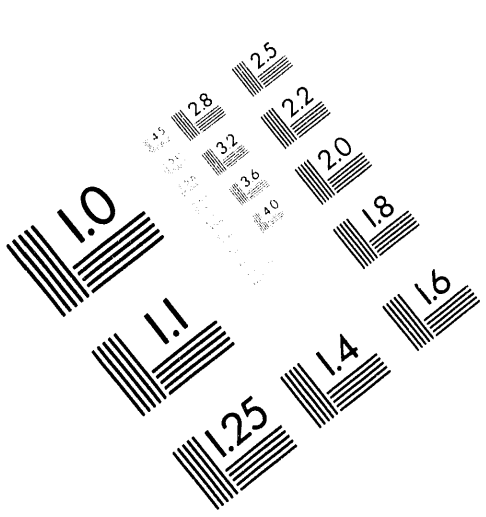

Association for Information and Image Management

1100 Wayne Avenue, Suite 1100
Silver Spring, Maryland 20910

301/587-8202

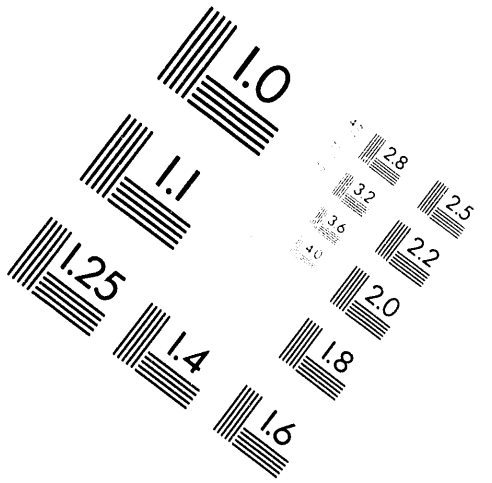

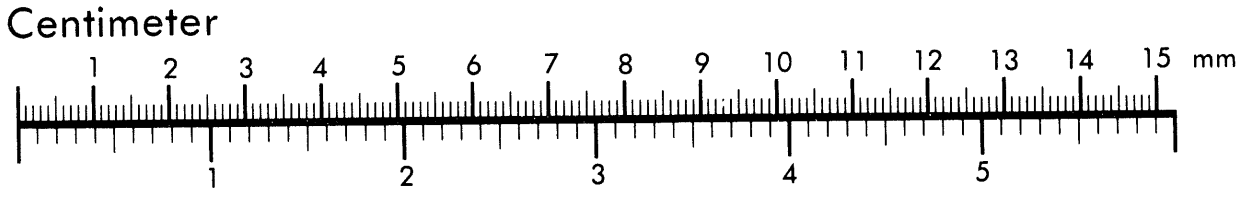

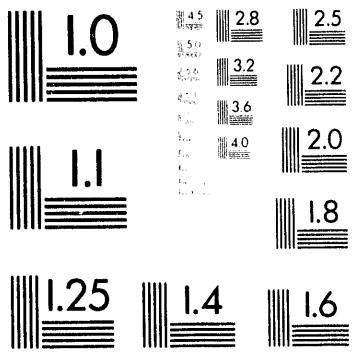

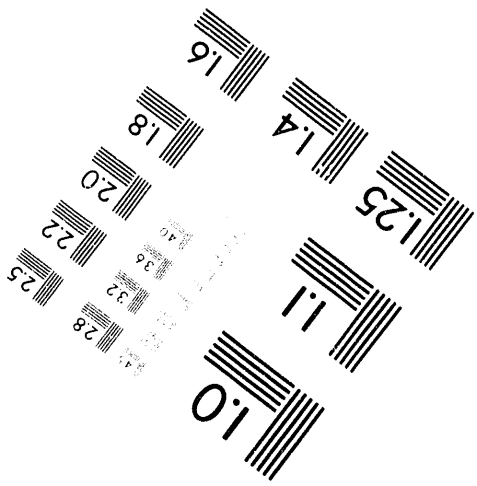

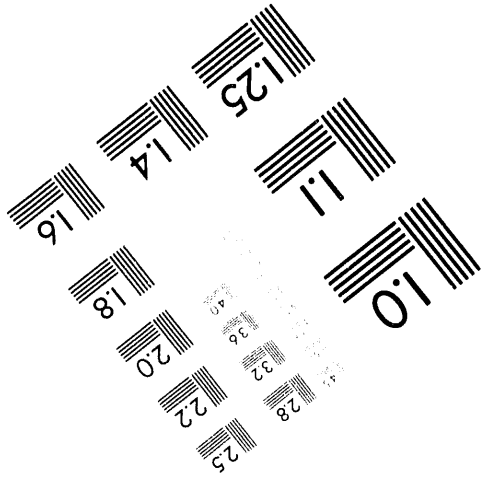

MANUFACTURED TO AIIM STANDARDS
BY APPLIED IMAGE, INC.

1 of 1

GA-A21595
UC-224

CESIUM RESERVOIR AND INTERCONNECTIVE COMPONENTS FINAL TEST REPORT TFE VERIFICATION PROGRAM

Prepared under
CONTRACT DE-AC03-86SF16298
FOR THE SAN FRANCISCO OPERATIONS OFFICE
DEPARTMENT OF ENERGY

GENERAL ATOMICS PROJECT 3450
MARCH 1994

GENERAL ATOMICS

CESIUM RESERVOIR AND INTERCONNECTIVE COMPC
FINAL TEST REPORT
TFE VERIFICATION PROGRAM

1. INTRODUCTION

1.1 Objective of TFE Verification Program

The program objective is to demonstrate the technology readiness of a TFE suitable for use as the basic element in a thermionic reactor with electric power output in the 0.5 to 5.0 MW(e) range, and a full-power life of 7 years. A TFE for a megawatt class system is shown on Figure 1-1. Only six cells are shown for simplicity; a megawatt class TFE would have many more cells, the exact number dependent on optimization trade studies.

1.2 Technical Approach

The TFE Verification Program built directly on the technology and data base developed in the 1960s and early 1970s in an AEC/NASA program, and in the SP-100 program conducted in 1983, 1984 and 1985. In the SP-100 program, the attractive features of thermionic power conversion technology were recognized but concern was expressed over the lack of fast reactor irradiation data. The TFE Verification Program addressed that concern.

The technical approach followed to achieve the program objective is shown on Fig. 1-2. Five prior programs form the basis for the TFE Verification Program:

1) AEC/NASA program of the 1960s and early 1970s.
1) SP-100 concept development program (Ref. 1-1).
3) SP-100 thermionic technology program (Ref. 1-2).
4) Thermionic irradiations program in TRIGA in FY-86 (Ref. 1-3).
5) Thermionic Technology Program in 1986 and 1987 (Refs. 1-4, 1-5).

These programs provided both the systems and technology expertise necessary to design and demonstrate a megawatt class TFE.

A TFE was designed that met the reliability and lifetime requirements for a 2 MW(e) conceptual reactor design. Analysis showed that this TFE could be used over the range of 0.5 to 5 megawatts. This was used as the basis for designing components for test and evaluation. The demonstration of a 7-year component lifetime capability was through the combined use of analytical models and accelerated, confirmatory tests in a fast test reactor. Iterative testing was performed where the results of one test series led to evolutionary improvements in the next test specimens.

The TFE components underwent screening and initial development testing in ex-reactor tests. Several design and materials options were considered for each component. As screening tests permitted, down selection occurred.

In parallel with ex-reactor testing, and fast reactor component testing, components were integrated into a TFE and tested in the TRIGA test reactor at GA. Realtime testing of partial

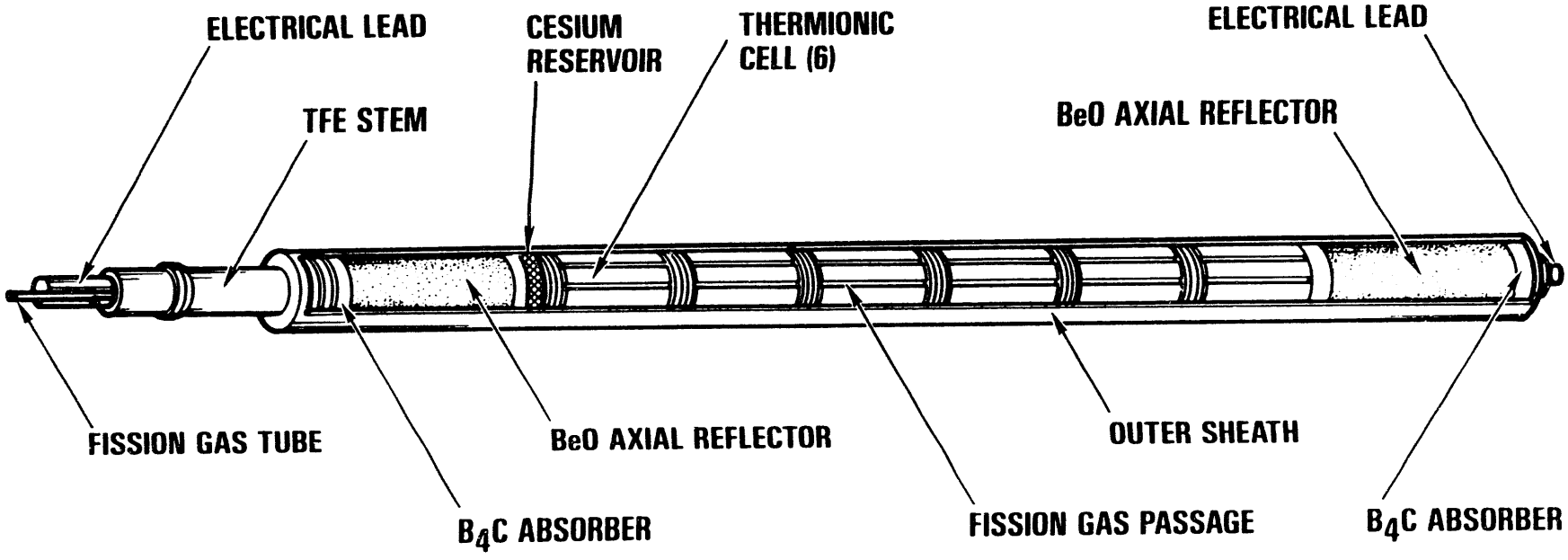

Figure 1-1. TFE for Megawatt Class System

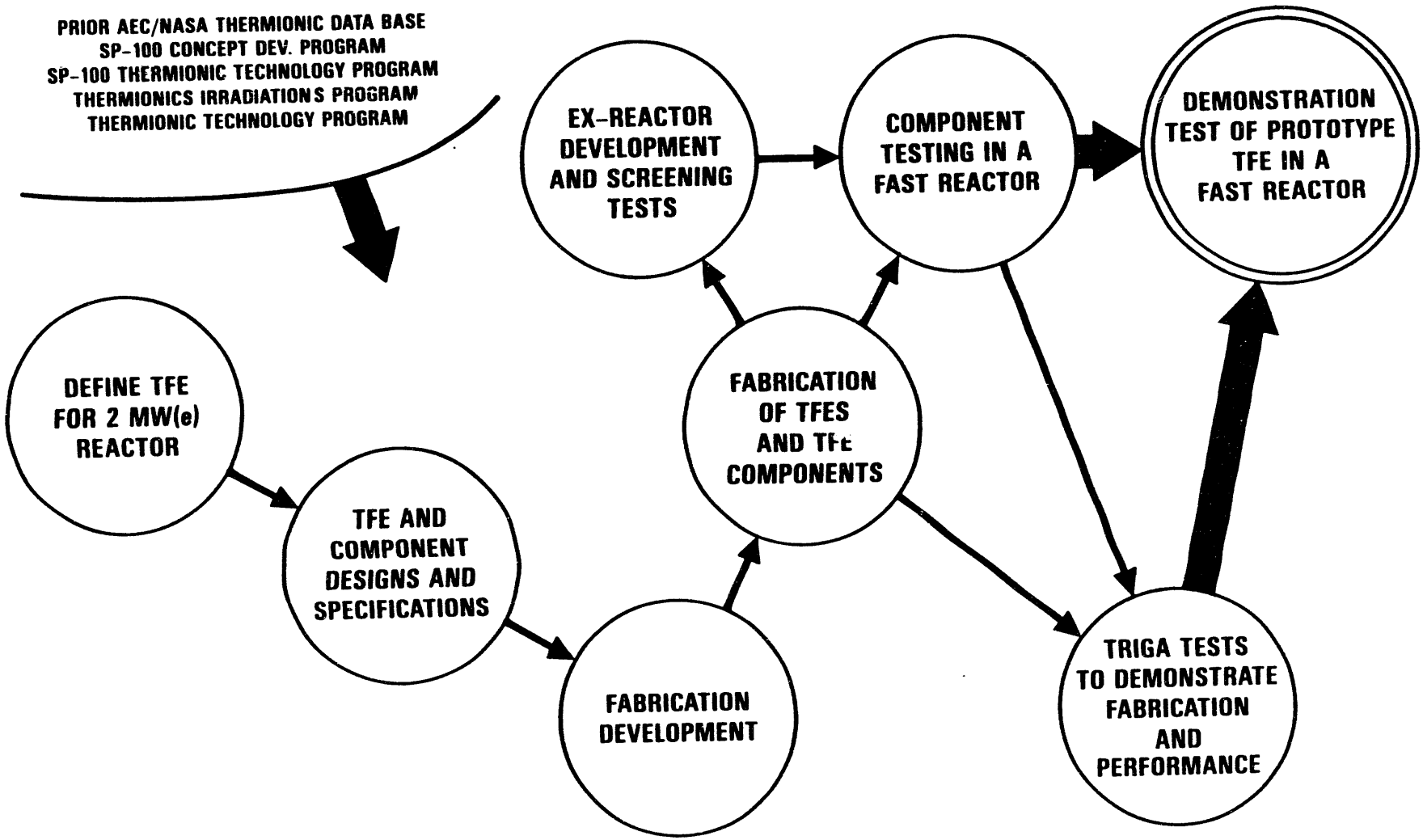

Figure 1-2. Logic to Demonstrate Technology Readiness of Megawatt Class TFE

length TFEs was used to test support, alignment and interconnective TFE components, and to verify TFE performance in-reactor with integral cesium reservoirs. Realtime testing was also used to verify the relation between TFE performance and fueled emitter swelling, to test the durability of intercell insulation, to check temperature distributions, and to verify the adequacy over time of the fission gas venting channels.

Predictions of TFE lifetime rested primarily on the accelerated component testing results, as correlated and extended to realtime by the use of analytical models.

1.3 Organization of the Program

Contracting Agency: Department of Energy, San Francisco Operations Office

Prime Contractor: General Atomics (GA)

Subcontractors:

ThermoTrex Corporation (TTC), a subsidiary of Thermo Electron Corporation
Rasor Associates, Incorporated (RAI)
Space Power Incorporated (SPI)

Fast reactor testing manager:

Westinghouse Hanford Corporation (WHC)

Fast reactor facilities:

Fast Flux Test Reactor (FFTF), with testing managed by WHC.
EBR-II, with testing managed by Argonne National Laboratory-West (ANL-W)

Technical oversight for DOE: Los Alamos National Laboratory (LANL).

1.4 Structure of Test Program

The TFE-VP was broken down into 7 tasks, generally corresponding to the components of a TFE. Figure 1-3 shows a thermionic cell with the various components identified.

Figure 1-4 shows a one cell TFE fabricated for test in the program. A multi-cell TFE has 2 or more cells in series.

When compared to Figure 1-1, it is clear that this test article is not quite prototypical. The test conditions dictate the design to some extent. Also, the test approach is to first test simple TFEs and then gradually test TFEs more prototypic.

For each component, the work involved:

1) Component design and analyses

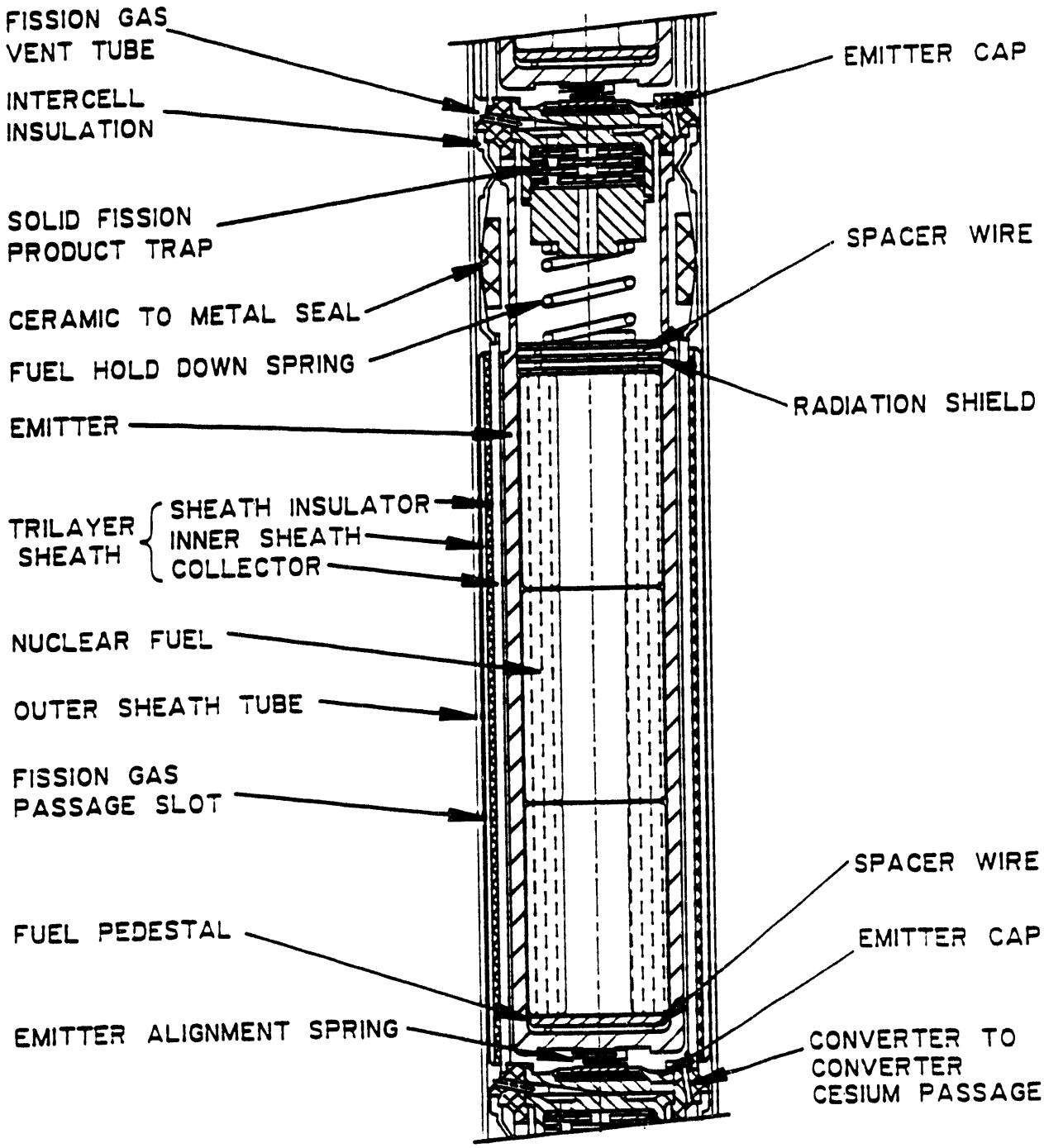

Figure 1-3. Thermionic Cell

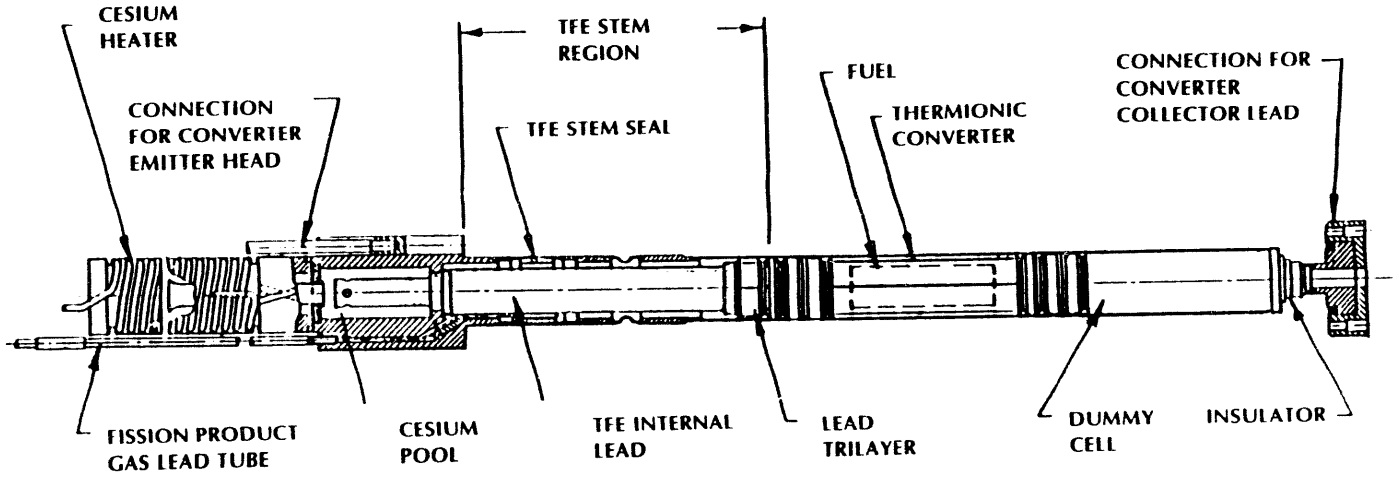

Figure 1-4. One Cell TFE Test in TFE Verification Program

2) Materials evaluation and selection
3) Performance testing
4) Life testing, both accelerated and real time.

In addition, performance models were developed for converter performance, fueled emitters and cesium reservoirs.

A brief description of each task is given below. For each of the component tasks, fabrication process specifications were developed and materials were chosen.

1.4.1 Conceptual Design. A TFE optimized for a 2 MW(e) system was designed. Its scalability over the range of 500 kW to 5 MW was demonstrated.

1.4.2 Converter Performance. The performance of converters of interest for megawatt class systems was measuredd and existing models on converter performance were refined.

1.4.3 Insulator Seals. The insulator seal isolates the space filled with gaseous fission products from the cesium filled interelectrode gap. It also assures that electrons flow from the collector of one cell to the emitter of an axially adjacent cell.

1.4.4 Sheath Insulators. The sheath insulator is a structure composed of 3 layers:

- The inner layer is the collector.
- The middle layer is an insulator electrically isolating the collector from the reactor coolant and structure. It also must conduct reject heat to the reactor coolant.
- The outer metallic layer assures the structural integrity of the sheath.

1.4.5 Fueled Emitters. The fueled emitter is the emitter component inside of which are the following components:

- UO_2 fuel.
- Fuel holddown device to prevent damage to the cell during launch and ascent.
- Fission product trapping components to prevent solid and condensable fission products from exiting the cell.
- Heat shields to protect the upper and lower parts of the emitter from the high temperatures of the UO_2 fuel.

1.4.6 Cesium Reservoir and Interconnective Components

The cesium reservoir provides cesium vapor to the interelectrode gap. A graphite cesium reservoir was demonstrated in the program.

Interconnective components are those metal parts and insulators which are necessary to attach one cell in series with another.

1.4.7 TFEs

The TFE is an axial series of one or more cells. It also contains a cesium reservoir. TFEs with one, three and six cells were fabricated and tested.

The TFEs fabricated under the TFE Verification Program are designated the "H" series TFEs, being the next series following the "E", "F" and "G" series which were studied in the 1960s and 1970s. The E series TFEs had an emitter diameter of 0.625 inch; the F series, 1.1 inches; and the H series, 0.5 inches.

A specific TFE has a designation xHy, the "x" being the number of cells in the TFE and the "y" being the specific TFE in question. For example, the TFEs fabricated and tested in the program were:

TFE-1H1, the first of the 1-cell TFEs.
TFE-1H2, the second of the 1-cell TFEs.
TFE-1H3, the third of the 1-cell TFEs.
TFE-3H1, the first of the 3-cell TFEs.
TFE-3H5, the fifth of the 3-cell TFEs. Numbers 2, 3 and 4 were eliminated early in the program.
TFE-6H1, the first of the 6-cell TFEs.

1.5 Semiannual Progress Reports

Semiannual progress reports provide a running account of technical progress which reflects the work done at GA, TTC, RAI and SPI. These reports also summarize the status and results of the irradiation program at WHC, ANL-W and LANL.

Table 1-1 shows a complete list of all semiannual progress reports.

1.6 Final Reports

Final test reports give details on each of the major components outlined in Section 1.4. A list of these final reports is given in Table 1-2. It is assumed in these reports that the reader is familiar with thermionic technology and the structure and operation of thermionic fuel elements and their components.

1.7 Westinghouse Hanford Company Reports on Cesium Reservoirs

WHC issued several reports dealing with the fabrication, testing and postirradiation examination of cesium reservoirs. These are listed in Table 1-3. The reader is referred to these reports for detail on the irradiation of cesium reservoirs and their subsequent postirradiation examination (PIE).

Table 1-1

SEMIANNUAL PROGRESS REPORTS

Period Ending	Date Issued	Report Number
March 31, 1987	April 1987	GA-A18780
September 30, 1987	March 1988	GA-A19115
April 30, 1988	June 1988	GA-A19269
October 31, 1988	January 1989	GA-A19412
April 30, 1989	September 1989	GA-A19666
September 30, 1989	March 1990	GA-A19876
March 31, 1990	July 1990	GA-A20119
September 30, 1990	January 1991	GA-A20335
March 31, 1991	April 1991	GA-A20493
September 30, 1991	December 1991	GA-A20804
March 31, 1992	April 1992	GA-A20911
September 30, 1992	January 1993	GA-A21210
March 31, 1993	May 1993	GA-A21326
September 30, 1993	January 1994	GA-A21511

Table 1-2

FINAL TEST REPORTS OF TFE VERIFICATION PROGRAM

Report Title	Document No.
Conceptual Design	GA-A21590
Converter Peformance Final Test Report	GA-A21591
Insulator Seal Final Test Report	GA-A21592
Sheath Insulator Final Test Report	GA-A21593
Fueled Emitter Final Test Report	GA-A21594
Cesium Reservoir and Interconnective Components Final Test Report	GA-A21595
TFE Performance Final Test Report	GA-A21596
TFE Design Package	GA-A21597

TABLE 1-3

WESTINGHOUSE HANFORD COMPANY REPORTS ON CESIUM RESERVOIR TESTING

Test Documentation

1. Williams, L.S., "Test Design Description for the Materials Open Test Assembly HM115 (MOTA-1E)", Experiment Description - Volume II, HEDL-TC-2851, July 1986.

2. Williams, L.S., "Final Data Package As-Built Documentation for the Installation of the Test Train into the Materials Open Test Assembly Vehicle - HM115 (MOTA-1E)" HEDL-TC-2855, July 1986.

3. Williams, L.S., "Test Design Description for the Materials Open Test Assembly HM116 (MOTA-1F)", Experiment Description - Volume II, WHC-SP-0028, August 1987.

4. Williams, L.S., "Final Data Package As-Built Documentation for the Installation of the Test Train into the Materials Open Test Assembly Vehicle - HM116 (MOTA-1F)" WHC-SP-0085, September 1987.

5. Engineering Test Plan for EBR-II Tests UFAC-2B and UFAC-3, WHC-SP-0469, May 1989.

6. Experiment Description and Safety Analysis for EBR-II Tests UFAC-2B and UFAC-3, WHC-SP-0470, July 1989.

7. Engineering Test Plan (ETP) for UCA-3, WHC-SD-SP-DB-001, August 1990.

8. QA and As-Built Data Package for UCA-3 Experiment (Capsule SC3-3), WHC-SD-SP-DP-001, November 1991.

9. QA and As-Built Data Package for UCA-3 Experiment (Capsule SC3-4, SC3-5 and SC3-6), WHC-SD-SP-DP-002, April 1991.

Test Data Reports

1. Lawrence, L.A., N.S. Cannon and K.E. Ard, "Irradiation and Examination of the Thermionic Fuel Element (TFE) Verification Program UCA-1 Samples", WHC-SP-0585, May, 1990.

2. Lawrence, L.A., K.E. Ard and D.M. Paxton, "Irradiation and Examinations of the Thermionic Fuel Element (TFE) Varification Program UCA-2 Samples", WHC-SP-0656, June 1991.

3. Lawrence, L.A. and D.M. Paxton, "Irradiation and Examinations of the Thermionic Fuel Element (TFE) Verification Program UCA-3 Samples", WHC-SP-1055, September 1993.

2. OBJECTIVES OF THE TEST PROGRAM

2.1 Function of the Cesium Reservoir

A thermionic converter must be supplied with cesium vapor for two reasons. Cesium atoms adsorbed on the surface of the emitter cause a reduction of the emitter work function to permit high current densities without excessive heating of the emitter. The second purpose of the cesium vapor is to provide space-charge neutralization in the emitter-collector gap so that the high current densities may flow across the gap unattenuated. This is accomplished by positive cesium ions in the interelectrode plasma that are produced both by surface ionization on the emitter, and by electron-atom collisions within the plasma volume.

The function of the cesium reservoir is to provide a source of cesium atoms, and to provide a reserve in the event that cesium is lost from the plasma by any mechanism. This can be done with a liquid cesium metal reservoir, as is done routinely in laboratory converters, in which case it is heated to the desired temperature with auxiliary heaters. In a TFE, however, it is desirable to have the reservoir passively heated by the nuclear fuel. In this case, the reservoir must operate at a temperature intermediate between the emitter and the collector, ruling out the use of liquid reservoirs. Intergral reservoirs contained within the TFE will produce cesium vapor pressures in the desired range at typical electrode temperatures.

The reservoir material that appears to be best able to meet requirements is graphite. Cesium intercalates easily into graphite, and the cesium pressure is insensitive to loading for a given intercalation stage.

2.2 Goals of the Test Program

The goals of the cesium reservoir test program were to verify the performance of Cs-graphite reservoirs in the temperature-pressure range of interest to TFE operation, and to test the operation of these reservoirs after exposure to a fast neutron fluence corresponding to a seven year mission lifetime. In addition, other materials were evaluated for possible use in an integral reservoir. Finally, the time response of the cesium graphite compounds to a temperature change was determined.

2.3 Requirements of the Cesium Reservoir

The design of the TFE places the following requirements upon the cesium reservoir:

Minimum operating temperature	1070 K
Design point cesium pressure	2 torr
Maximum neutron fluence	3.5×10^{22} nvt

In addition to the primary design requirements noted above, there are many subordinate requirements:

1) The cesium vapor pressure in the interelectrode gap must remain constant for small variations in the cesium load in the reservoir. Cesium will be absorbed on various metal surfaces and this absorption may change with time. In addition, small leaks may develop. The vapor pressure should not change significantly if and when these changes occur.

2) The reservoir material must exhibit thermo-chemical stability in its operating environment over long periods of time. There should be no chemical reaction between the reservoir material and its environment.

3) The cesium vapor pressure in the interelectrode space should increase when the emitter temperature increases. This is essential for stable thermionic operation.

4) The reservoir pressure/temperature relationship must not change significantly under fast neutron irradiation. The reservoir material itself should have properties which are not sensitive to fast neutrons.

2.4 Technical Approach

All in-reactor testing was done with graphite reservoir materials, as prompted by previous experience. Two materials were studied: highly oriented HOPG and isotropic POCO CZR-2. The cesium pressure-graphite temperature characteristics were measured before and after exposure to a neutron environment in FFTF or EBR-II. In addition, a few other materials were subjected to ex-reactor testing. None were found to be suitable and were not tested incore.

2.5 Interconnective Components

The objective of this part of the program was to establish a method of coating the intercell components to prevent an arc from being established between them and the surrounding sheath tube. In normal operation, this would not be possible since the spacing is sufficient to prevent arcing. However if a leak should occur between the cesium and fission product spaces, a cesium arc could occur and the TFE could be damaged. The design requirements for intercell insulation are:

Minium breakdown voltage	7.5 v
Operating temperature	1150 K maximum
Nominal fast fluence	3.5×10^{22} nvt
Lifetime	7 years
Operating environment	Fission gases; possible 2 torr Cs in event of a leak

3. EX-REACTOR TEST REPORT

3.1 Test Articles

3.1.1 Test Articles to Support In-Core Tests

The test article used for characterizing graphite reservoir materials prior to in-core testing is shown schematically in Fig. 3-1. This same test article was also used for determining the cesium loading characteristics of other candidate reservoir materials that were not subsequently irradiation tested.

The test article was a niobium cylinder about .56 inch in diameter and slightly larger in length. During laboratory testing, it was connected to a test manifold via a niobium tube, which was subsequently pinched off, as shown in Fig. 3-1. The reservoir sample was located within a perforated tantalum liner located within the niobium canister. The function of the liner was to prevent physical contact between the graphite/carbon materials, and the niobium, thereby reducing the possibility of carbide formation during long periods at high temperature in-core.

The thin section at the bottom of the niobium canister is essential in the post- irradiation examination (PIE) of the reservoir sample. In PIE, the canister is punctured and the pressure/temperature characteristics of the reservoir determined.

Table 3-1 lists all test articles that were used for in-core testing after the ex-reactor testing was complete. HOPG is a highly oriented pyrolytic graphite. PC-113 is a porous carbon material. Fibers are oriented pitch-derived graphite. POCO is an isotpic graphite, CZR-2 being one of several POCO grades. All of these materials are commercially available.

Test articles were also prepared that contained PC-113, Al_2O_3, MoS_2, and high surface area Mo. These tests, which were not followed by in-core testing, are not included in the table.

3.1.2 Test Articles for Dual Reservoir Tests

Ex-reactor tests were also undertaken to assess the performance of a Cs-graphite reservoir operating in a temperature gradient, such as indicated in Fig. 3-2(a). In the idealized case, the temperature decreases linearly from T_1 to T_2 along a stack of chunks of graphite that are only loosely connected. This situation was idealized with an experimental configuration in which two samples were operated isothermally at T_1 and T_2, but are in the same vacuum envelope, as shown in Fig. 3-2(b). In the actual experiments, there was three times as much graphite in the left-hand chamber as in the other chamber. The connection to the test stand was made through a flanged fitting on the tube indicated at the right of Fig.3-2.

3.1.3 Test Articles for Time Response Tests

Ex-reactor tests of the time response of the cesium pressure to design modifications in the reservoir chamber were also conducted. The test articles for two time response tests were the same as shown in Fig. 3-1, except that instead of the specimens of POCO or HOPG graphite, they contained 5 graphite pins approximately .125 in. in diameter and .375 in. long. In one of these two tests, the pins were loose within the Ta liner, and in the other they were

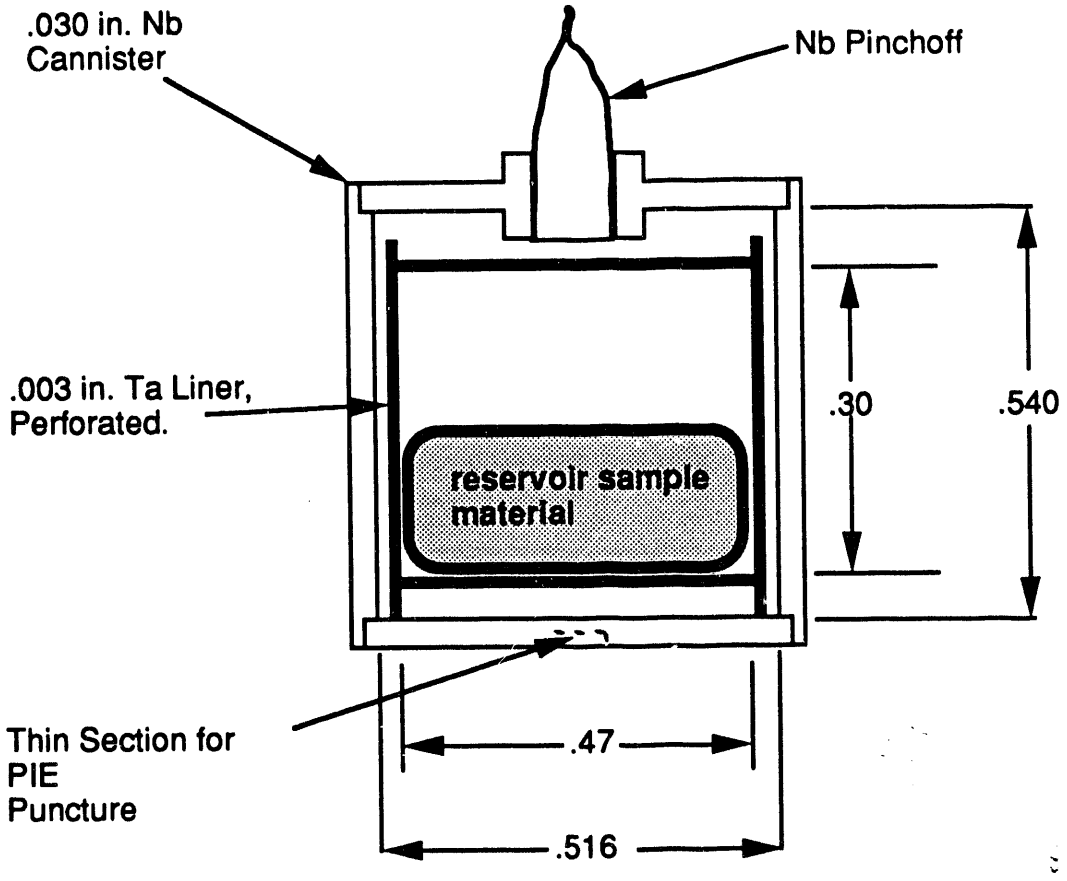

Figure 3-1. Test Article for Characterizing Cesium Reservoir Materials

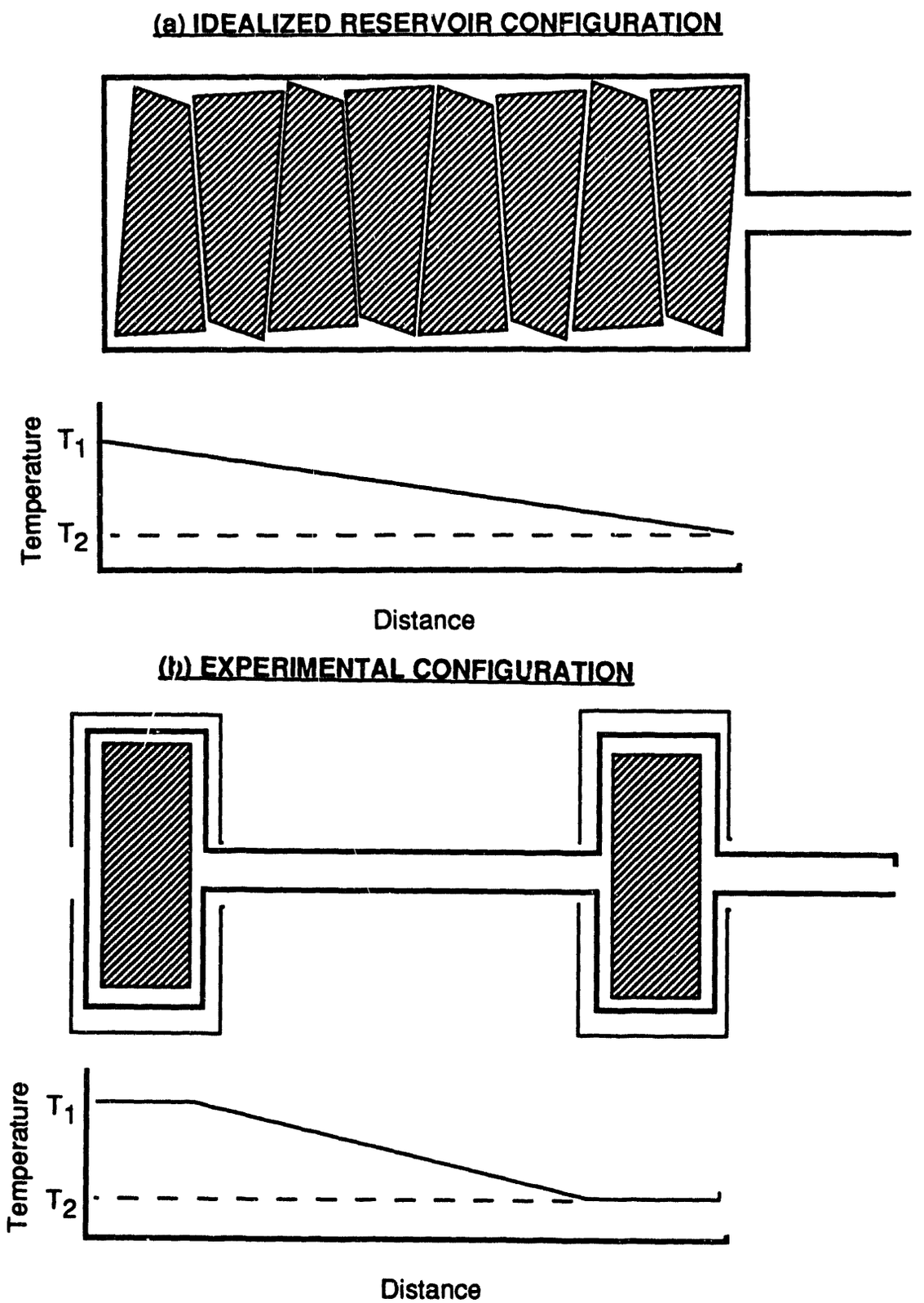

Figure 3-2. Schematic Configuration for Assessing Reservoir Performance in a Temperature Gradient

Table 3-1

GRAPHITE SAMPLES CHARACTERIZED IN EX-REACTOR TESTS AND SUBSEQUENTLY IRRADIATED

Identification Number	EBR-II (FFTF) Test Designation	Material	Size/Weight
9A	UCA-1	HOPG	0.408 cm^3
B	UCA-1	PC-113	0.437 cm^3
C	UCA-1	HOPG	0.191 cm^3
		PC-113	0.225 cm^3
		POCO	0.226 cm^3
		Fibers	N/A
D	UCA-1	HOPG	0.393 cm^3
E	UCA-1	PC-113	0.450 cm^3
197A	UCA-2	HOPG-ZYH	0.7474 g
199D	UCA-2	POCO CZR-2	0.7410 g
929D	UFAC-3	POCO CZR-2	0.2895 g
930D	UFAC-3	POCO CZR-2	0.2803 g
960D	UFAC-3	POCO CZR-2	0.2915 g
961A	UFAC-3	HOPG-ZYH	0.3188 g
962A	UFAC-3	HOPG-ZYH	0.2564 g
413D	UCA-3	POCO CZR-2	0.3020 g
1247D	UCA-3	POCO CZR-2	0.3005
1300D	UCA-3	POCO CZR-2	0.3030 g
1301D	UCA-3	POCO CZR-2	0.3010 g

contained in a porous Mo barrel shown schematically in Fig. 3-3. This design is patterned after a prototypic design for an integral reservoir that would prevent migration of graphite fragments within the TFE.

The test article for a third time response test was similar to that used in the dual reservoir tests, as shown in Fig. 3-4. The purpose here was to model the behavior of a large amount of the porous material between the Cs-graphite and the interelectrode gap of a converter.

3.2 Test Procedures

3.2.1 Preirradiation Test Procedures

A schematic of the apparatus used for the preirradiation testing is shown in Fig. 3-5. The same apparatus was also used for limited testing of certain non-carbon reservoir materials. There are four controlled heat zones:

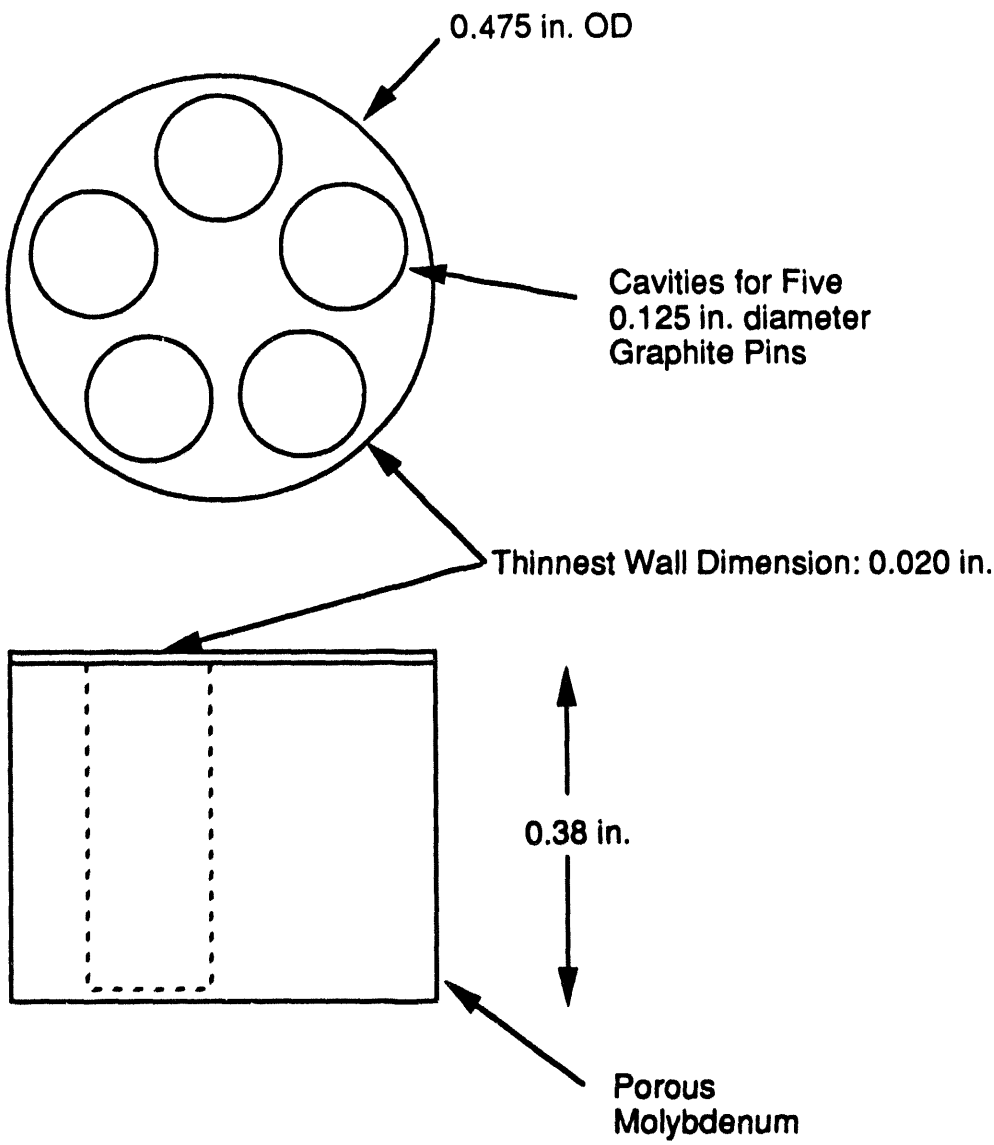

Figure 3-3. Porous Molybdenum Reservoir Barrel

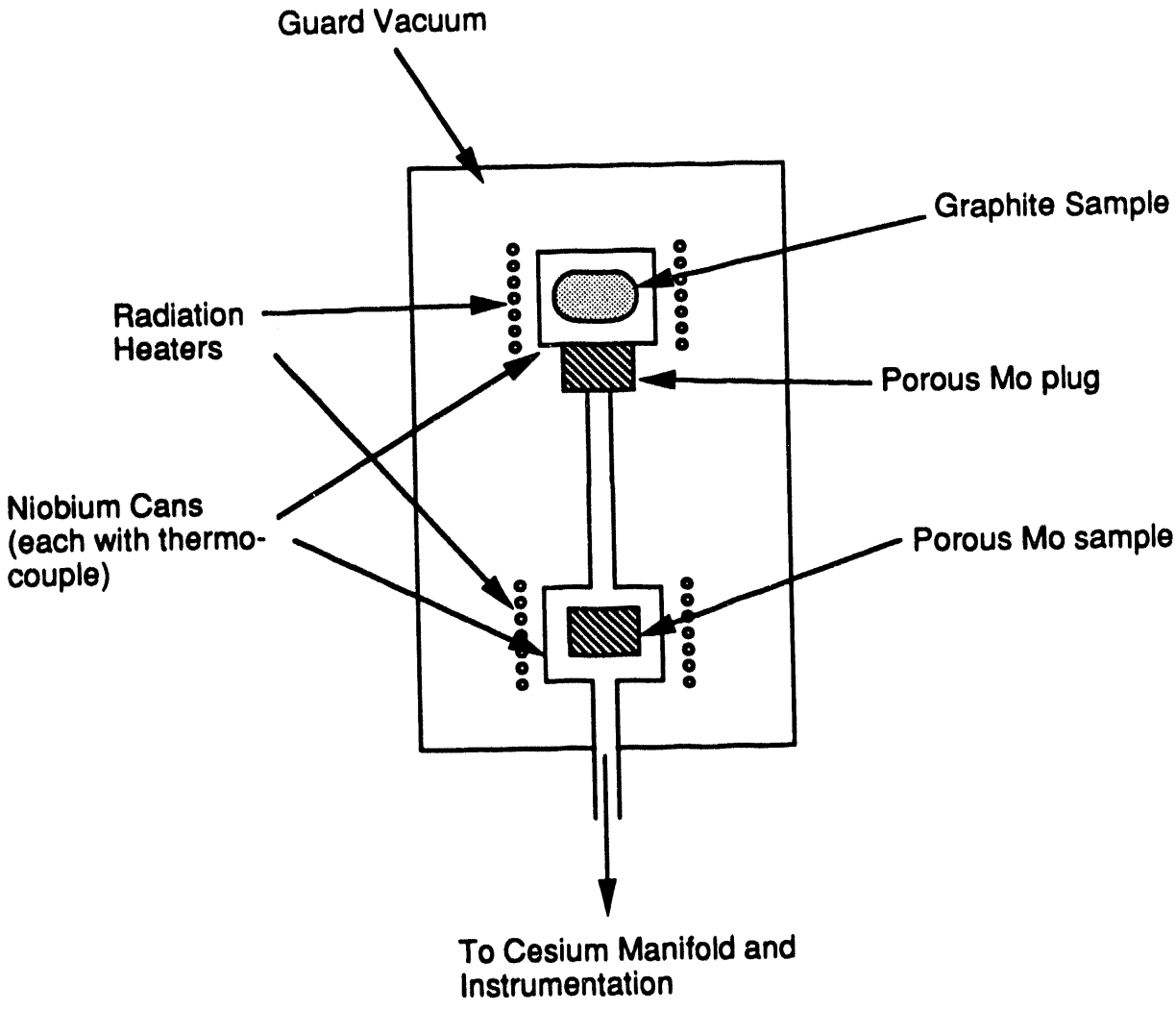

Figure 3-4. Schematic of Test Fixture for Porous Plug Tests

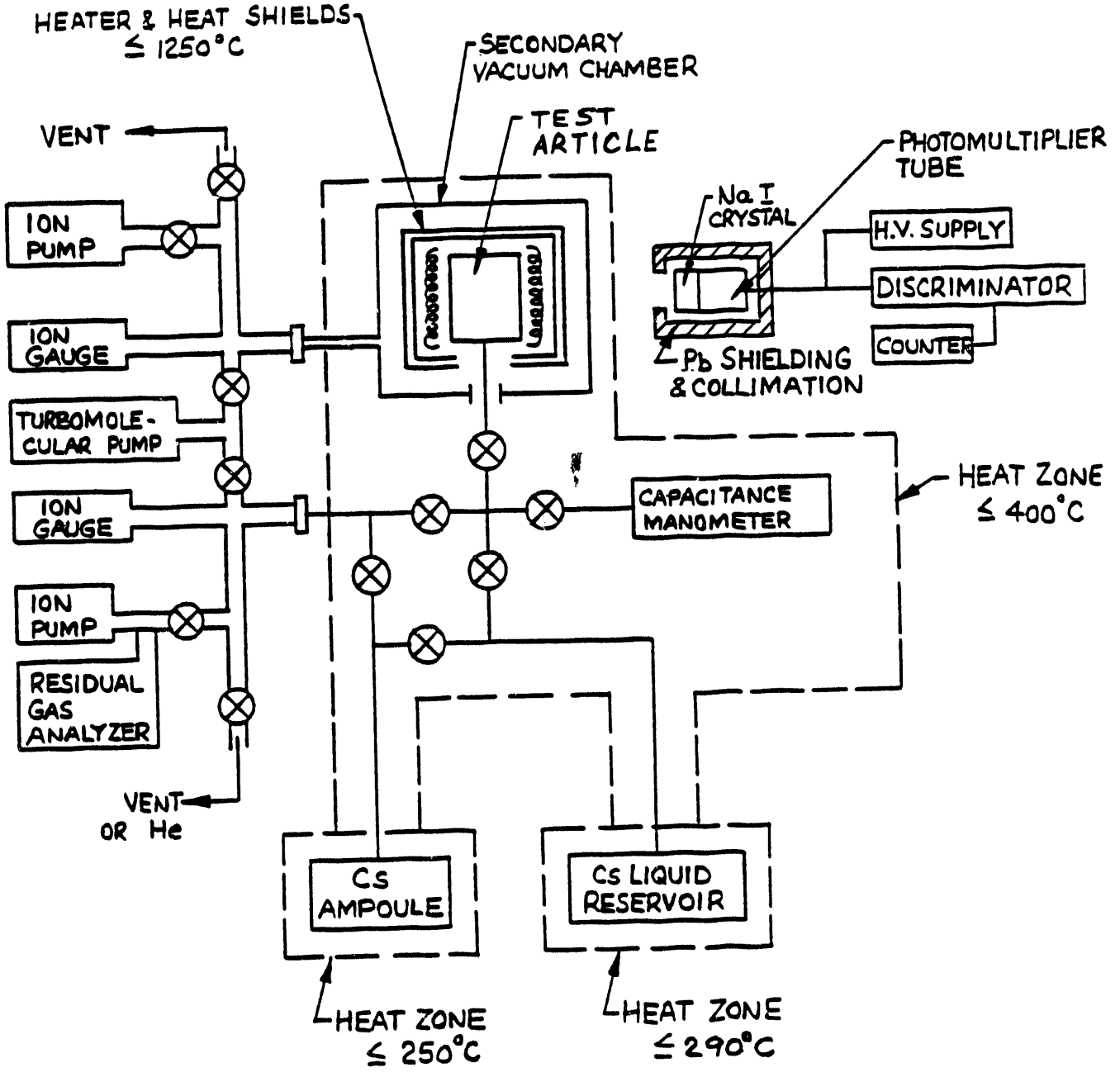

Figure 3-5. Schematic of Cesium Reservoir Ex-Reactor Test Stand

1) A heat zone for use in the initial charging of the apparatus with cesium from ampoules that had been activated in the TRIGA test reactor at GA.

2) A heat zone to control the liquid cesium reservoir temperature to establish the loading pressure of the reservoir materials;

3) A heat zone that maintains the cesium manifold and the capacitance manometer at a temperature that prevents condensation of cesium; and

4) A heat zone that contains the reservoir test article.

Heat zones 1 and 2 consist of coaxial heater wires wound upon the components and suitably insulated, whereas heat zone 3 is a commercial oven. Heat zone 4 consists of a tungsten radiation heater and radiation heat shields that surround the test article. The cesium manifold and the secondary vacuum chamber (guard vacuum) are initially evacuated with a turbomolecular pump and ion pumps as shown.

The amount of cesium in the graphite is determined using gamma ray spectroscopy. TRIGA activation of the cesium in the ampoules produces Cs-134. During the activation run, another ampoule of $CsNO_3$ is placed next to the Cs ampoule to provide an activity standard for subsequent measurements. A NaI scintillator crystal is located outside of the guard vacuum, in view of the test article, so that the activity of the reservoir material can be measured and compared with the $CsNO_3$ standard. In this manner, accurate determination of the cesium loading is obtained.

The test sequence begins when the test article is attached to the cesium manifold at a port in the guard vacuum, and the heater coil and heat shields are put in place. The guard vacuum space is evacuated, and the test article is outgassed 1200°C for 1 to 2 hours. The temperature of heat zone 4 is then lowered to the desired loading temperature and the pumping manifold is valved off. The desired cesium pressure is established in the liquid Cs reservoir and the valve to the cesium manifold is opened. The loading is monitored with the Cs-134 counting system until steady state is reached, then the valve to the liquid reservoir is closed.

The cesium pressure versus (graphite) temperature is measured using the capacitance manometer to measure the pressure. The system is then cooled down and the test article is backfilled, typically with He. The guard vacuum is opened so that the pinchoff in the tube attached to the test article may be made. The pinchoff is electron-beam welded and a serial number if etched into the Nb cylinder before it is ready for shipment. The samples which are subjected to ex-reactor testing only are not backfilled or welded shut.

3.2.2 Dual Reservoir Test Procedures

The same basic test stand shown in Fig. 3-5 is employed for the dual reservoir tests. Heat zone 4 is modified as shown in Fig. 3-6 and the gamma counting capability is not used

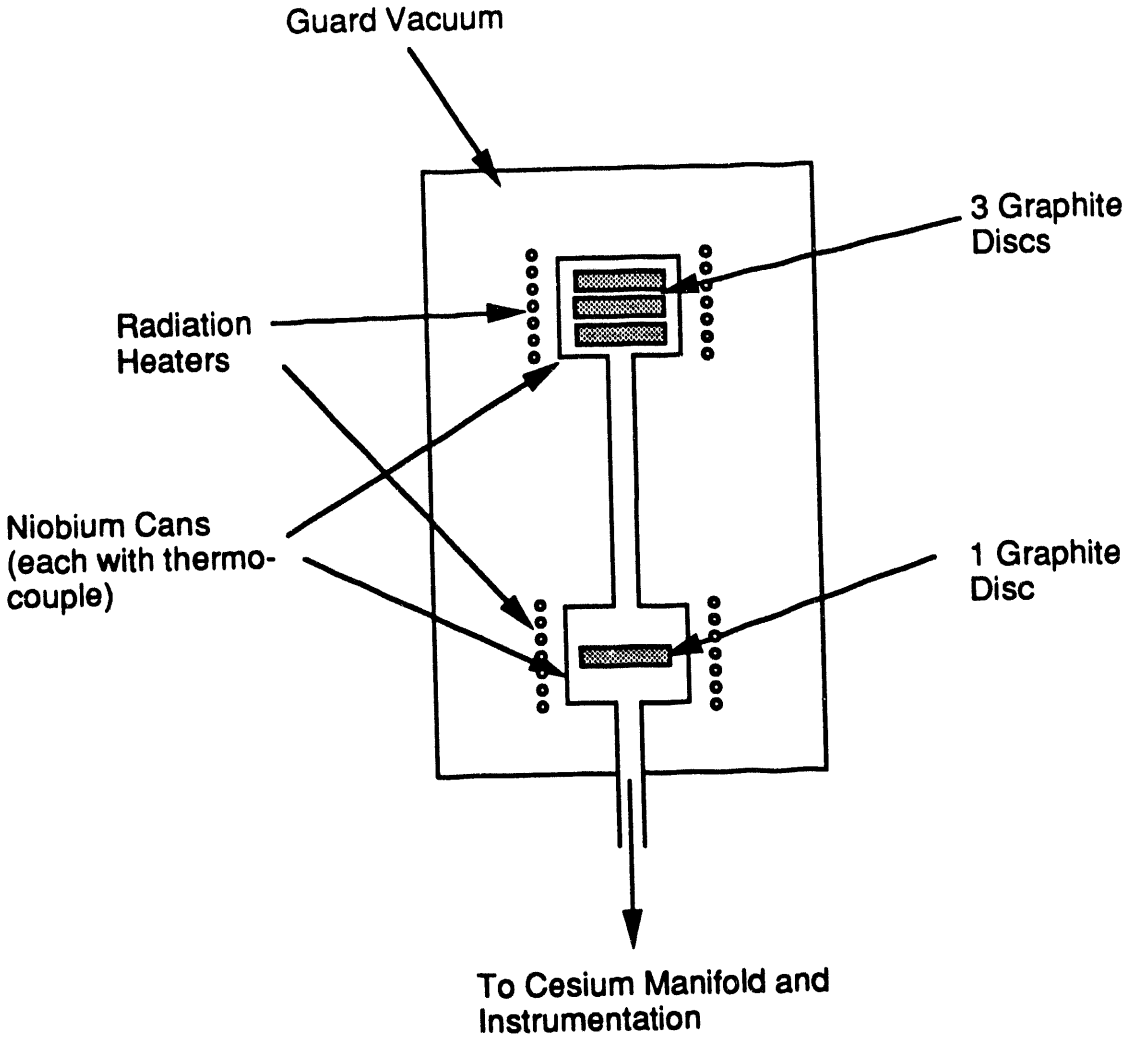

Figure 3-6. Schematic of Test Fixture for Asymmetric Reservoir Tests

(non-activated Cs is employed). In the dual reservoir tests, one chamber of the test article contains three graphite discs and is located in an isothermal heat zone. The other chamber contains one graphite disc and is located in a second (independent) isothermal heat zone. The connection to the cesium manifold is made at the same flange used to connect the preirradiation test articles to the cesium manifold shown in Fig. 3-5.

After initial outgassing, both reservoirs are brought to the same temperature and exposed to cesium for several hours, until equilibirum is achieved. This is determined by closing the valve to the liquid reservoir and monitoring the pressure as a function of time. If the pressure drops, the graphite is absorbing cesium, and the loading is continued for another time interval. If the pressure remains contant after the valve is closed, then equilibrium has been achieved, and the loading is complete.

Both reservoirs were loaded to the same specific loading, but the total cesium inventory of the upper reservoir in Fig. 3-6 was 3 times that in the lower reservoir. The tests were performed by maintaining one reservoir at constant temperature and varying the other, while monitoring the cesium pressure. Measurements were repeated by reversing the roles of the two reservoirs, then loading them at a different specific loading and repeating the series, as will be discussed in Section 3.3.2 below.

3.2.3 Time Response Test Procedures

The apparatus for these measurements was the same as described in Section 3.2.2. Only one of the heat zones was employed, however, and the pressure and temperature were recorded on a strip charge recorder, so that short time resolution could be obtained.

The test procedure, after loading the graphite in the manner described above, was to impose a temperature change on the graphite and monitor the pressure response. The time resolution was limited to about 30 seconds by the temperature response of the system.

3.3 Test Results

3.3.1 Preirradiation Test Results

Table 3-2 lists the preirradiation samples and the final loading values achieved just before pinchoff. The P vs T isosteres at the values of loading listed in the table are shown in the figures contained in Appendix A, with the exception of the UCA-1 test articles. Neither the loading nor the P vs T relationships were determined for the UCA-1 samples. The UCA-1 values quoted in the table were obtained from x-ray densitometric and dimensional measurements just prior to final encapsulation at the FFTF site, and are subject to some error.

Table 3-2

PREIRRADIATION LOADING OF RESERVOIR TEST MATERIALS FOR THE TEST ARTICLES THAT WERE SUBSEQUENTLY IRRADIATED

Identification Number	EBR-II(FFTF) Test Designation	Material	Loading, mg Cs/gC*
A	UCA-1	HOPG	610-1110
B	UCA-1	PC-113	940
C	UCA-1	HOPG	0
		PC-113	0
		POCO	0
		Fibers	0
D	UCA-1	HOPG	610-1110
E	UCA-1	PC-113	1010
197A	UCA-2	HOPG-ZYH	230
199D	UCA-2	POCO CZR-2	222
929D	UFAC-3	POCO CZR-2	790
930D	UFAC-3	POCO CZR-2	0
960D	UFAC-3	POCO CZR-2	260
961A	UFAC-3	HOPG-ZYH	0
962A	UFAC-3	HOPG-ZYH	295
413D	UCA-3	POCO CZR-2	278
1247D	UCA-3	POCO CZR-2	586
1300D	UCA-3	POCO CZR-2	348
1301D	UCA-3	POCO CZR-2	396

*The loading values of the UCA-1 samples A-E were estimates.

The preirradiation test results on graphite can be used to provide an analytical form for the cesium pressure that can be employed in thermionic models and design applications. These reservoir model developments are given in Section 5 below.

Two other candidate reservoir materials were examined in the preirradiation tests: a high surface area alumina, and a porous carbon material. Both materials were found to absorb Cs; Al_2O_3 absorbed up to 100 mg Cs per gram of material, and PC-113, a porous carbon material, absorbed up to about 1300 mg Cs per gram of material. However these two materials are not useful candidates for integral Cs reservoirs because of the extreme sensitivity of the cesium pressure to reservoir loading. This is demonstrated for alumina in Fig. 3-7 and for PC-113 in Fig. 3-8.

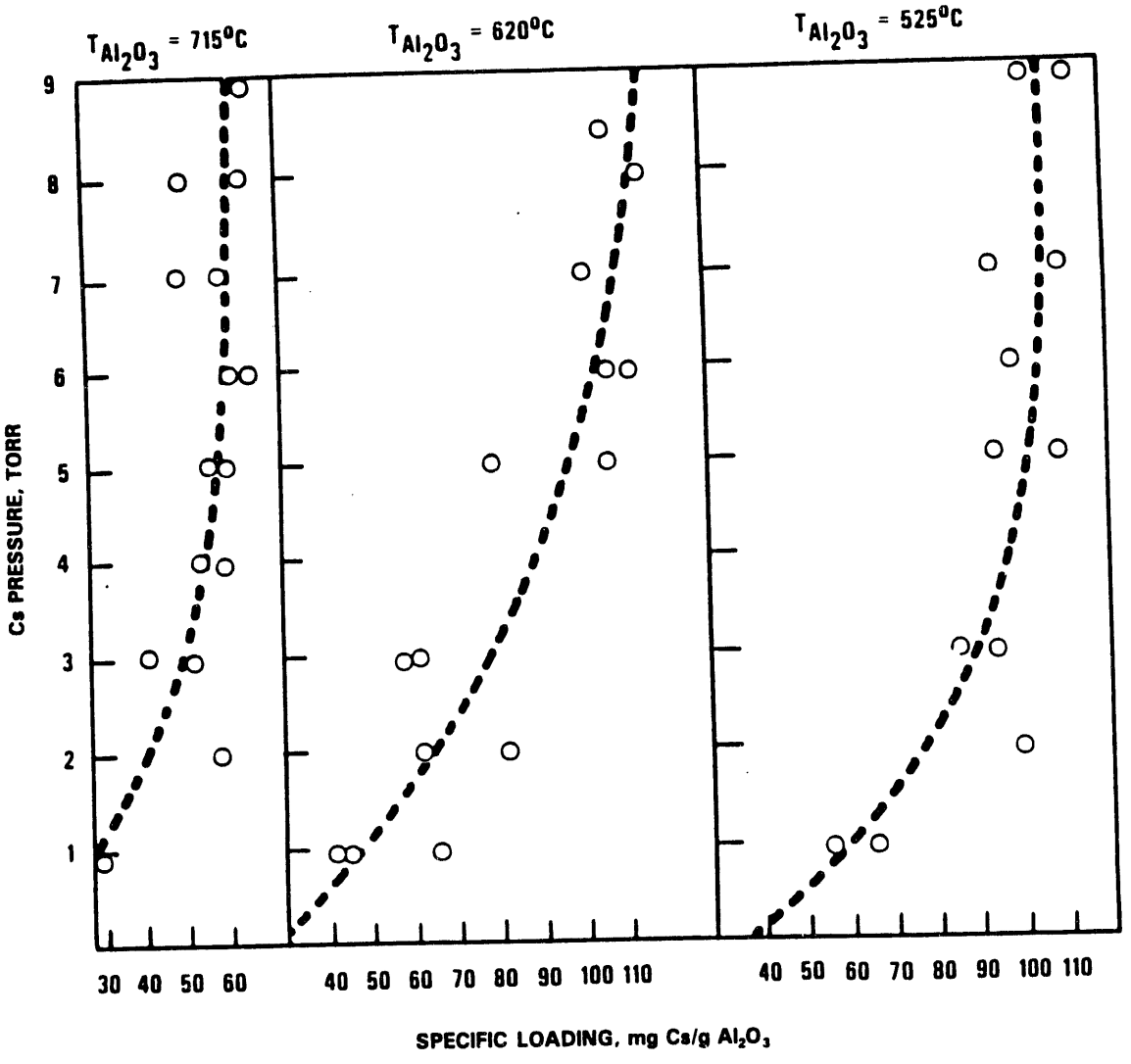

Figure 3-7. Cesium Pressure-Loading Curves for Alumina Reservoirs

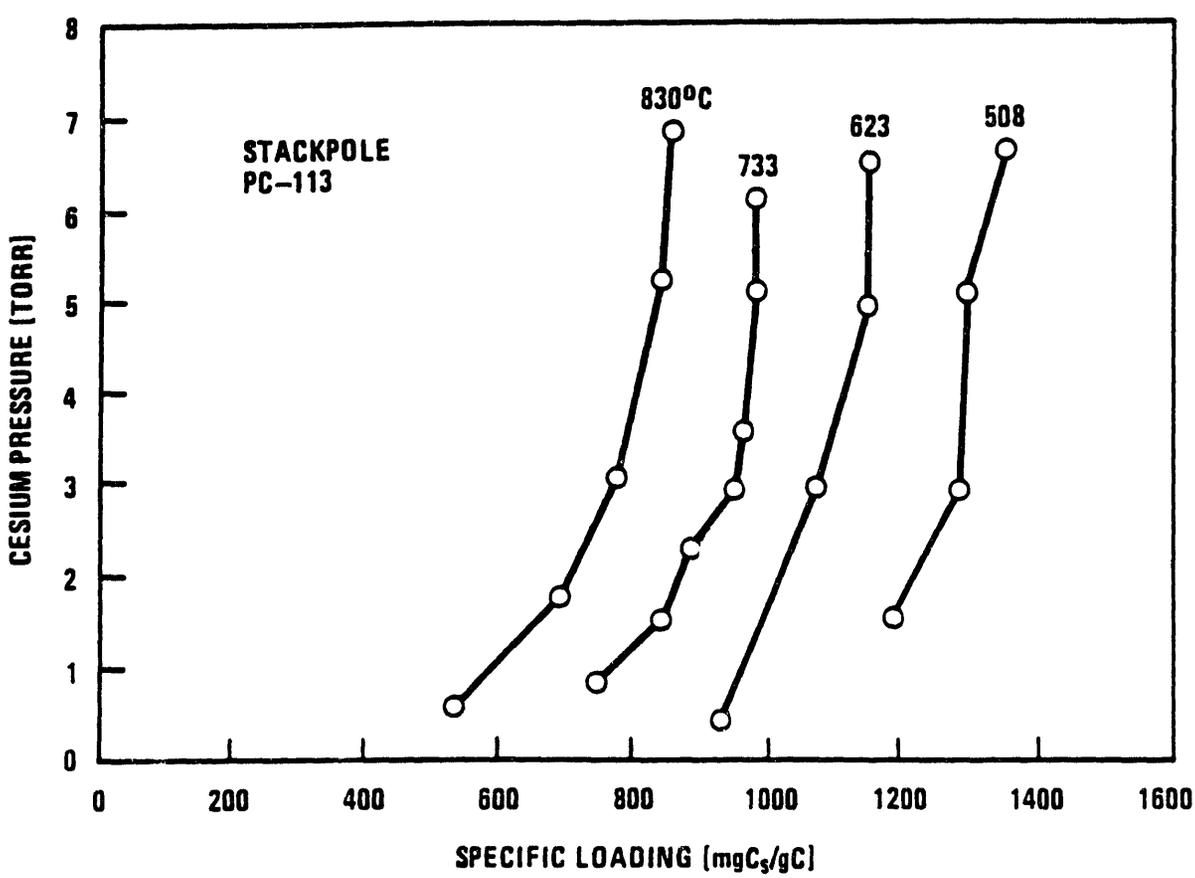

Figure 3-8. Cesium Pressure vs Loading Curves for Porous Carbon Reservoir

3.3.2 Dual Reservoir Test Results

The test vehicle for dual reservoir tests is shown schematically in Fig. 3-6. One reservoir contains 3 one-gram discs of POCO graphite and the other contains a single disc. Two isothermal loading conditions were used as indicated in Table 3-3. The loading was estimated from UCA-3 and UFAC-3 preirradiation data using Cs-134.

Table 3-3

DUAL RESERVOIR ISOTHERMAL LOADING CONDITIONS

Cesium Pressure, torr	Graphite Temperature, °C	Estimated Loading, mg Cs/gC
3	730	~600
1	800	~300

Cesium pressure data sets as indicated in Table 3-4 were obtained. In addition, isothermal measurements were made, i.e., the Cs pressure was measured as a function of graphite temperature with the two reservoirs at the same temperature. Comparisons of the isothermal data with the UCA-3 results are shown in Figs. 3-9 and 3-10. Agreement between the data sets was good.

Table 3-4

CESIUM PRESSURE DATA SETS

Estimate Loading, mg Cs/gC	Temperature Range of 3 Gram Reservoir, °C	Temperature Range of 1 Gram Reservoir, °C
600	655	650-780
	765	660-765
	650-825	655
	670-765	765
300	800	743-963
	890	750-894
	751-950	800
	730-840	890

The asymmetric data sets are plotted in Figs. 3-11 and 3-12. Qualitatively, the pressure is controlled by the 3 gram reservoir in all cases. For example, if both reservoirs were initially at 800°C (for the 300 mg Cs/gC case), the pressure was about 1.3 torr. If the 3 gram reservoir was held at 800°C and the 1 gram reservoir heated to 960°C, the cesium pressure increased only to about 2.3 torr. If the situation is reversed, however, and the 3 gram reservoir was increased to 950°C, the pressure increased to about 4.1 torr.

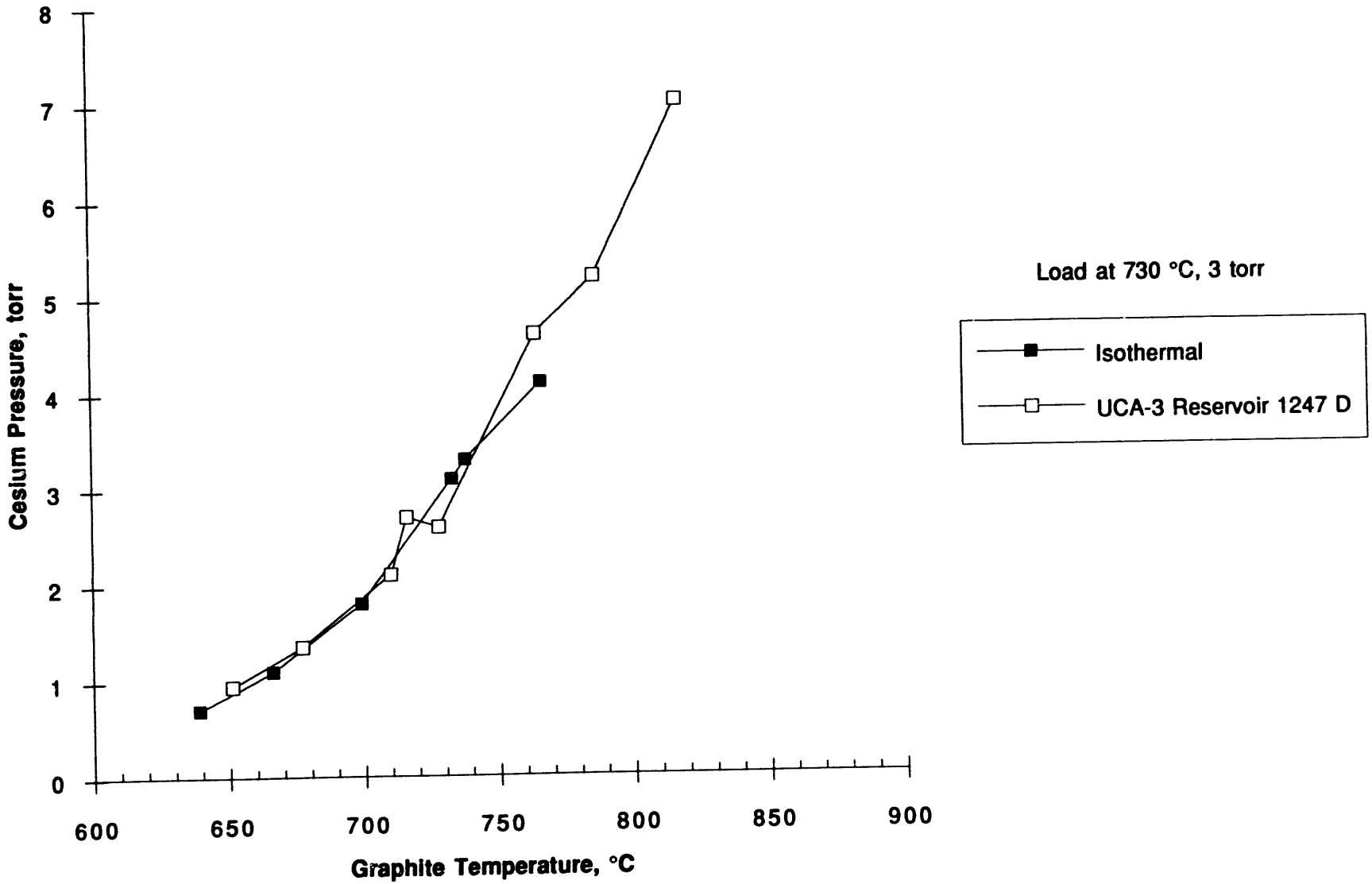

Figure 3-9. Isothermal Pressure vs UCA-3 Data

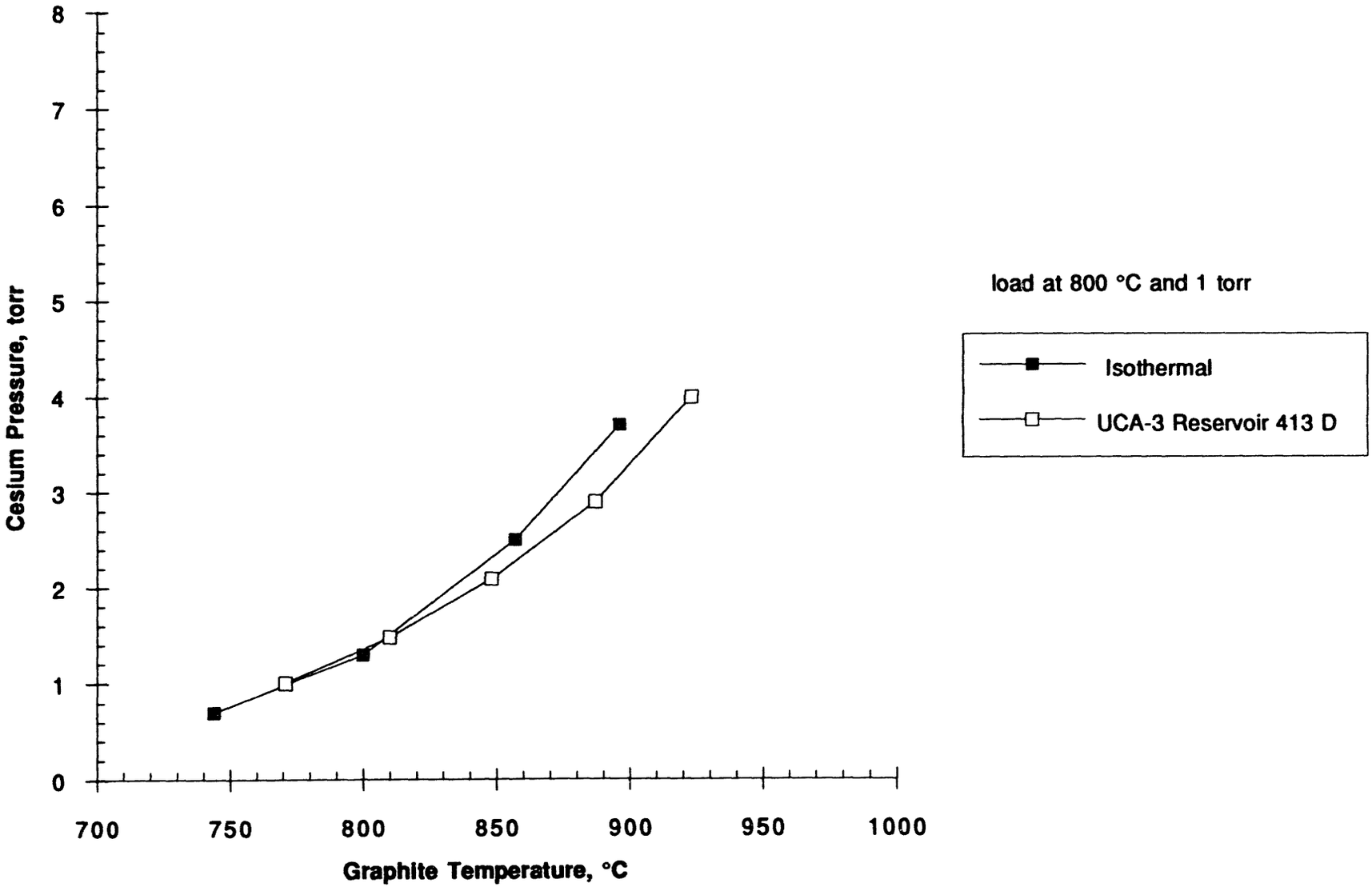

Figure 3-10. Isothermal Pressure vs UCA-3 Data

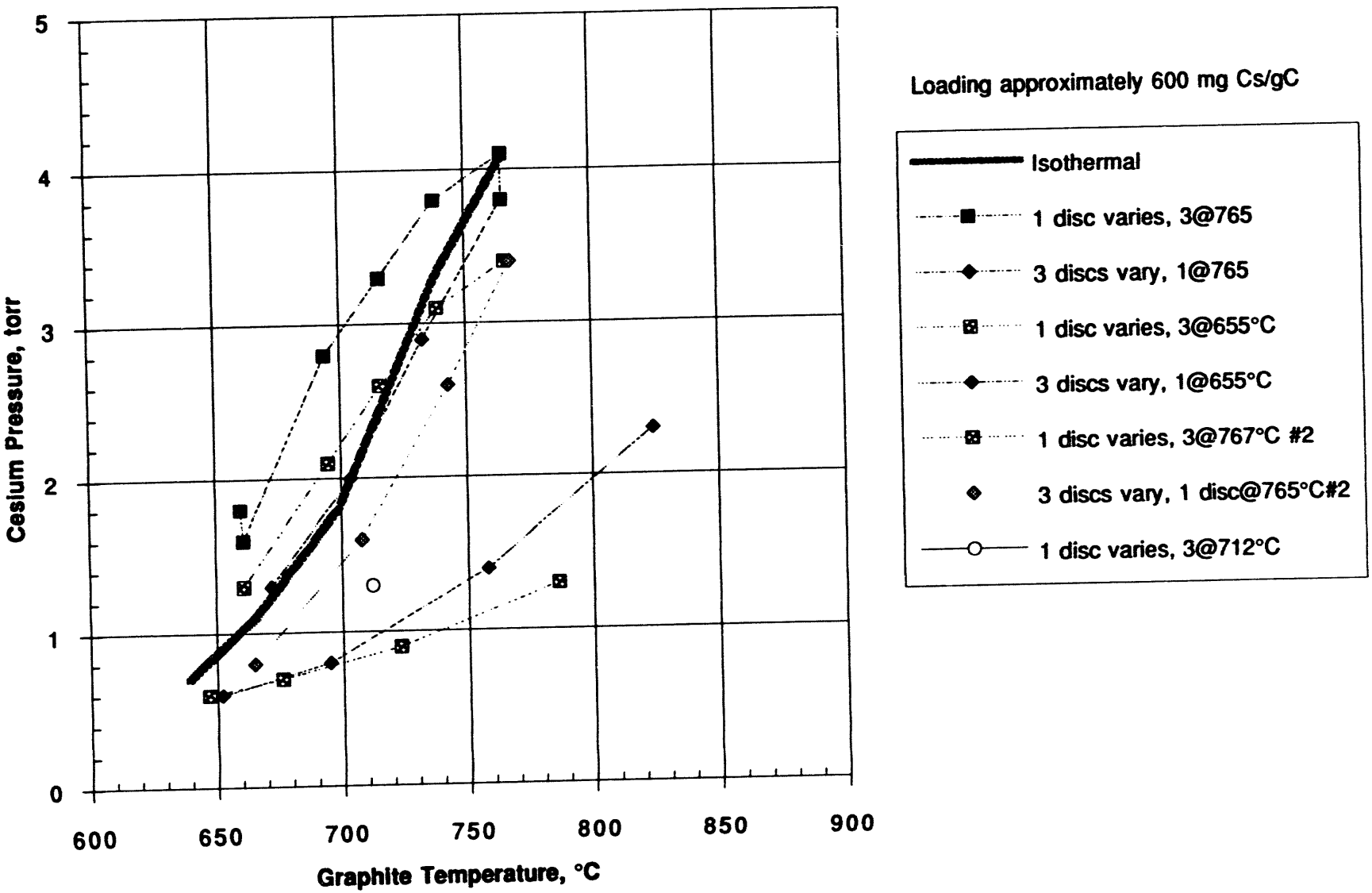

Figure 3-11. Cesium Pressure-Temperature Curves for Temperature Gradient Across Reservoir

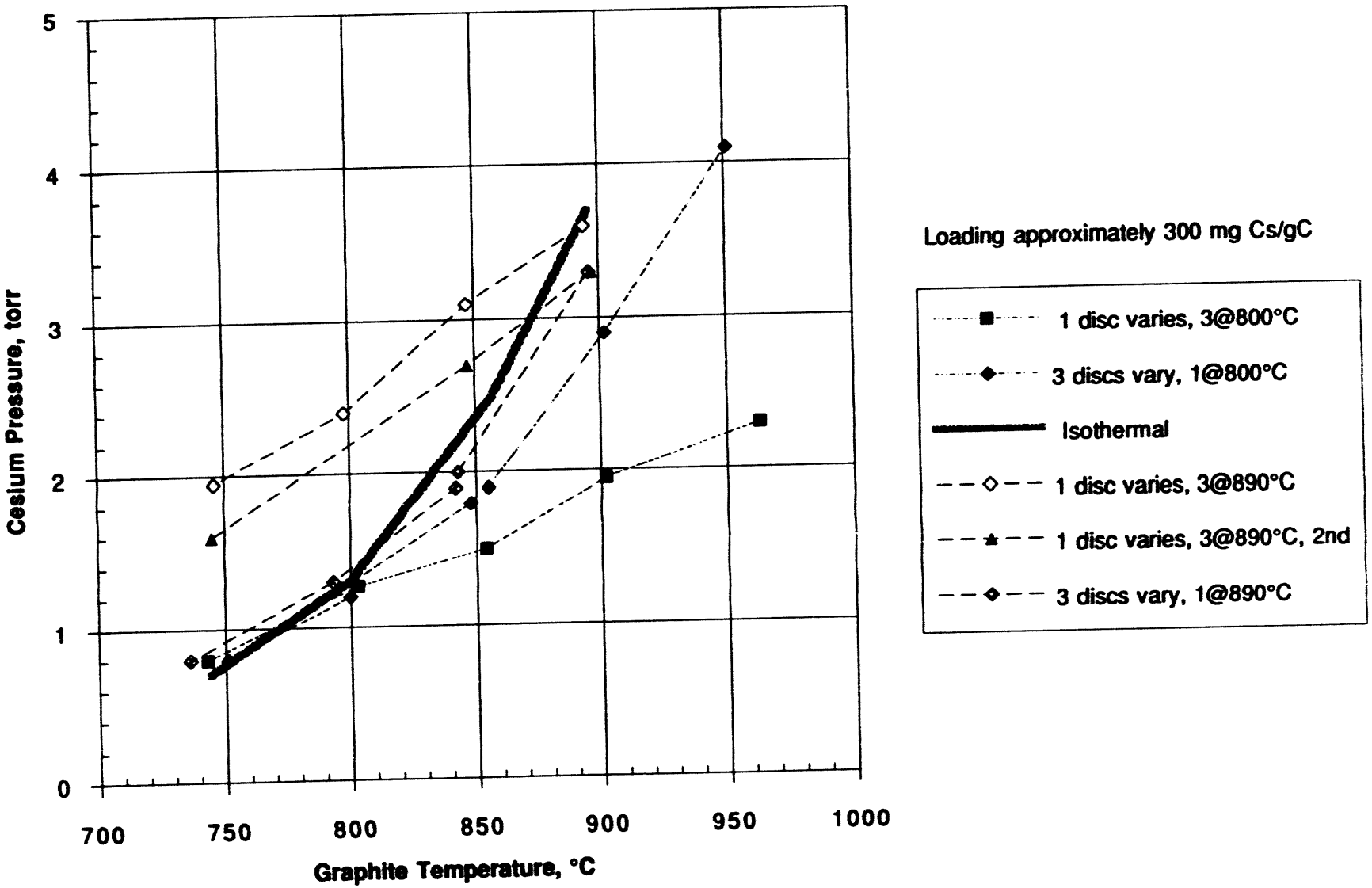

Figure 3-12. Cesium Pressure-Temperature Curves for Temperature Gradient Across Reservoir

When either reservoir was heated there was a transfer of cesium from the hot the cold reservoir. This transfer stopped only when each reservoir was in equilibrium with the new system pressure. Since the pressure-temperature response of Cs-graphite depended on the specific loading, not the absolute loading, and since the same amount of cesium left one reservoir and entered the other, the equilibrium pressure over the larger reservoir was less effected, and it dominated the system pressure.

3.3.3 Time Response Test Results

The temperature of the graphite in these tests must be inferred from the measured temperature of the niobium can depicted in Fig. 3-6. Since a knowledge of the instantaneous temperature of the graphite is crucial to these tests, a thermal model was developed to relate the graphite temperature to the can temperature. This model development was described in GA A21511, the Semiannual Progress Report for the Period Ending September 30, 1993 (see Section 1.5), and will not be repeated here.

The experimental data obtained for the two loadings, using the pins alone and the pins in the molybdenum barrel, are given in Figs. 3-13 for a loading of 300 mg Cs/gC and Fig. 3-14 for a loading of 600 mg Cs/gC. The data are also shown in a more intuitive format in Figs. 3-15 to 3-18. The model results in each figure account for the time lag in heating the graphite reservoir and assume that the cesium pressure changes instantly once the graphite changes temperature.

The temperature of the niobium can (the thermocouple reading) reached its final value within 10 to 30 seconds in the experiments, and this fact is included in the model calculations. The time constants that were observed in this study after the niobium can temperature was stabilized are summarized in Tables 3-5 and 3-6.

The data for a loading of 600 mg Cs/gC are shown for completeness only. When the data were taken, it was difficult to control the temperature of the test vehicle. Hence the experimental errors are believed to be relatively large.

Table 3-5

TIME CONSTANTS FOR GRAPHITE PINS ALONE

	Time Constant	
	High Loading	Low Leading
Model Calculation	43 sec	34 sec
Experimental Data	48 sec (est.)	57 sec

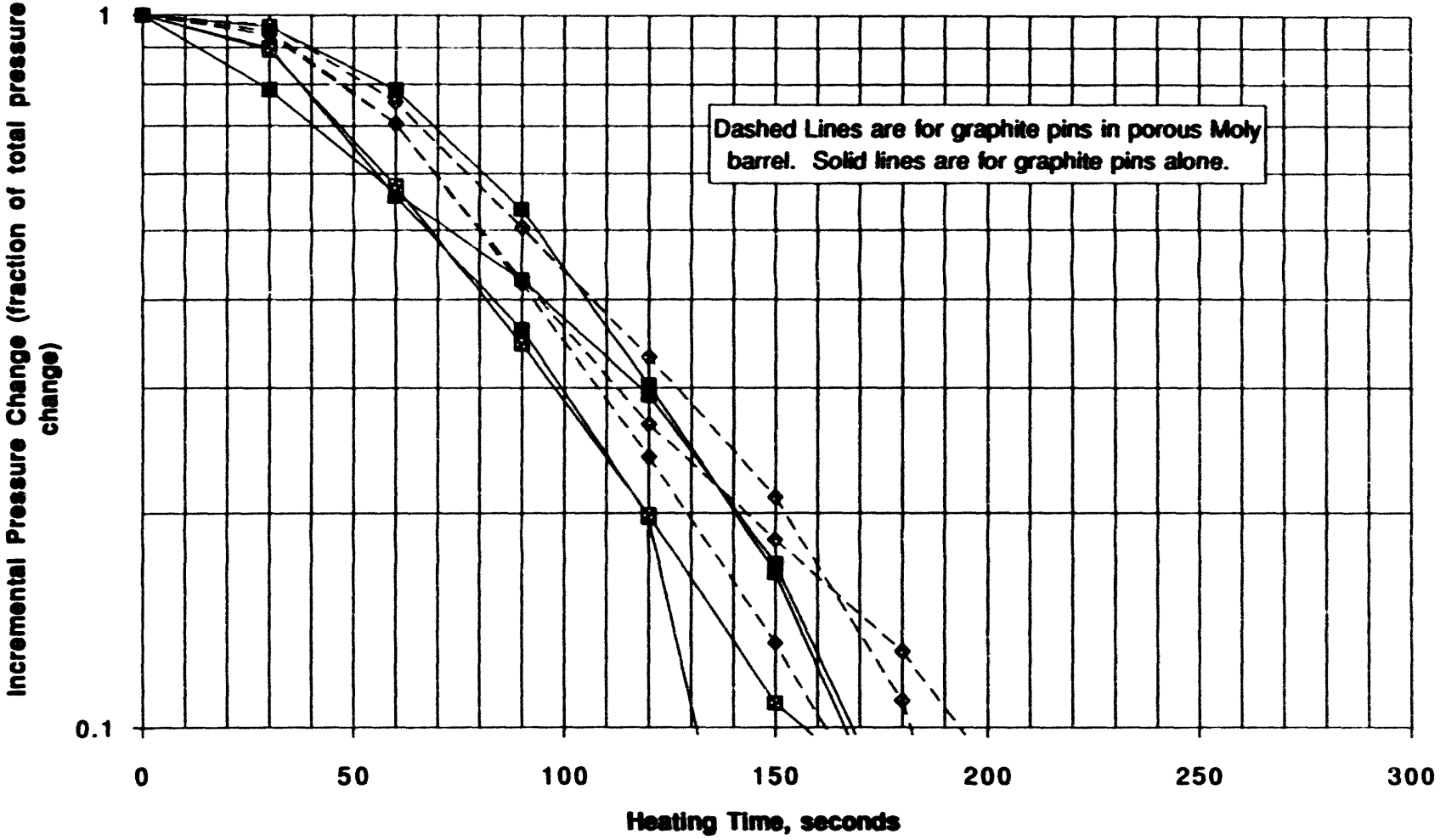

Figure 3-13. Incremental Cesium Pressure Change Upon Heating; Loading 300 mgCs/gC.

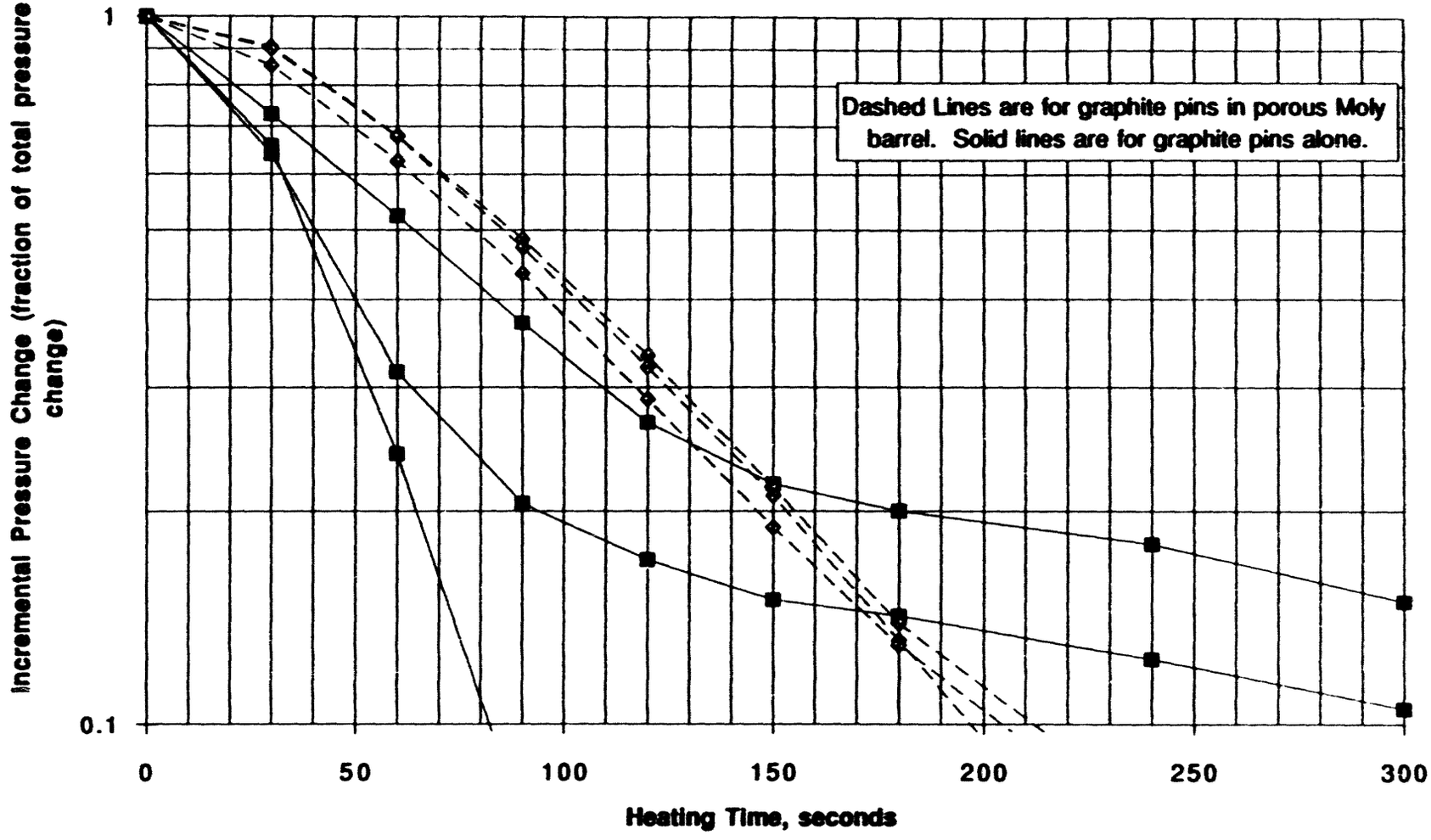

Figure 3-14. Incremental Cesium Pressure Change Upon Heating; Loading 600 mgCs/gC.

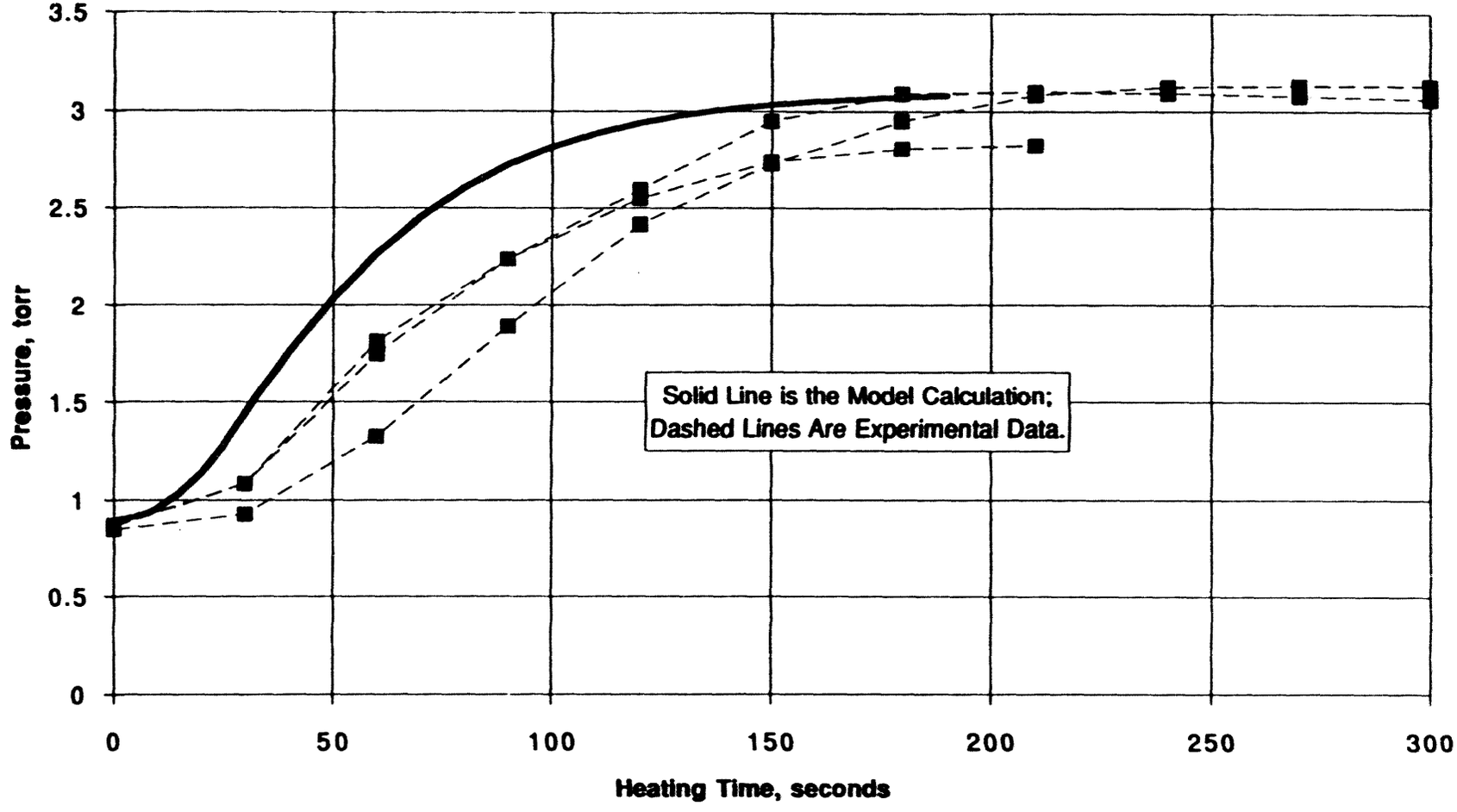

Figure 3-15. Response of Graphite Pins Alone; Loading 300 mg Cs/gC.

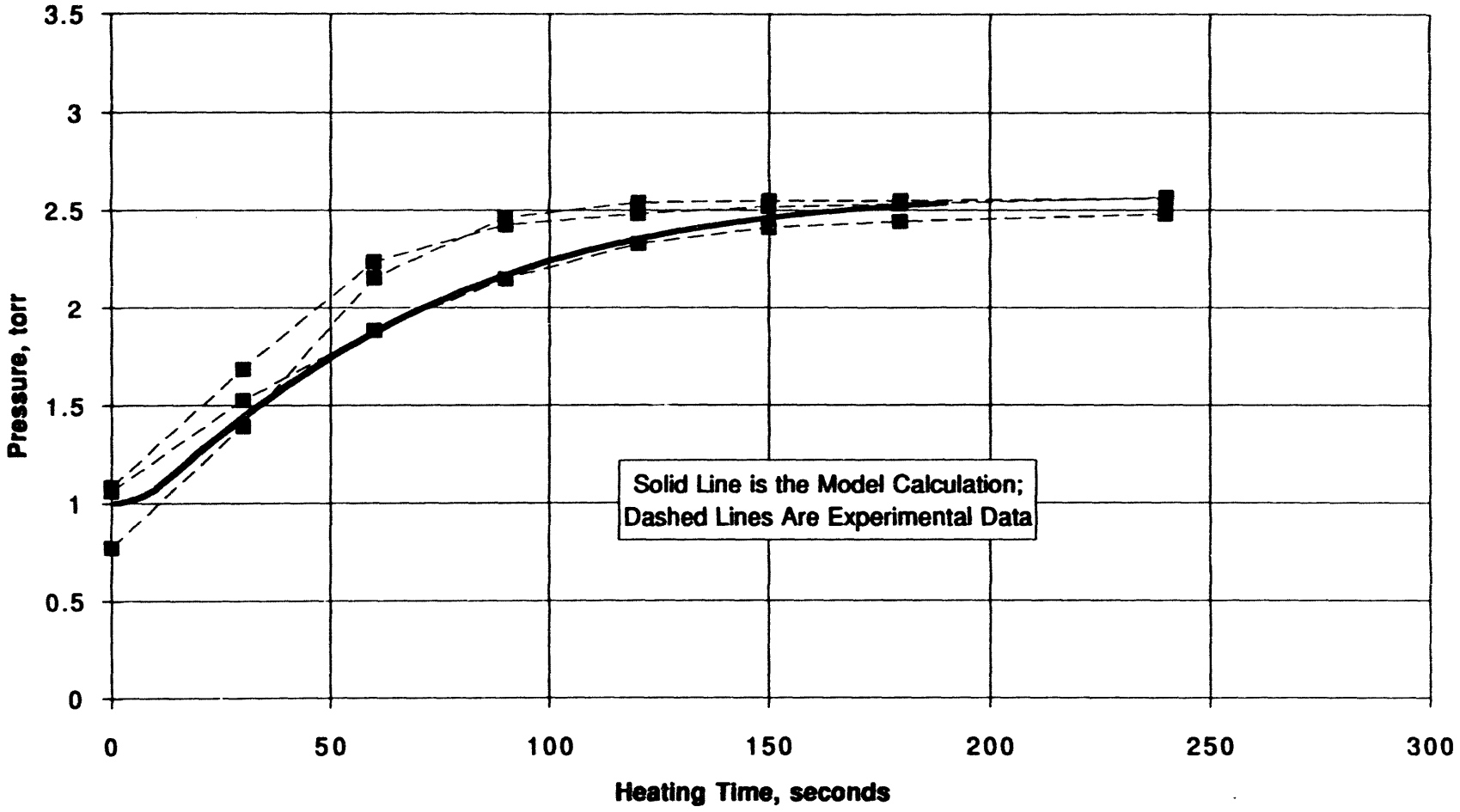

Figure 3-16. Response of Graphite Pins Alone; Loading 600 mg Cs/gC.

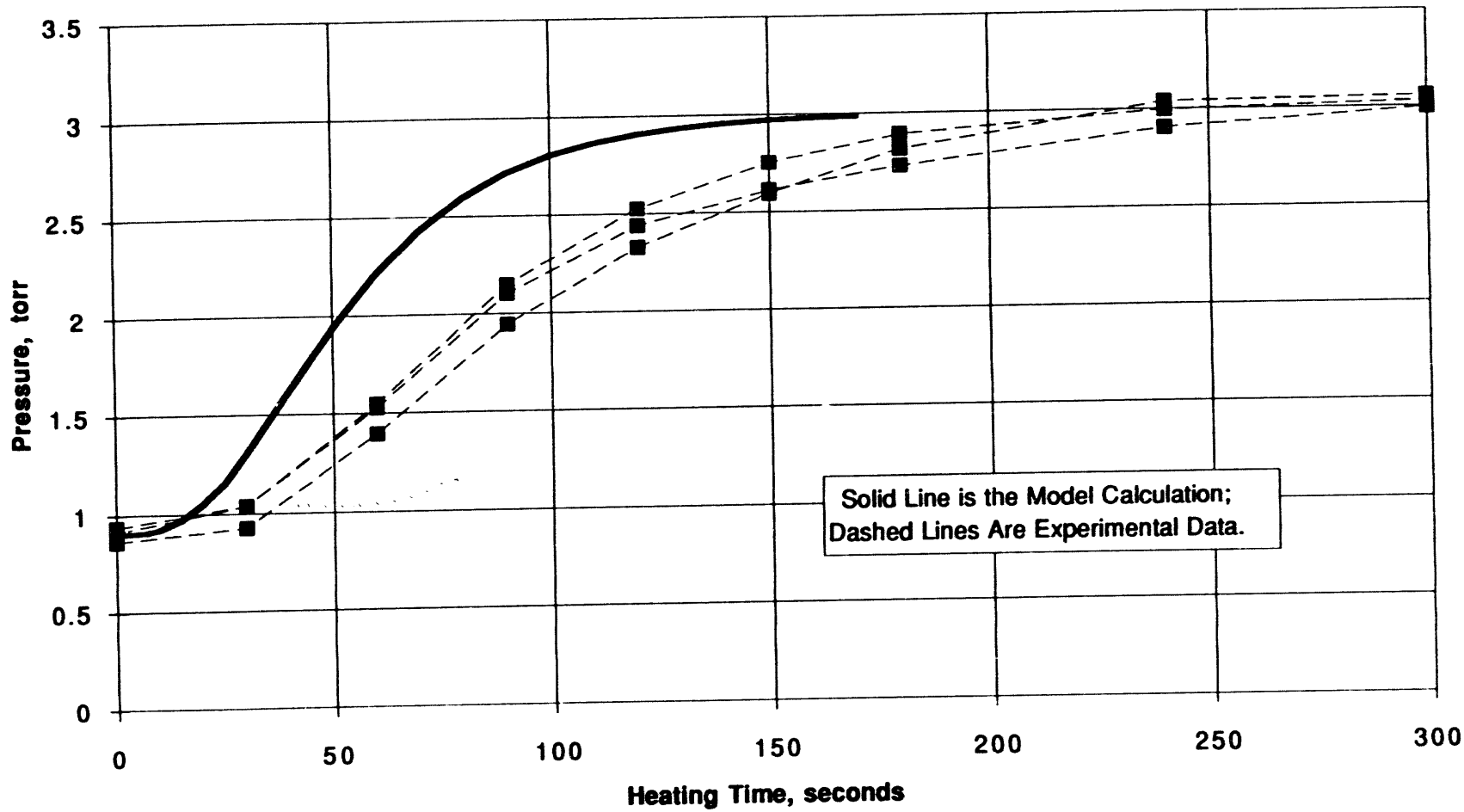

Figure 3-17. Response of Graphite Pins Inside Porous Molybdenum Housing Loading, 300 mg Cs/gC

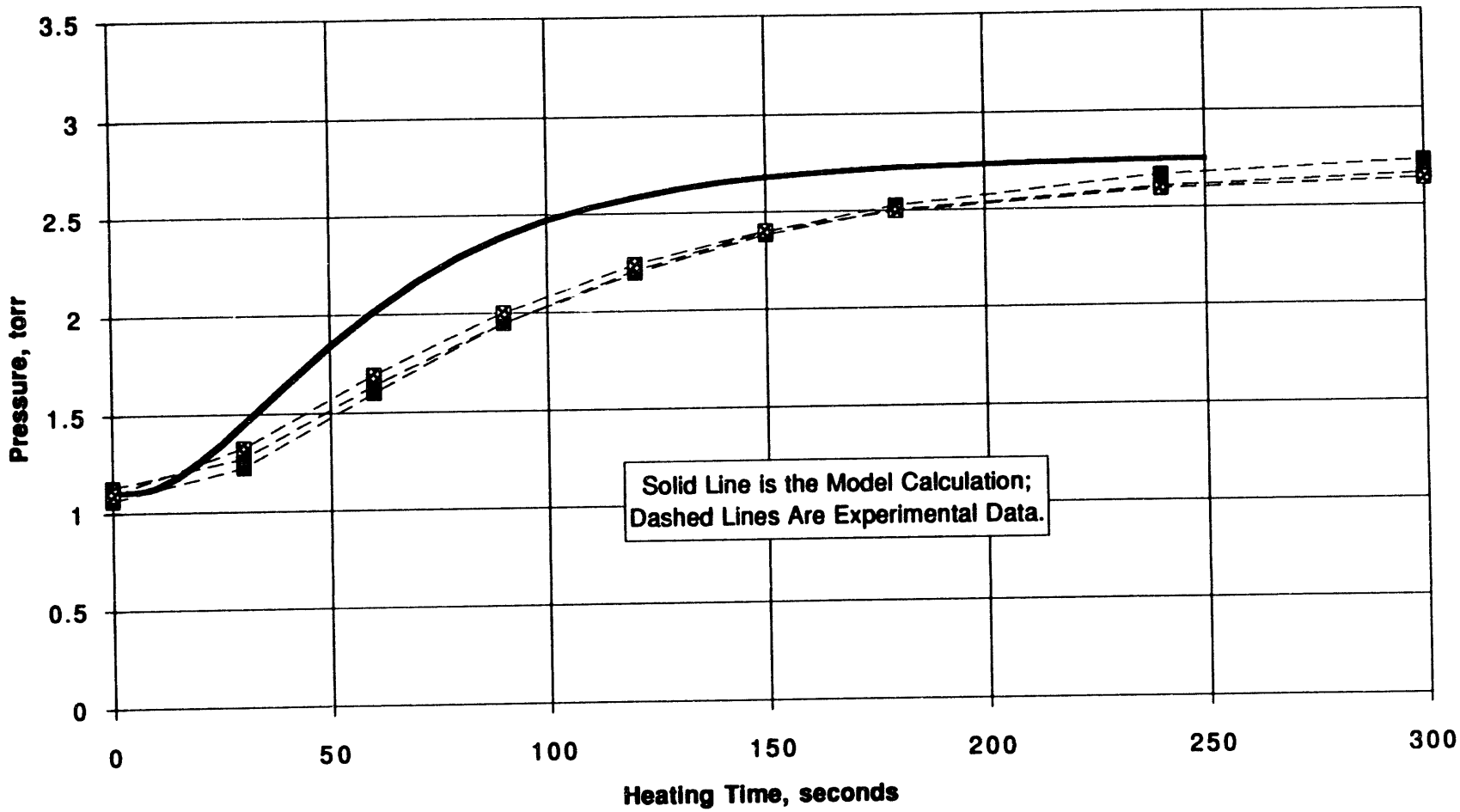

Figure 3-18. Response of Graphite Pins Inside Porous Molybdenum Housing Loading, 600 mg Cs/gC

Table 3-6

TIME CONSTANTS FOR GRAPHITE PINS IN MOLYBDENUM BARREL

	Time Constant	
	High Loading	Low Loading
Model Calculation	40 sec	28 sec
Experimental Data	69 sec	57 sec

For the graphite alone, the equilibration of the cesium pressure to a change in graphite temperature was characterized by an experimental time constant that was more than 20 seconds longer than that calculated for an instantaneous response. For the graphite pins located in the porous molybdenum, the time constant was nearly 30 seconds longer. This difference is probably not due to inadequacies in the model since most reasonable improvements to the model, e.g., inclusion of point-contact conduction, would cause the model to equilibrate faster and therefore broaden the gap between calculation and experiment. Therefore the additional time lag in the experimental results must be attributed to the Cs-graphite compound and permeation through the porous molybdenum.

It is instructive to estimate the amount of cesium in the gas phase in these tests, and to compare it with the amount of cesium in the near-surface region of the Cs-graphite compound. For a volume of 273 cm^3, and a temperature of about 600 K (the temperature of the cesium manifold), the perfect gas law says that 1.3×10^{19} Cs atoms are present in the vapor phase at 3 torr. The POCO graphite used in these tests has a density of 1.7 g/cm^3. For $C_{36}Cs$, the cesium atom density in the graphite is 2.2×10^{21} atoms per cm^3. The geometrical surface area is 4.8 cm^2, so at a pressure of 3 torr, the volume of the test manifold contains an amount of cesium equivalent to that found within the first 12 μm from the surface of the graphite pins. Since chemical equilibrium within the graphite will prevent total cesium depopulation of any region, a depth of much greater than 12 μm must be involved. The particle size in the ultra fine POCO grpahites is in the vicinity of 5 μm or less, therefore diffusion (permeation) of Cs in the open porosity of the graphite must be playing a role.

To estimate the magnitude of the effect of cesium transport in the open porosity of the graphite pins, consider a one dimensional slab of thickness d=.16 cm, the radius of the pins. The time constant in this simple geometry is given by $\tau = d^2/\pi K$, where K is the permeation coefficient. For Xe, which has nearly the same size and atomic radius as Cs, in a porous graphite a value of $K = 3 \times 10^{-3}$ cm^2/sec has been reported (Ref. 3-1). The resultant value of the time constant is $\tau = 2.7$ seconds, nearly an order of magnitude smaller than the observed time delay. This may be due in part to the difference between the present POCO graphite and the Morgan EY9-166 graphite used by Weller and Watts in Ref. 3-1.

The observed time constant when the pins are located within the porous Mo barrel is 5 to 10 seconds longer than the time constant for the pins alone, and probably due to permeation time through the walls of the barrel. The design of the barrel, shown in Fig. 3-3, provides a wall thickness of 20 mils throughout the length of the pins. The rapid response of the reservoir enclosure is due to this short permeation length.

Some degree of mitigation of the problem of the time response of the Cs-graphite reservoir, including that due to the thermal coupling, was anticipated from the cesium adsorbed in the porous molybdenum material. Since the thermal coupling of the reservoir housing, or an auxiliary porous Mo reservoir, can be made much tighter than the thermal coupling to the graphite, the limited amount of cesium adsorbed on the former material would be injected into the gas phase much more rapidly, providing electron cooling while the Cs-graphite was equilibrating. This effect was not observed in these experiments, nor could it be expected, given the volume of the Cs manifold and the volume of the porous Mo used.

To quantify this assertion, it is necessary to solve the gas law equation and satisfy the adsorption isotherms for Cs on Mo simultaneously. The gas law may be written

$$P_{Cs} = 760(N^{o}_{Cs} - A_{Mo}\Theta_{Mo}\sigma_{Cs})\frac{RT_{volume}}{VN_{o}} \text{ (torr)}$$

where N^{o}_{Cs} is the total amount of cesium in the system, A_{Mo} is the surface area of the Mo, Θ_{Mo} is the surface coverage of the Mo, σ_{Cs} is the coverage at one monolayer (5×10^{14} atoms per cm^2), R=82 cm^3-atm/mole-K, and $N_o=6.02\times10^{23}$ atoms/mole. The second term in the parentheses is the amount of cesium adsorbed on the molybdenum. The difference between that term and the first term is simply the amount of cesium in the gas phase. The adsorption isotherms for Cs on Mo are approximated by those for W, given by Langmuir (Ref. 3-2), in the graphical form $P_{Cs}=f(T_{Mo}, \Theta_{Mo})$.

If the value of N^{o}_{Cs} is adjusted to yield a pressure of 1 torr at 1100 K, (and the molybdenum is assumed to have a specific surface area of 1 m^2/g), then the equilibration pressure at 1200 K is 1.2 torr, neglecting the influence of the graphite. This small increase in pressure would not have been noticed in the present experimental setup. If, on the other hand, the gas phase volume had been reduced to 1 cm^3, the same numerical manipulations result in an equilibration pressure at 1200 K of 3.5 torr.

Measurements were also undertaken in other geometries to assess the performance of porous tungsten (Ref. 3-3) in a well defined geometry. The test fixture is shown in Fig. 3-4. The graphite sample was completely isolated from the cesium manifold by a porous plug 0.25 in. in diameter and 0.25 in. long, weighing 1.802 g. A second can held an identical specimen of the porous material for ancillary testing. Each can was independently heated, and its temperature monitored by a separate thermocouple. The graphite sample was a short cylinder, 0.322 in. high and 0.425 in. in diameter and weighed 1.199 g. The pressure response in the cesium manifold after an increase in temperature of the can containing the graphite is shown in

Fig. 3-19. The temperature increase from 800°C to 900°C took about 1.5 minutes, as exemplified by the initial concave-upward part of the curve. The data displays an exponential behavior, with a time constant of 14 minutes. This is attributed to the porous plug.

The conductance of this material should scale with size according to the ratio of the cross-sectional area to the length of the plug, since the conductance of a given pore is inversely proportional to its length and conductances in parallel combine additively. Therefore

$$\tau_{porosity} \approx \frac{V_{porosity}}{\frac{0.75}{14x60} x \frac{A_{porosity}}{.317} x \frac{.635}{d_{porosity}}} \approx 560 V_{porosity} (\frac{d_{porosity}}{A_{porosity}}) \quad \text{(seconds)}$$

when d, A and V are given in cm, cm^2 and cm^3 respectively. To compare this result with that of the previous section, it is necessary to estimate the corresponding dimensions. The length is about 0.020 in. which is the thickness of the wall opposite each pin, or $d_{porosity} \approx 0.051$ cm. The appropriate area is area of this portion of the wall, or about 0.1 in. x 0.375 in., yielding $A_{porosity} \approx 1.21$ cm^2. The volume between the pin and the wall of the cavity in the barrel is $V \approx 0.065$ cm^3. The result is

$$\tau_{porosity}^{barrel} \approx 560(0.065)\frac{0.051}{1.21} = 1.53 \quad \text{(seconds)}$$

This does not compare too well with the observed value of 5 to 10 sec estimated from the data in the last section, but the expression provides a useful way to estimate the time constant of these (46% porous) materials.

The intercalation and deintercalation of the graphite in these measurements was a very slow process. Equilibrium was "declared" if the pressure in the cesium manifold did not change when the valve to the liquid reservoir was closed. During intercalation, the liquid reservoir was at a temperature corresponding to a pressure in the range of 1 to 3 torr. For deintercalation, it was near room temperature so as to condense the cesium expelled by the graphite. The behavior of the manifold pressure during deintercalation is given in Fig. 3-20. At periodic times during deintercalation, the valve to the liquid reservoir was closed and the resulting cesium pressure observed as a new equilibrium pressure was reached by the cesium remaining in the graphite reservoir.

Before the valve to the liquid reservoir is closed, the pressure in the manifold is essentially zero in all cases, as required by the low temperature of the liquid. When the valve is closed, the pressure rises slowly as the graphite expels cesium until it is once again at equilibrium at its new value of Cs loading. After only one minute of deintercalation, the pressure rises to its original value of 3 torr after a period of time. By contrast, the pressure only rises to about 0.6 torr after 17 hours of deintercalation. Only after about 100 hours of deintercalation did the pressure remain at zero torr when the valve was closed.

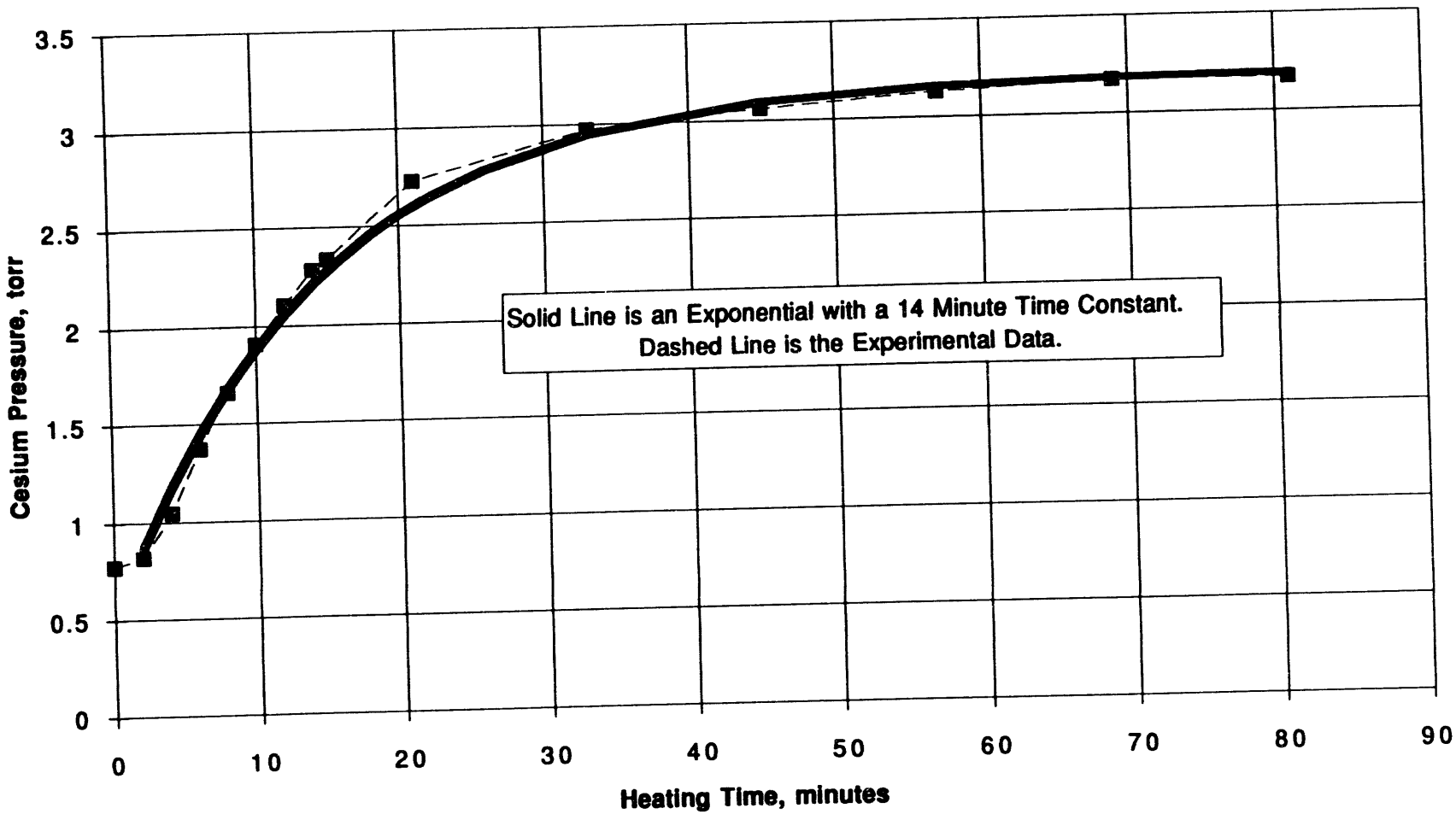

Figure 3-19. Response of Graphite Cylinder Behind Porous Molybdenum Plug Loading, 300 mg Cs/gC

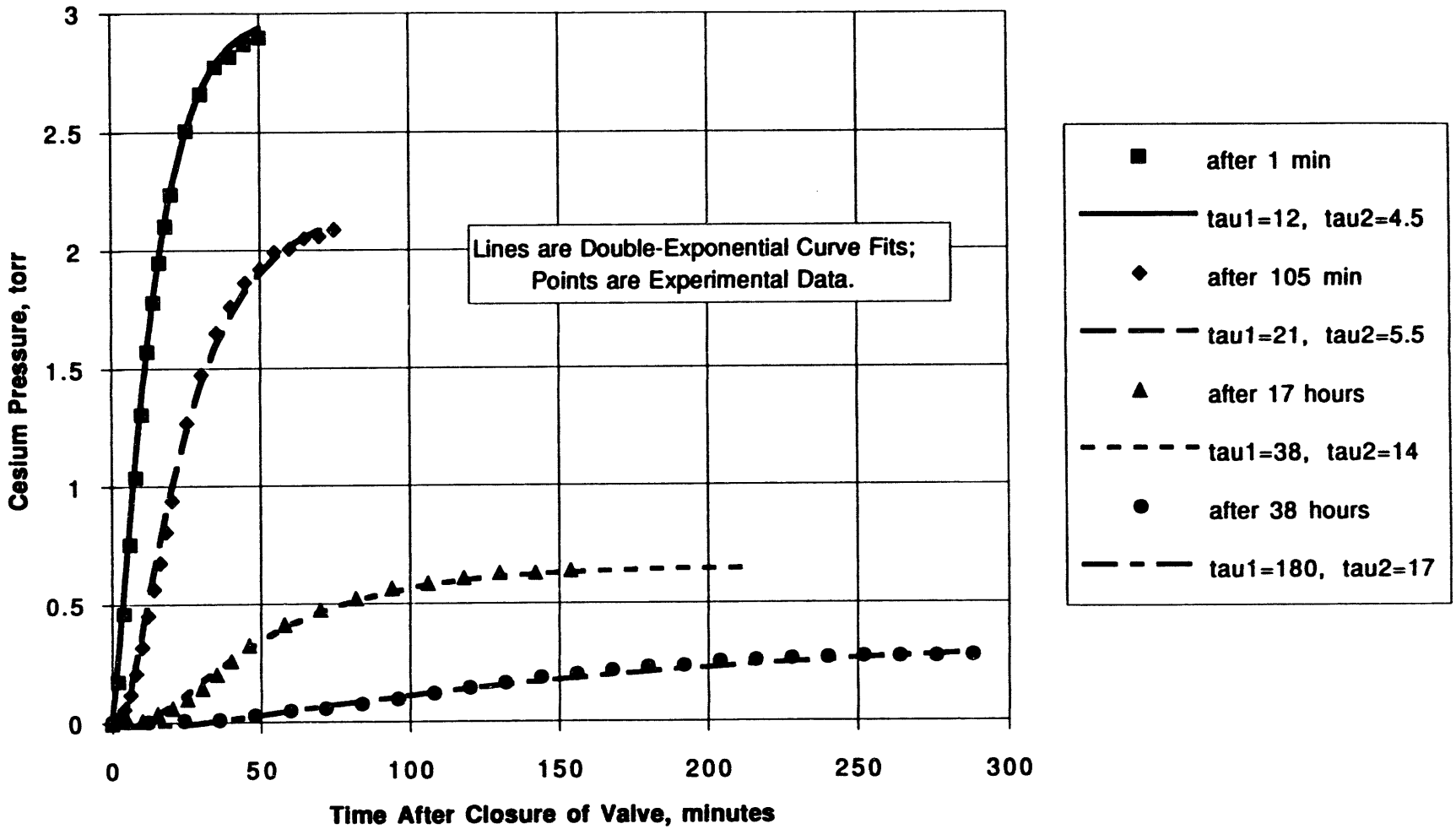

Figure 3-20. Pressure Transients During De-Intercalation

The time to reach steady-state after the valve closing grew larger as the deintercalation time increased. In general, the pressure behavior was characterized by two time constants, as indicated by the values of τ given in the legend of Fig. 3-20. The longer of the two time constants at each interval is to be associated with the porosity of the W plug, while the shorter time constant is associated with the porosity in the graphite cylinder. As the steady-state pressure decreases, these time constants increase. The time constants are inversely proportional to the corresponding conductances, and the inverse τ is plotted versus steady-state pressure in Fig. 3-21. For both the porosus W (tau 1) and the graphite (tau 2), there is a quasi-linear dependence of τ^{-1} upon pressure that suggests viscous flow in both media.

If the flow is viscous, the Knudsen number (ratio of the mean free path to a characteristic dimension of the flow geometry) should be ≤ 0.01. In the case of the porous W, the pore diameter, as measured with a traveling microscope, ranges from 100 to 300 μm (0.1 to 0.3 mm). At 1000 K and 3 torr, the mean free path of Cs is about 3×10^{-3} cm, whether calculated from the total collision cross section of 110Å (Ref. 3-4) or taken to be equal to that for Xe (Ref. 3-5). Thus the Knudsen number, based on the pore diameter, is 0.15, in the middle of the range for transition flow ($0.01 < K_n < 1.0$). While this result does not confirm viscous flow, it clearly shows that free-molecule flow (and, therefore, constant conductance) is not occurring in the porous W. It should be noted here that the pore diameter of the porous Mo described in the previous section, though it has about the same net porosity, is in the range from 20 to 30 μm, much lower than the 100 to 300μm of the porous W. The flow through that material, therefore, should nearly free-molecular and the conductance may not be pressure dependent. In the case of the graphite (tau 2) all that may be said from the data is that it behaves as if viscous flow were occurring.

4. IN-REACTOR TEST REPORT

4.1 In-Reactor Test Article Description

The same test article employed in the preirradiation testing and characterization (Fig. 3-1) was used for the in-reactor tests. It was double encapsulated before insertion in-core. Each Nb can was sealed in a stainless steel canister which was backfilled with a He/Ar mixture for thermal control. Several such SS canisters were loaded into a common SS capsule which, in turn, was backfilled with pure helium. This capsule was in contact with the core Na coolant fluid of the FFTF or EBR-II test reactors.

4.2 In-Reactor Test Procedure

Table 3-7 lists the irradiation temperature and accumulated fluence for each of the reservoir test articles in the in-reactor test. The temperatures were calculated with a two-dimensional heat transfer code, using the nuclear heating rates determined for the reactor utilized (FFTF or EBR-II). The fluences were similarly determined from the flux profiles. Neither temperature nor fluence were measured directly.

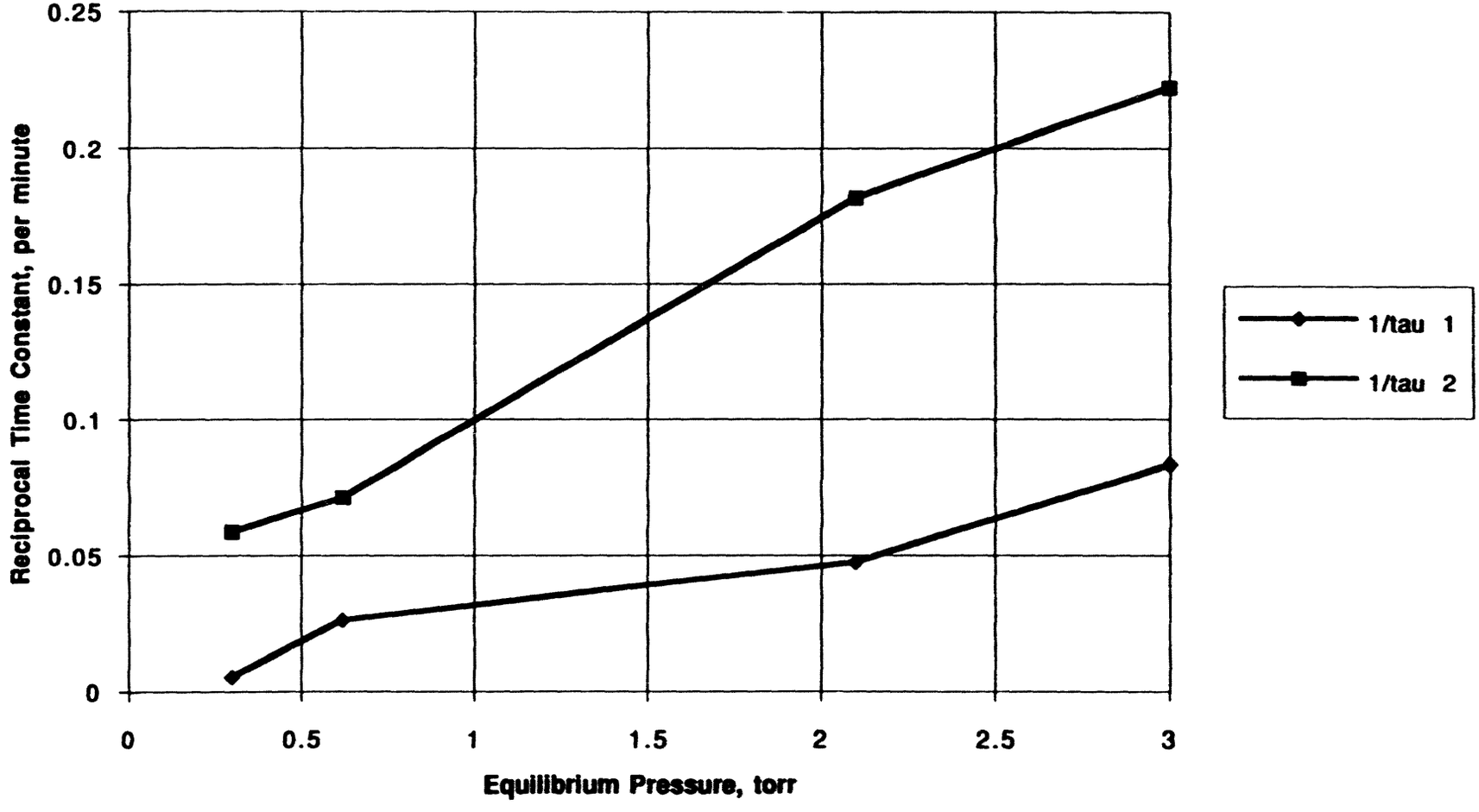

Figure 3-21. Pressure Dependence of Apparent Time Constants Observed During De-Intercalation

Table 3-7

IN-REACTOR TEST PARAMETERS

Identification Number	EBR-II (FFTF) Test Designation	Irradiation Temperature, K	Accumulated Fluence, n/cm^2
A	UCA-1	1157	2.8×10^{22}
B	UCA-1	1147	2.8×10^{22}
C	UCA-1	1217	2.8×10^{22}
D	UCA-1	1171	2.8×10^{22}
E	UCA-1	1142	2.8×10^{22}
197A	UCA-2	1359	3.2×10^{22}
199D	UCA-2	1308	3.2×10^{22}
929D	UFAC-3	1250	3×10^{22}
930D	UFAC-3	1250	3×10^{22}
960D	UFAC-3	1250	3×10^{22}
961A	UFAC-3	1250	0.9×10^{22}
962A	UFAC-3	1250	0.9×10^{22}
413D	UCA-3	1087	1.5×10^{22}
1247D	UCA-3	967	1.3×10^{22}
1300D	UCA-3	1087	1.5×10^{22}
1301D	UCA-3	1033	1.4×10^{22}

At the conclusion of the in-core irradiation, the test articles were examined with neutron radiography, and removed to a hot cell for further study.

4.3 In-Reactor Test Results: Post Irradiation Examination (PIE)

4.3.1 Cesium Meter

The principal objective of the PIE was to determine the pressure-temperature relationship of the graphite-cesium reservoir after irradiation and to compare it to the before-irradiation curve. The concern was that fast neutron damage to the graphite might significantly change the crystal structure of the graphite and change the pressure-temperature relationship. This could significantly affect the projected lifetime and performance of the thermionic system.

The device used to determine the pressure-temperature relationship in the WHC hot cell was a cesium meter, designed and built by ThermoTrex Corporation. This device is described in Appendix B.

4.3.2 UCA-1 PIE

At the end of the irradiation in FFTF, neutron radiographs of the subcapsules were obtained. After an ex-reactor cooldown period, the reservoir specimens were visually examined in the Hot Cell facility at WHC. Test articles A, C, and D, i.e., the three that contained HOPG, were ruptured at some stage in the irradiation. Test articles B and E contained only PC-113 porous carbon, and they appeared intact.

Neutron induced swelling was discounted as a contributory cause for the rupture of the test articles containing HOPG, since existing data precluded the swelling that would be required to produce the observed effect. However later data in UFAC-3 showed that, for Cs-loaded HOPG, c-axis swelling of 400 to 600% could occur. This fact is most certainly the reason the UCA-1 (and one UCA-2 HOPG sample, as will be mentioned below) samples were ruptured.

One of the PC-113 samples was examined for Cs, using the cesium meter described in Section 4.3.1. No Cs was observed. Apparently, a leak occurred during initial degassing, and the cesium was pumped out before the test began.

An extensive discussion of the UCA-1 PIE is presented in Ref. 4-1.

4.3.3 UCA-2 PIE

Sample 197A containing HOPG was ruptured during the irradiation due to the neutron induced swelling of the intercalation compound. Sample 199D containing POCO was intact, and was installed in a cesium meter and the vapor pressure of Cs vs temperature was determined. The data are given in Appendix C, Fig. C-1. The postirradiation Cs pressure exceeded the preirradiation Cs pressure by about 1 torr at 1087 K, and increased as the temperature increased to about 4 torr at 1163 K. The significance of this will be discussed later.

4.3.4 UFAC-3 PIE

Test article 962A, an HOPG sample, was removed from the reactor after a fluence of 0.9×10^{22}nvt, because neutron radiography showed that it had undergone extraordinary c-axis expansion. This peculiar behavior was examined and explained in terms of the island-like structure of the Cs-graphite intercalation compounds. The cesium vapor pressure was also measured, and was found to be nearly an order to magnitude lower than the preirradiation value. This is shown in Fig. C-2.

The two POCO samples, 929D and 960D, were irradiated to a fluence of 3×10^{22}nvt. Neutron radiography showed that there was no appreciable structural difference in the samples resulting from the irradiation. They were installed in cesium meters to measure the Cs vapor pressure. The results are shown in Appendix C, Fig. C-3. There was not substantial change after irradiation, unlike the HOPG sample.

4.3.5 UCA-3 PIE

Only neutron radiography has been done on these samples. There were no structural changes in the samples due to irradiation.

5. CESIUM RESERVOIR MODEL DEVELOPMENT

The dependence of the cesium pressure upon the temperature and specific loading (L) of the graphite can be described by:

$$P = P_2 + (P_1 - P_2) \exp(-t/\tau)$$

where $P_1 = P_0 \exp(-T_0/T_1)$, and P_0 and T_0 are functions of the specific loading. There is an equilibrium time τ associated with the change in pressure from P_1 to P_2 following a change of temperature from T_1 to T_2, that depends on the surface-to-volume ratio of the graphite, and the porosity of any housing material. There isn't sufficient data to quantify τ over a broad range, but in Section 3.3.3 it was shown that it is no more than about 30 seconds for high surface-to-volume, and can be as large as 15 minutes for low surface-to-volume reservoirs, with concurrent low pressure.

Values of P_0 and T_0 were determined for each of the preirradiation samples listed in Table 3-2, with the exception of UCA-1. The values are given in the empirical formulas shown in the figures of Appendix A. These values, plotted in Fig. 3-22, were employed to synthesize the cesium pressure as a function of loading and temperature shown in Fig. 3-23. Data taken in the 1968 thermionics program is also shown on Fig. 3-23. The staging of the intercalation compounds isn't obvious in the synthesized data due to the lack of data points. Figure 3-24 shows an isotherm obtained in this program at 1010 K, as well as synthesized data at the same temperature. The isotherm displays staging. The synthesized data agree best with the isothermal data taken on decreasing pressure (desorption).

The discrepancy between the isothermal data and the synthesized data in Fig. 3-24 is worst at low pressure. While there is no completely satisfactory explanation for this, it seems likely that it is associated with the time required for the graphite to absorb the cesium. The time between data points for the isothermal data of Fig. 3-24 was typically about 20 minutes. At high pressures, this would be adequate to reach steady state. However at low pressure, subsequent data suggests that the equilibration time could have been 3 to 5 times longer. This would have the effect of moving all low-pressure data points for the isothermal case to the right, more in agreement with the synthesized data.

The loading of the preirradiation samples at pinchoff is known, and shown in Appendix A. As long as the volume of the test system is small enough to require cesium atoms from only the near surface region of the graphite, the equilibration time for the isosteric data is much faster. Thus, the preirradiation data is valid, even though the time between data points is only

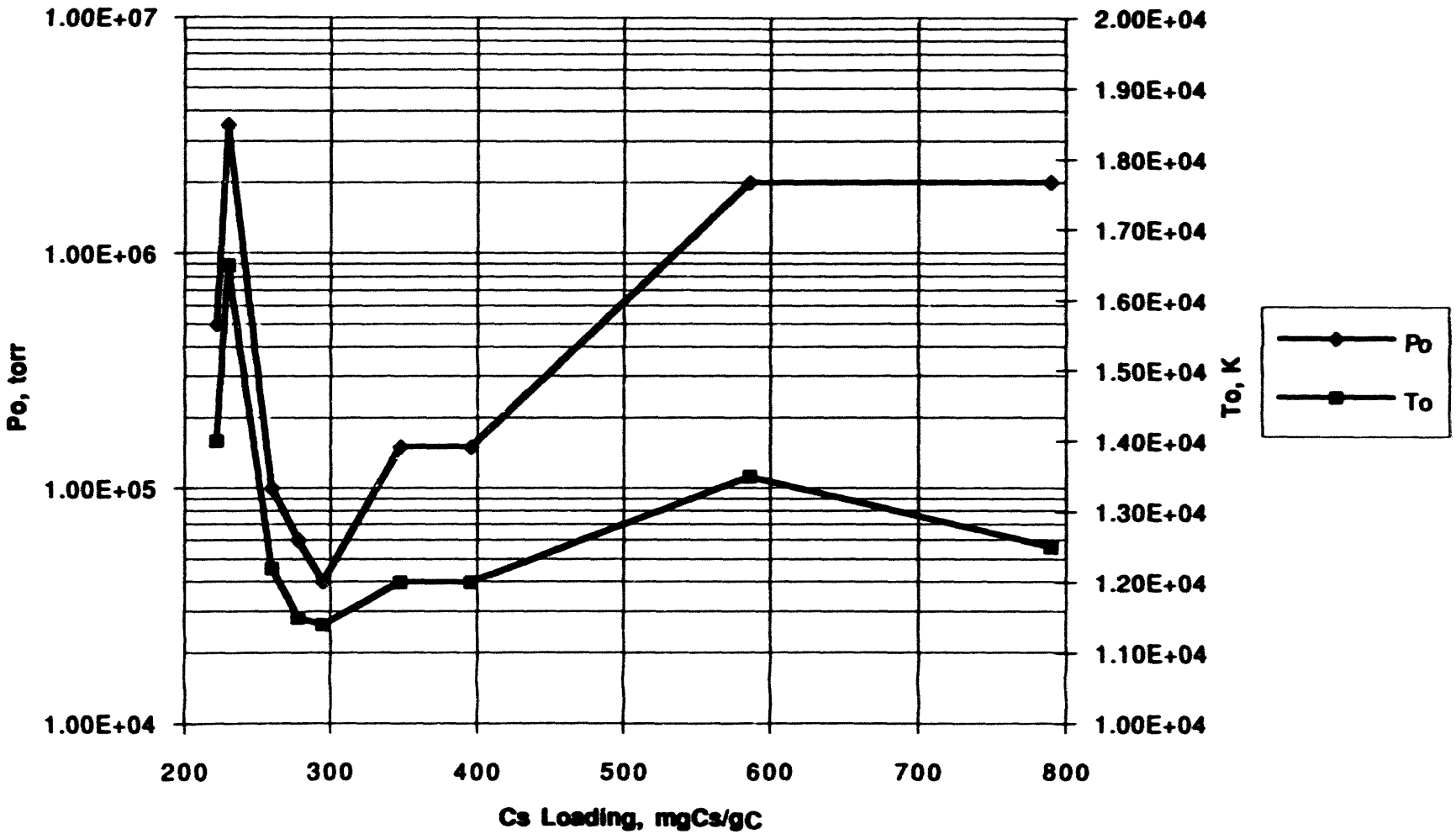

Figure 3-22. Analytical Fit Parameters

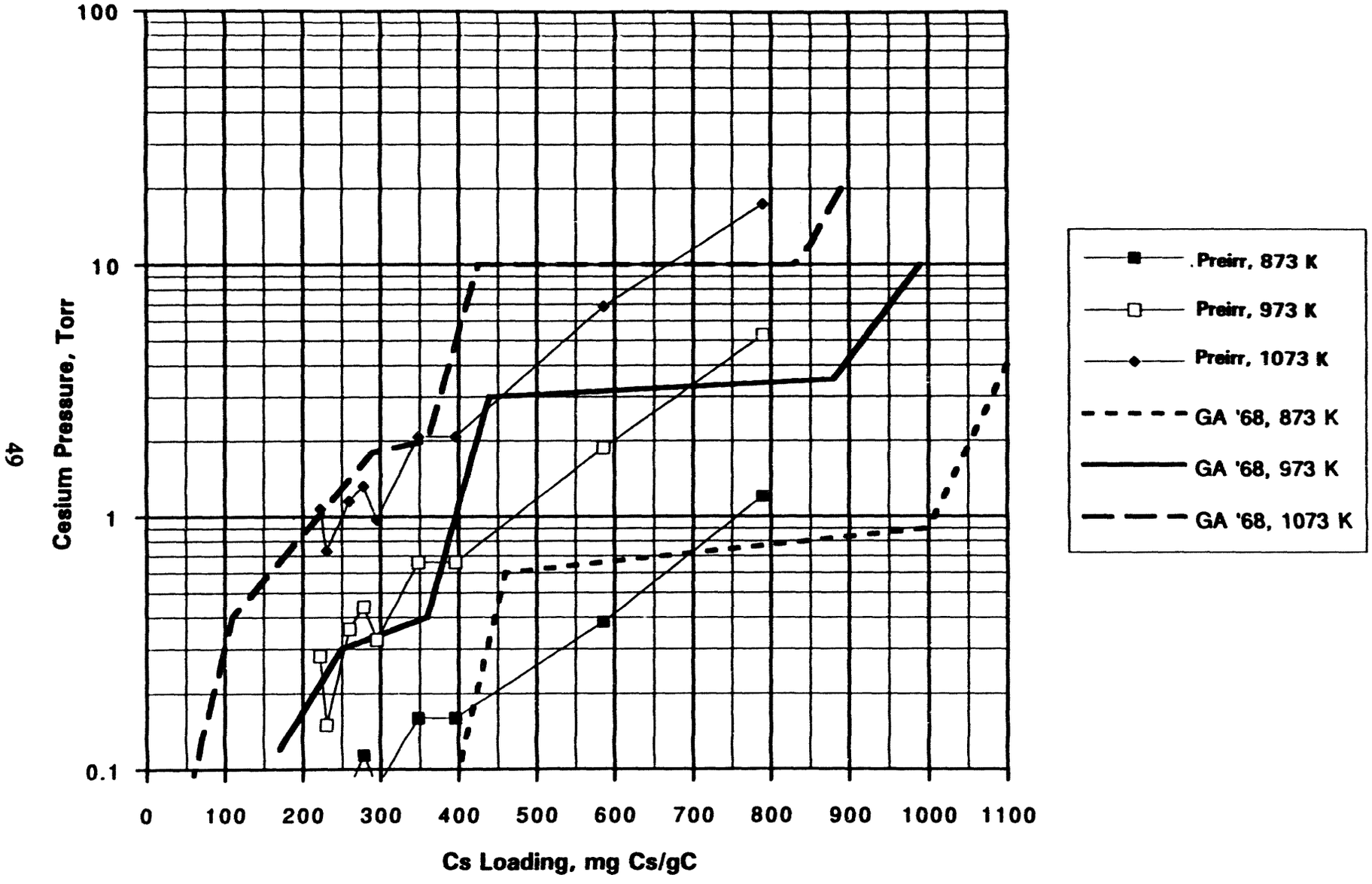

Figure 3-23. Cesium Pressure vs Loading

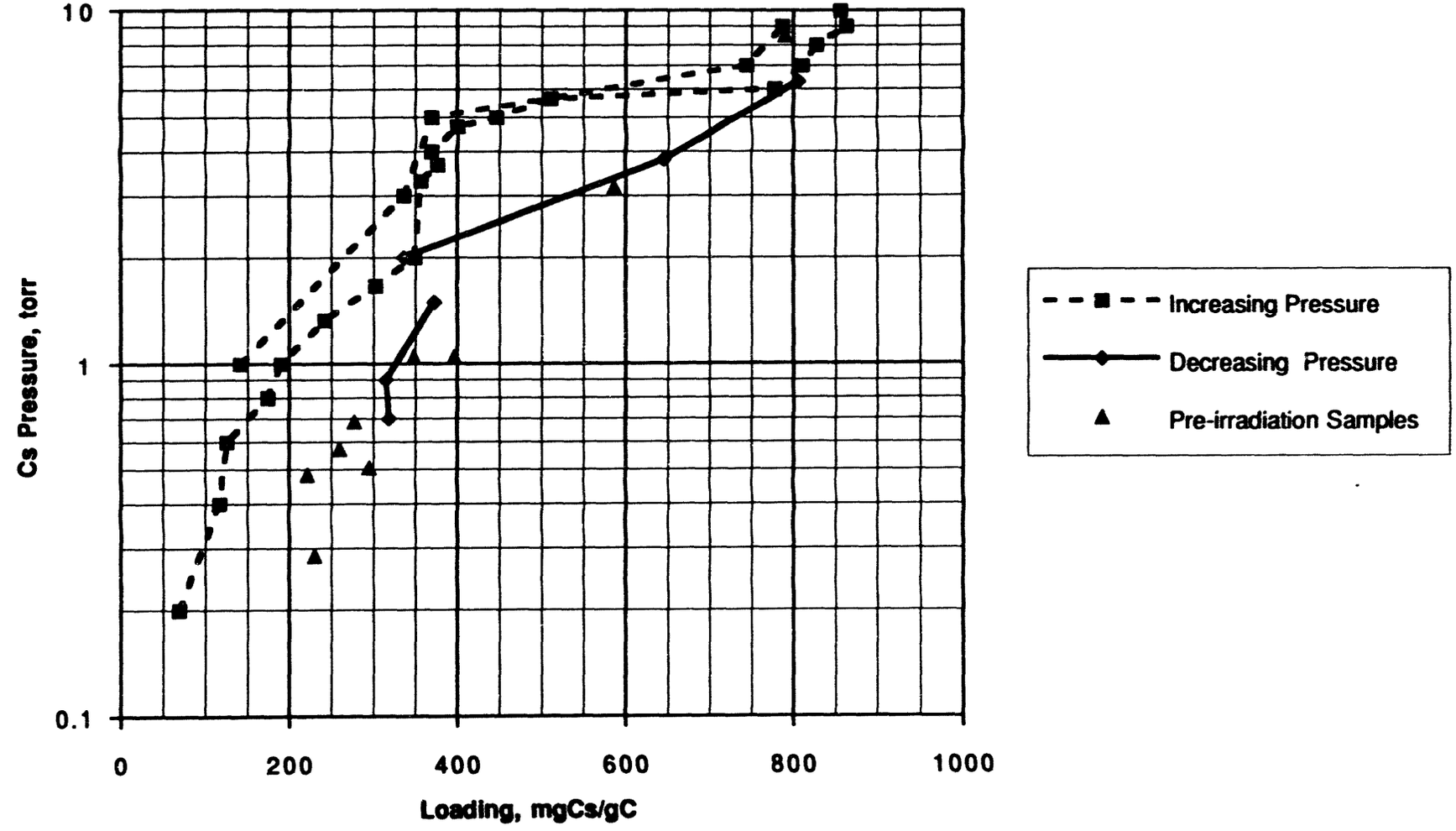

Figure 3-24. 1011 K Isotherms

about 10 minutes, typically. The values of T_o and P_o in Fig. 3-22 may be used for design calculations, though the uncertainty might be large in the vicinity of 400 and 800 mgCs/gC.

6. CESIUM RESERVOIR SPECIFICATION

6.1 Materials

POCO CZR-2 is identified as the material best for Cs-graphite integral reservoirs. Porous refractory metals may be utilized for the reservoir housing, although careful attention must be given to material compatibility. Of primary concern is the possible formation of metallic carbides.

6.2 Fabrication Process Description

Prior to assembly, the graphite should be vacuum degassed at 1500°C or above, for at least 2 hours at a pressure $< 10^{-6}$ torr. Outgassing in-situ, at a temperature exceeding its highest operating temperature for at least 2 hours at a pressure $< 10^{-6}$ torr should also be performed.

7. INTERCONNECTIVE COMPONENTS

In the presence of cesium vapor, the minimum breakdown voltage at an electrode temperature of 1073 K is slightly over 2 volts at a pd product of about 10 torr-mills. This is demonstrated by the Paschen curve for the bare electrode in Fig. 3-25. In the H-series TFEs, the pd product in the intercell region, in the event of a leak between the cesium space and the fission product spaces, could be as large as 100 torr-mils. For bare electrodes, Fig. 3-25 shows that breakdown could occur at about 5 volts. On the other hand, data obtained in the pre-1973 thermionics program (Ref. 7-1) demonstrate that a plasma-spray coating of Al_2O_3 can increase the breakdown voltage to approximately 15 volts at 100 torr-mils, as also shown in Fig. 3-25. As a further advantage, the situation improves at lower cesium pressures in the case of the plasma-spray alumina coating, rather than becoming worse.

The data available, an example of which is shown in Fig. 3-25, is adequate to assure that cesium arcs in the intercell region can be avoided. No further testing of the TFEVP was deemed necessary.

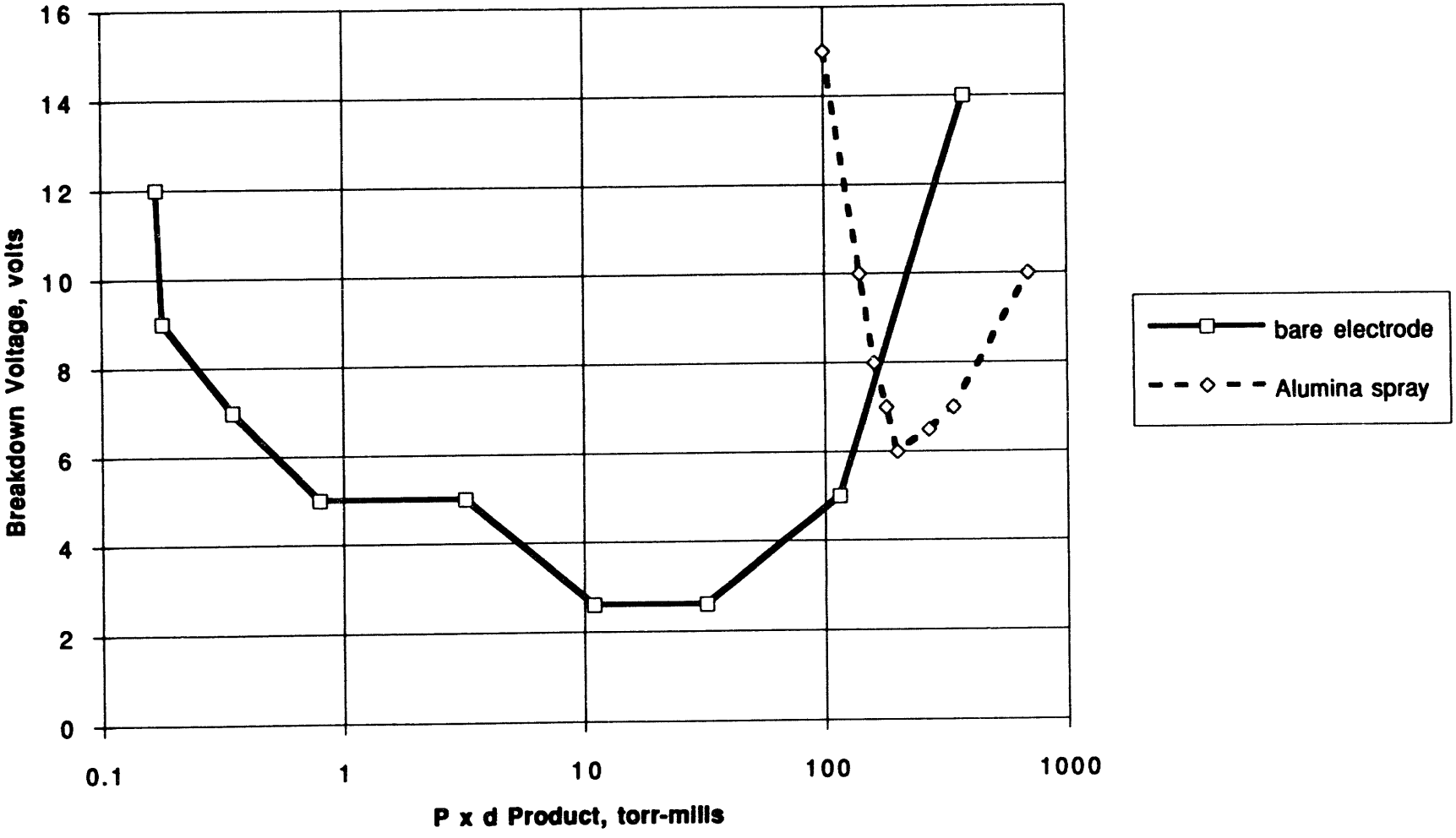

Figure 3-25. Effect of Plasma Sprayed Intercell Region

8. REFERENCES

1-1 General Atomics Report GA-C18062, GES Baseline System Definition and Characterization Study, Final Report for the Period December 1984 through July 1985; Prepared under JPL Contract 956472, August 9, 1985.

1-2 General Atomics Report GA-A18182 (1985), SP-100 Thermionic Technology Program Annual Integrated Technical Progress Report for the Period Ending September 30, 1985, by GA Technologies, Rasor Associates Inc., Space Power, Inc. and Thermo Electron Corporation, General Atomics, San Diego, CA, November 1985.

1-3 General Atomics Report GA-A18915 (1987), Thermionic Irradiations Program Final Report, General Atomics, San Diego, CA.

1-4 Cone, V. P. and J. Dunlay (1987), Thermionic Technology Program Fiscal Year 1986 and Final Technical Report, Thermo Electron Report No. TE4400-227-87.

1-5 Hatch, G.L. (1988), Thermionic Technology Program: Thermionic Converter Performance Final Report, NSR-25-25, E-533-003-B053188 (DOE Contract No. DE-ACO3-86SF15954).

3-1 Weller, K. R. and H. Watts (1965), Carbon, 2, 337.

3-2 Taylor, J. B and I. Langmuir (1933), Physical Review, 44, 423.

3-3 Porous tungsten was obtained from Spectra-Mat, Inc., Watsonville, CA. No certifications were received. The vendor characterized the material as 46% dense tungsten.

3-4 Hatsopoulos, G. N. and E. P. Gyftopoulos (1979), VII, MIT Press, Cambridge, MA, p.401.

3-5 Dushman, S. and J. M. Lafferty (1962), Second Edition, John Wiley, NY, p. 32.

4-1 General Atomics Document 910108, "UCA-1 Cesium Reservoir Test Report: Test Procedure and Discussion of Post Irradiation Examination", J. N. Smith, June 14, 1990.

7-1 Fitzpatrick, G., M. Yates and J. Chin, "Electric Discharges in Cesium in the Sheath Region of TFEs", General Atomics Report GACD-10316, April, 1971.

APPENDIX A

PREIRRADIATION ISOSTERES FOR Cs-RESERVOIR TEST SPECIMENS

SEE TABLE 3-2 FOR SAMPLE DEFINITION

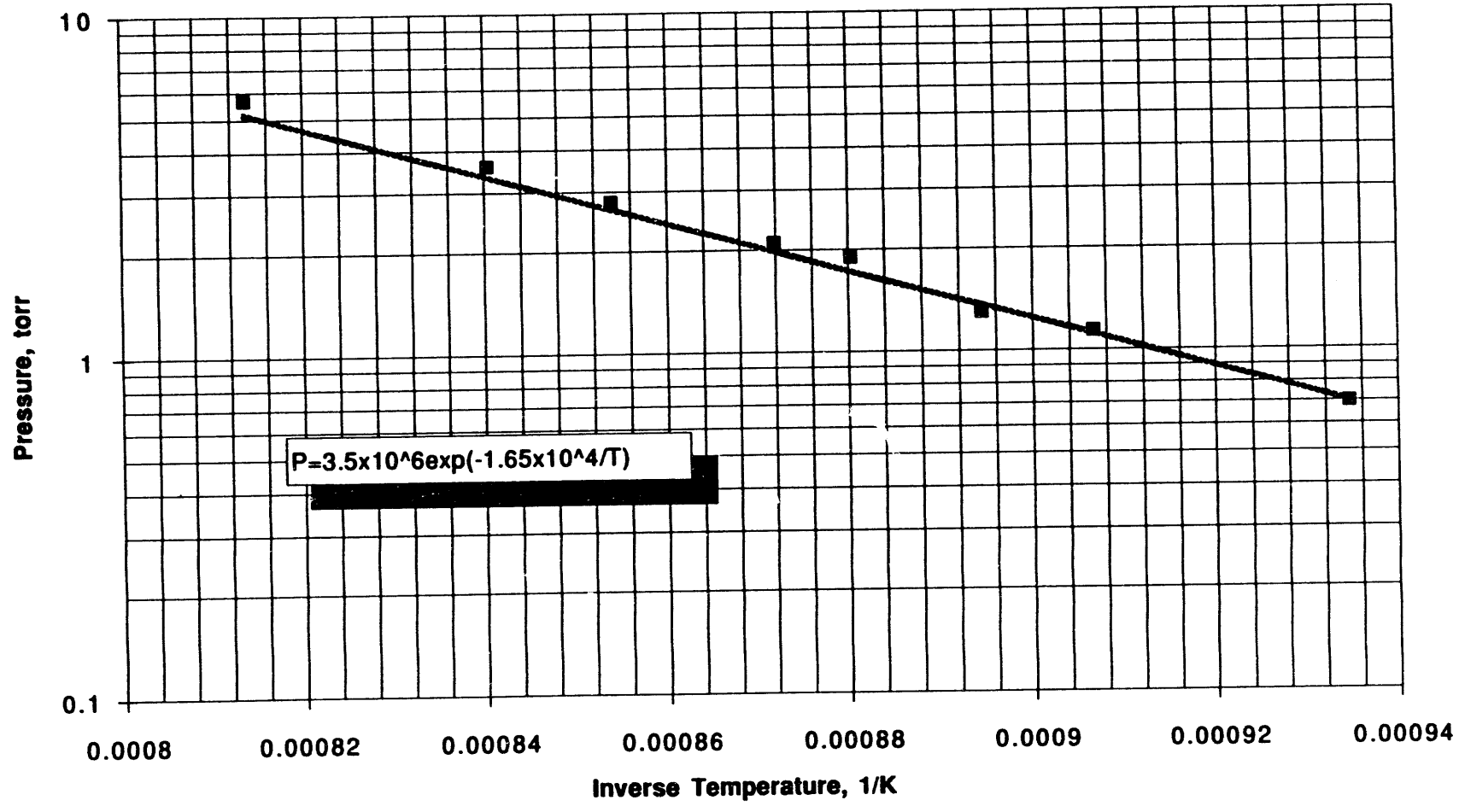

Figure A-1. Preirradiation Isostere, UCA-2 Sample 197 A 230 mg Cs/gC

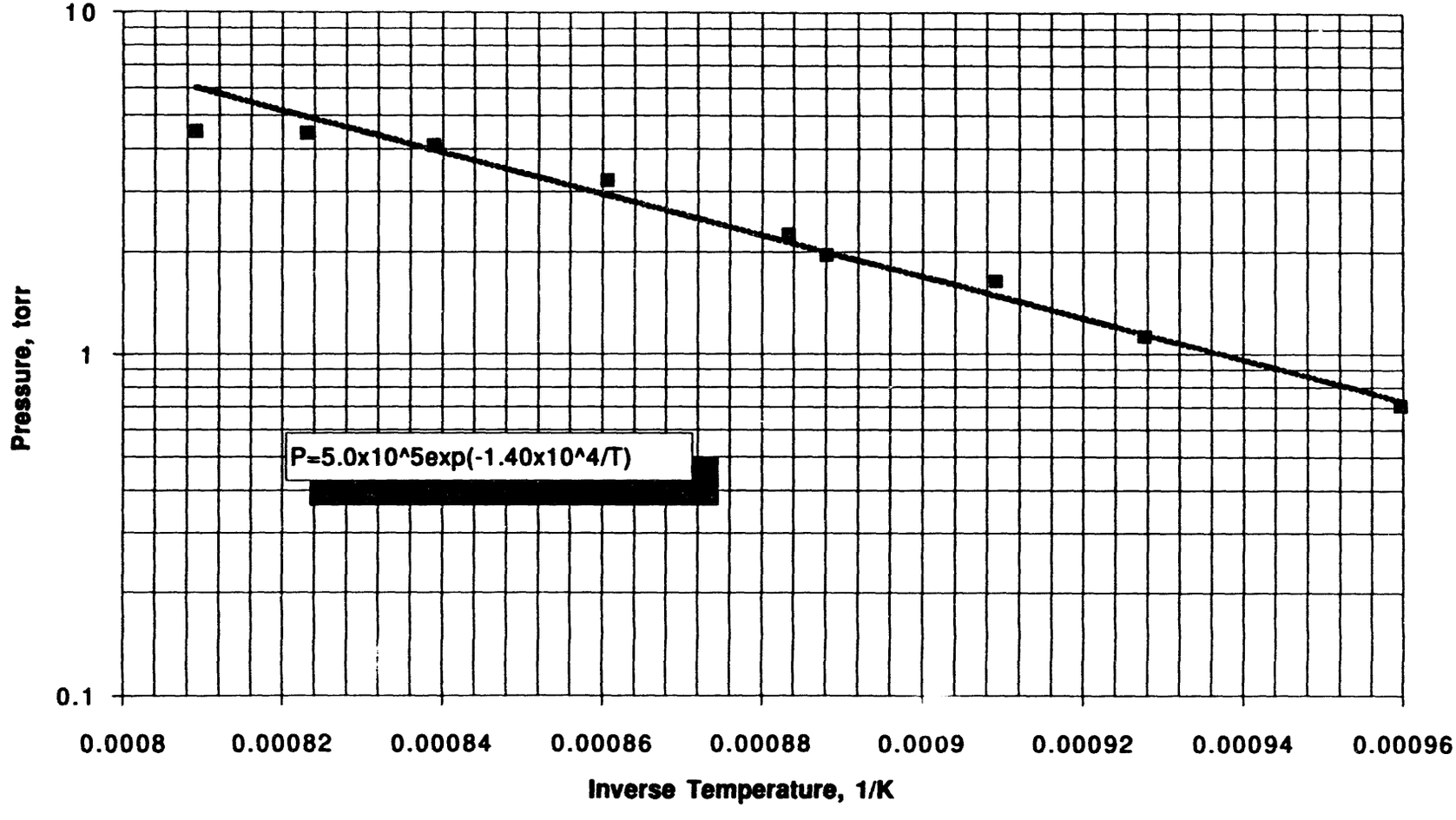

Figure A-2. Preirradiation Isostere, UCA-2 Sample 199 D 222 mg Cs/gC

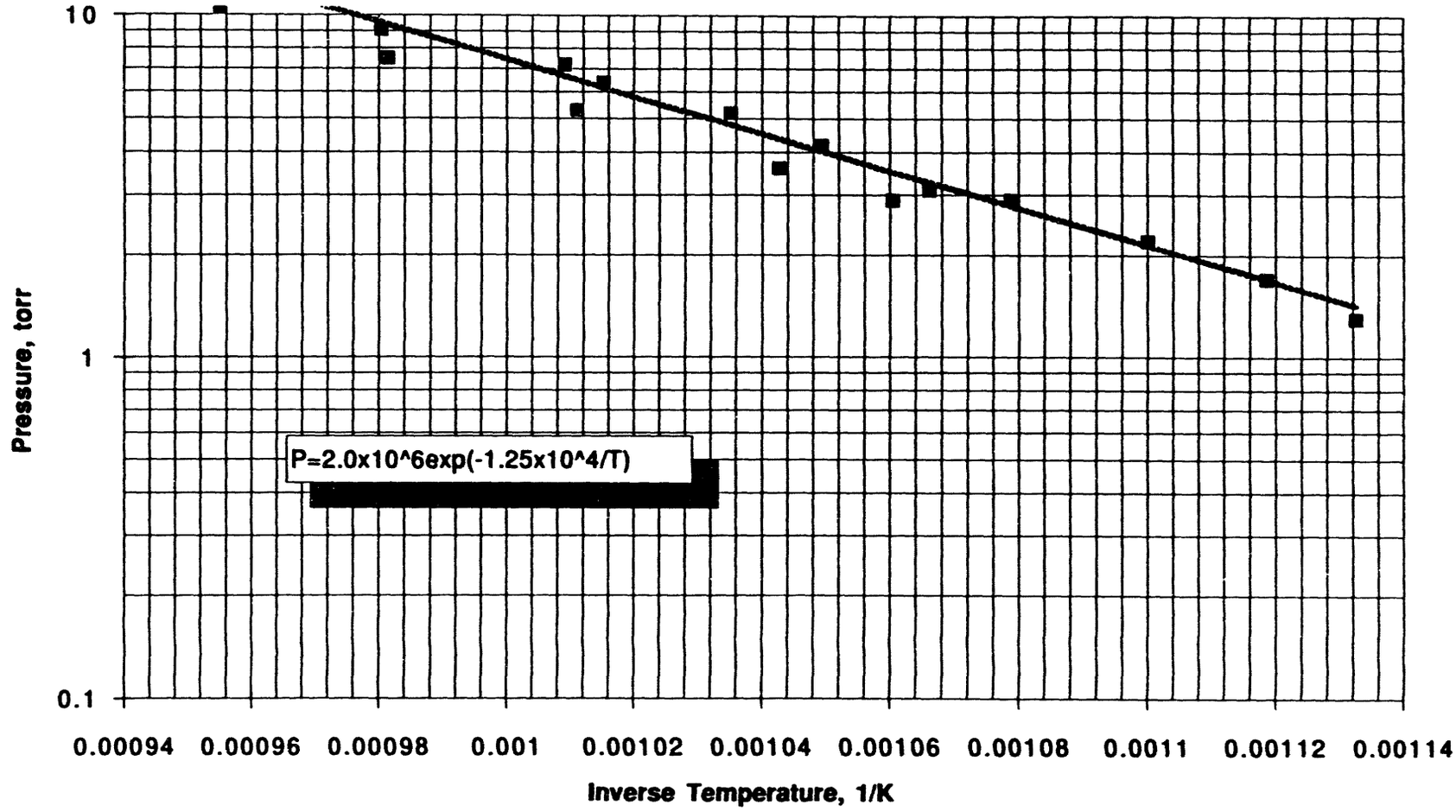

Figure A-3. Preirradiation Isostere, UFAC-3 Sample 929 D 790 mg Cs/gC

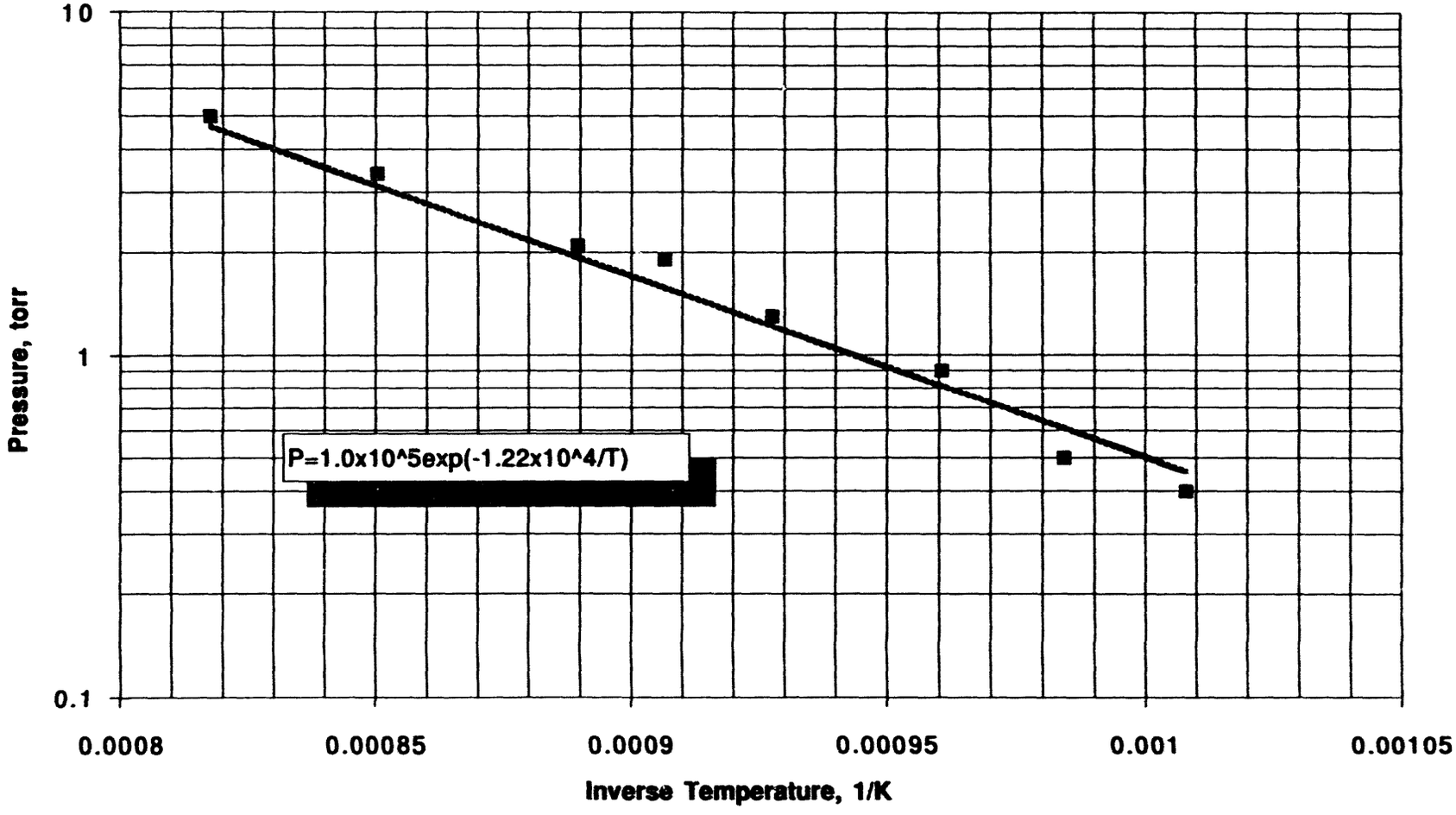

Figure A-4. Preirradiation Isostere, UFAC-3 Sample 960 D 260 mg Cs/gC

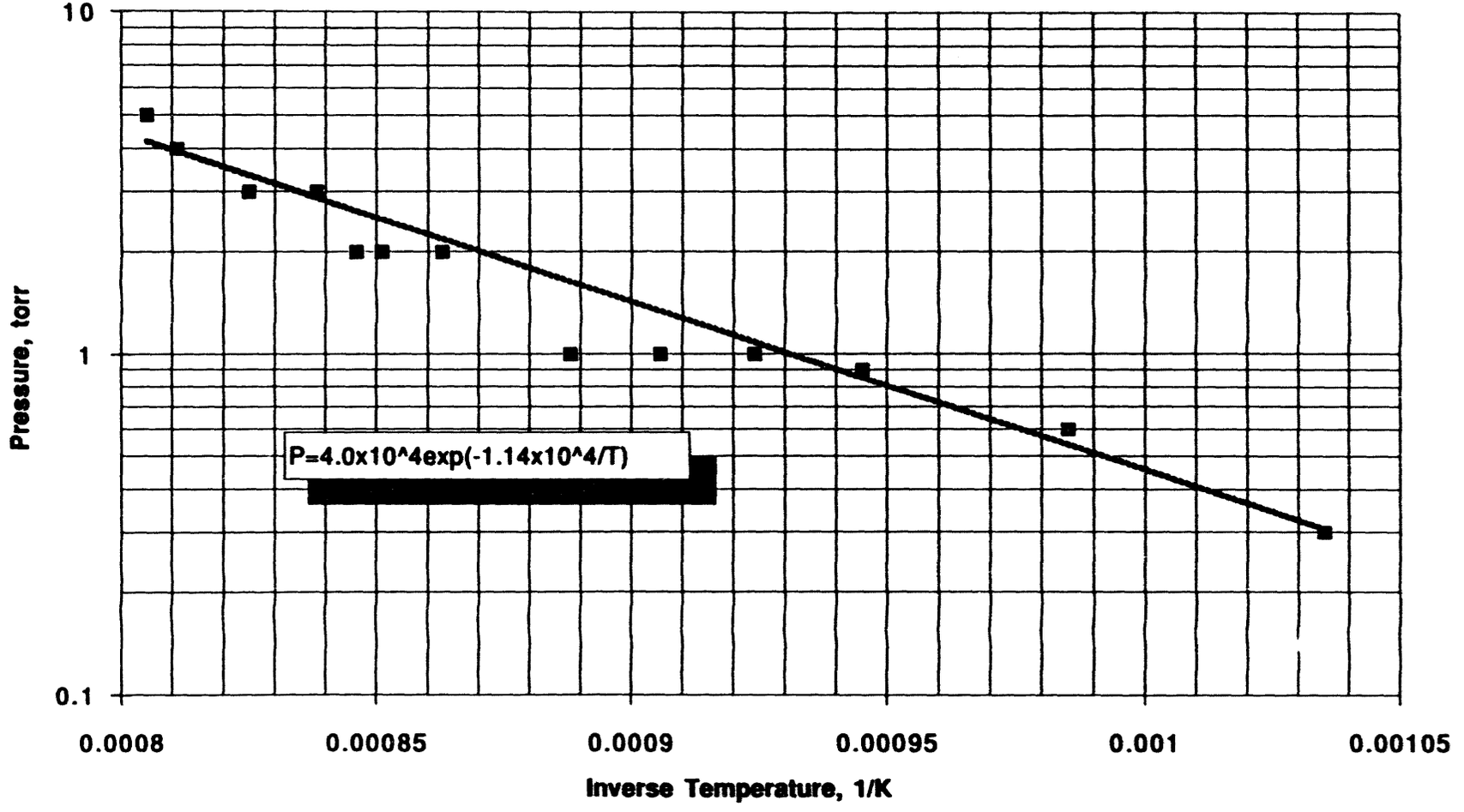

Figure A-5. Preirradiation Isostere, UFAC-3 Sample 962 A 295 mg Cs/gC

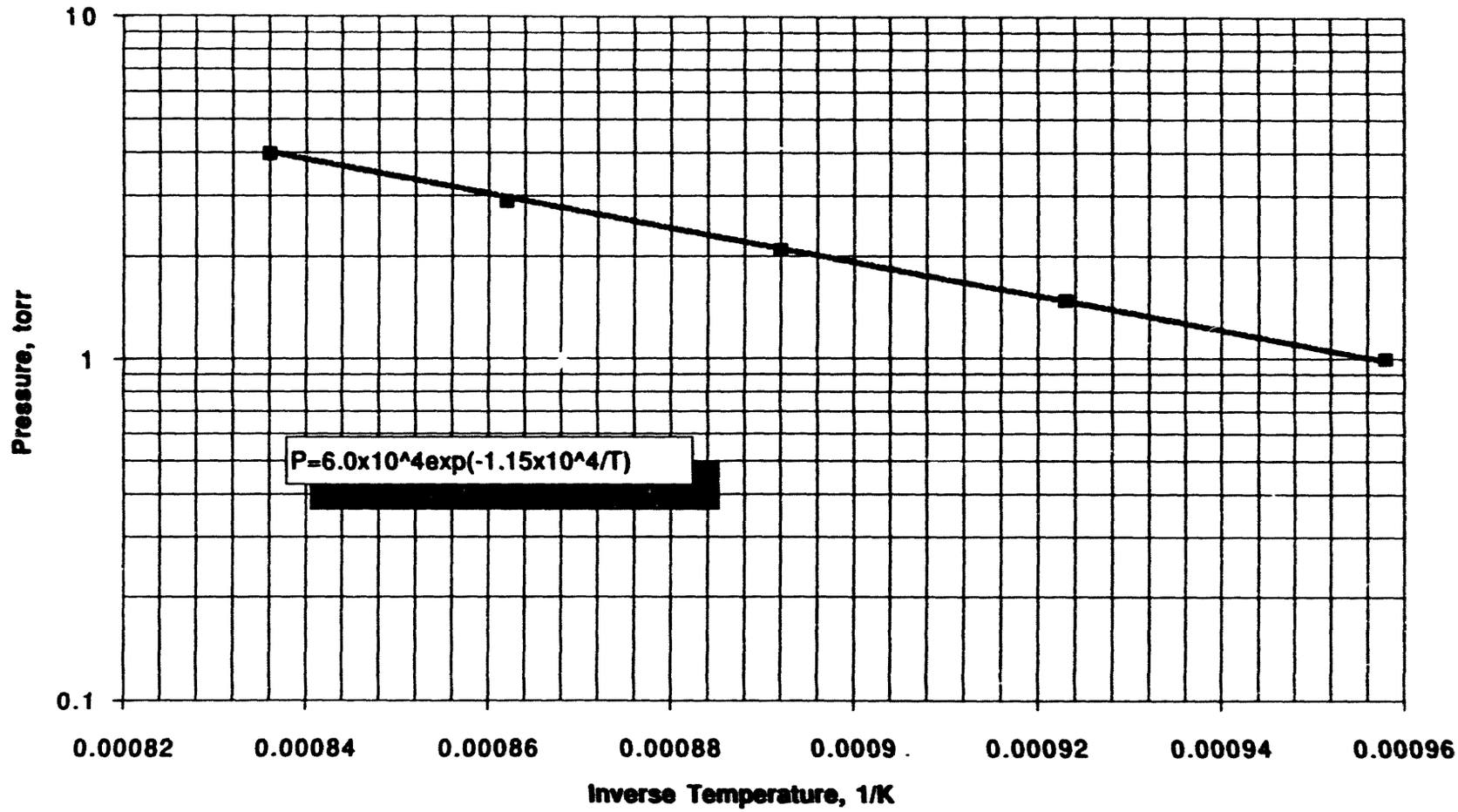

Figure A-6. Preirradiation Isostere, UCA-3 Sample 413 D 278 mg Cs/gC

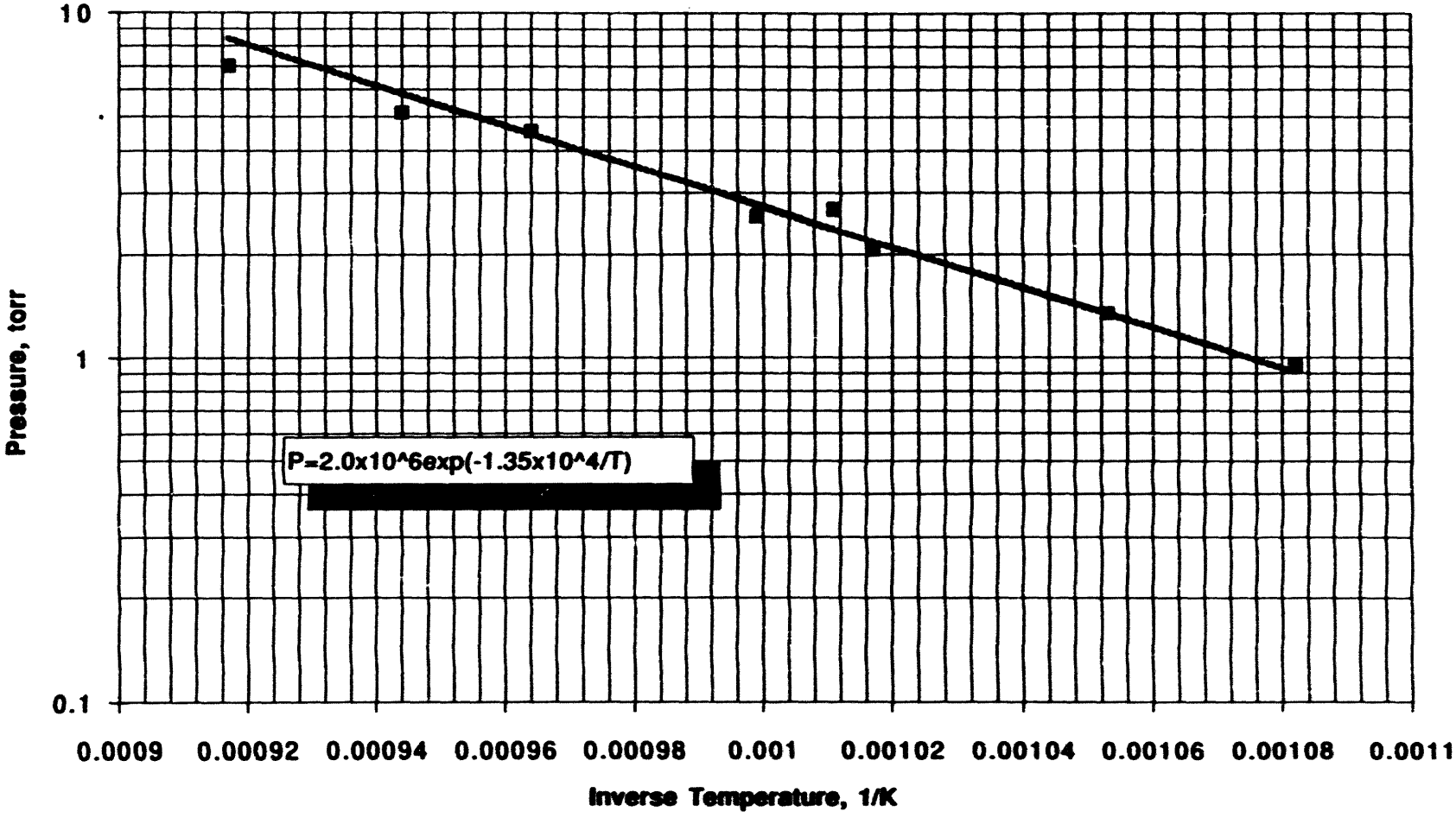

Figure A-7. Preirradiation Isostere, UCA-3 Sample 1247 D 586 mg Cs/gC

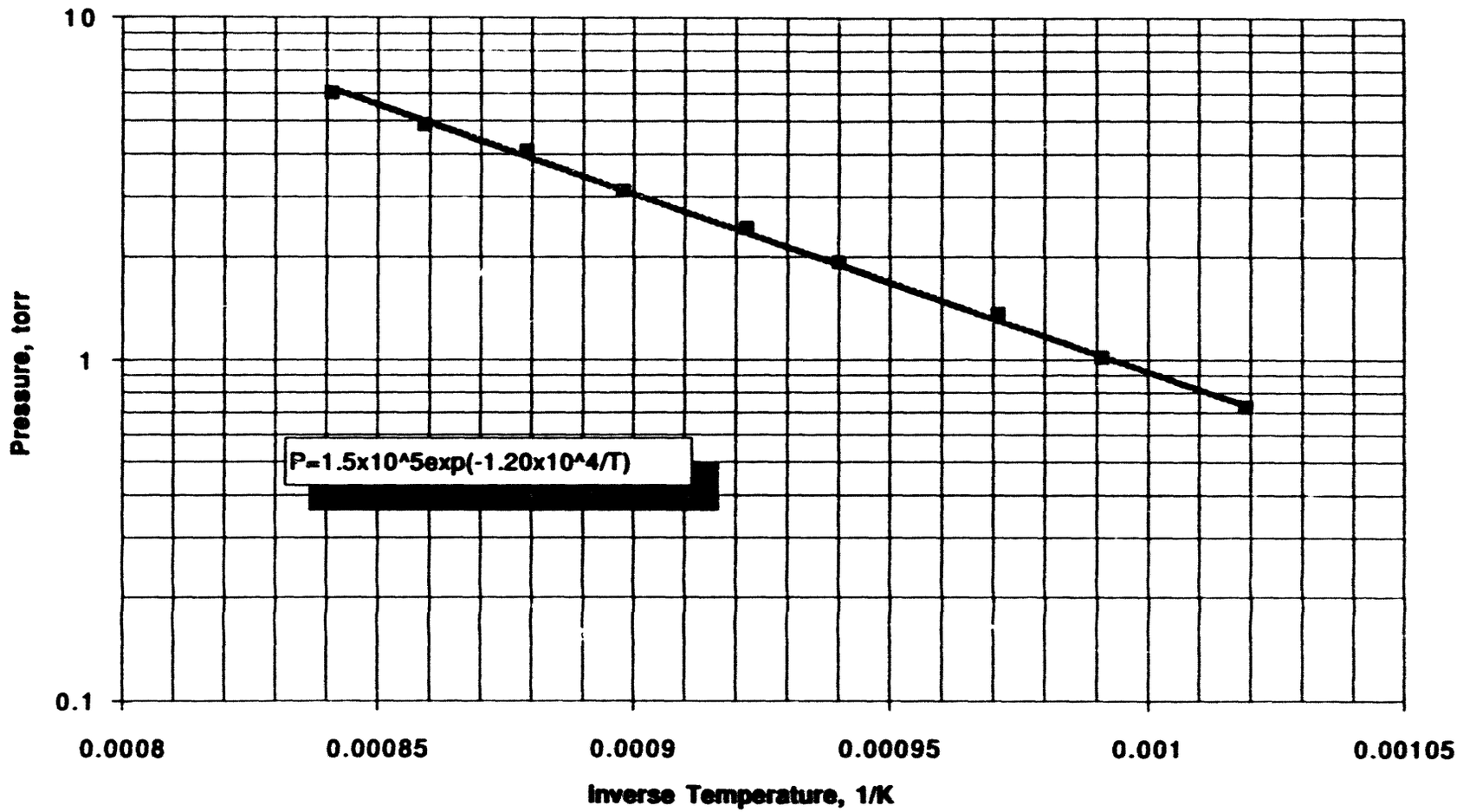

Figure A-8. Preirradiation Isostere, UCA-3 Sample 1300 D 348 mg Cs/gC

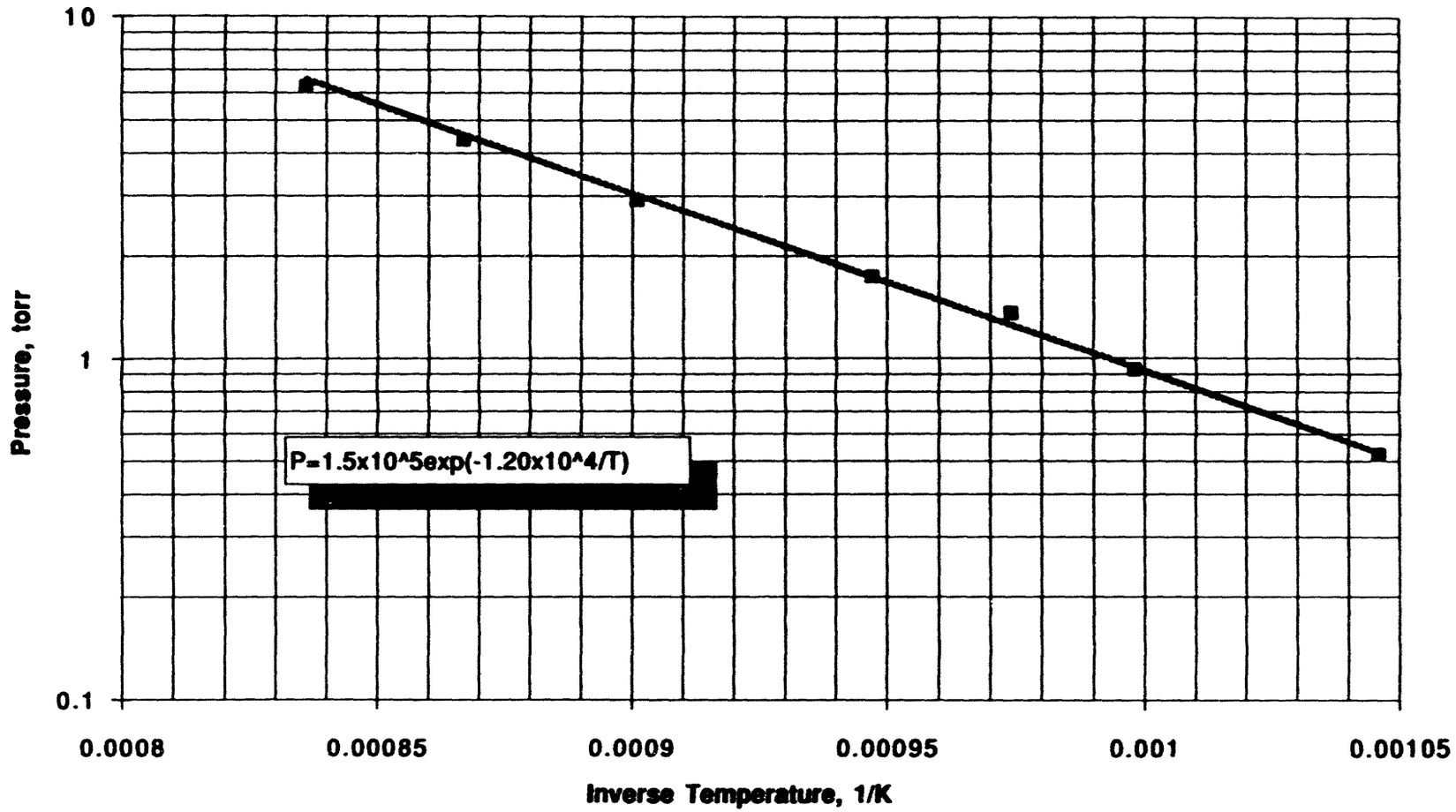

Figure A-9. Preirradiation Isostere, UCA-3 Sample 1301 D 396 mg Cs/gC

APPENDIX B

CESIUM METER DESCRIPTION

CESIUM METER

B.1 Introduction

The cesium meter was used to determine by remote control in a hot cell the cesium pressure of an intercalated cesium graphite compound which had been irradiated. It is not reusable. The device provides for the measurement of the deignition voltage of a cesium arc. The voltage-pressure characteristics of the device are derived from a separate test using liquid cesium.

B.2 Description of the Cesium Meter

The cesium meter is shown schematically in Fig. B-1, the various parts of which are defined in Table B-1. The test specimen, Part 21, is enclosed in the test specimen holder, Part 16, which also contains a thermocouple. A vacuum is established through Part 22, which when pinched off seals the test specimen in the cesium meter. At the time of the test, the test specimen, which itself is sealed, is punctured by a puncture rod, Part 6, which is activated by turning three puncturing screws, Part 25. The rod motion is accommodated by a bellows, Part 19. The subsequent cesium pressure is determined by the test specimen temperature as given by the thermocouple in Part 16. The arc across the cesium gap takes place in Part 15, the temperature of which is kept at 500°C, as measured by a TC in Part 17.

B.3 Cesium Meter System

The cesium meter is enclosed in two ovens, as shown in Fig. B-2, so that the test specimen and spark gap can be heated to two different temperatures. The spark gap component (Part 15) is kept at about 500°C while the test specimen temperature is varied typically over the range 700°C to 900°C. The test specimen temperature determines the cesium pressure.

The instrumentation schematic is shown on Fig. B-3.

Two insulated electrical leads for 200 V at 500°C, are attached to the test rig, one to Part 17 and one to Part 5. The thermocouple sheath and electrical lead attached to Part 17 must be insulated completely from the test rig. The Lindberg power supplies for the two furnaces are identical except they are connected to different voltages. The supply for the tube furnace is connected to 110 V while the supply for the box furnace is connected to 220 V as per the manufacturer's instructions.

B.4 Test Procedure

The test specimen is mounted in the tube furnace as shown in Fig. B-2. The cesium meter is outgassed by heating the test specimen to 900°C and the rest of the apparatus to 500°C. The vacuum system pressure should be at 5×10^{-5} torr at temperature.

Table B-1

DESCRIPTION OF CESIUM METER COMPONENTS

Part Number	Description
16	Test specimen holder
21	Test specimen
6	Puncture rod
7	Structural tube
22	Evacuation/pinch-off tube
15	Ceramic insulator (where arc occurs)
17	Spark gap electrode
5	Inner flange
19	Bellows to accommodate puncture rod motion
27	Bellows adapter
4	One of three puncturing screws
25	Capture nut for puncturing screws
9	Outer flange

The test specimen is then remotely punctured and the cesium meter is pinched off.

Measurements are then made over the range 700°C to 900°C.

The thermocouple in the spark gap (Part 17) is brought up on a 2-hour ramp to 500°C. The thermocouple in the specimen holder (Part 16) is brought up to 500°C at the same time, and then increased to 700°C and stabilized before stepping up the temperature at 25°C intervals from 700°C to 900°C. At each step, the arc voltage between points 1 and 2 are determined by simultaneously plotting the voltage 1-2 vs voltage 3-4 using the oscilloscope. Figures B-4 and B-5 show typical X-Y scope traces and the point at which to measure the "arc" (actually deignition) voltage. Figure B-6 is the calibration curve of arc deignition voltage vs cesium pressure above a liquid cesium reservoir for 500 $\pm$ 2°C spark gap temperatures.

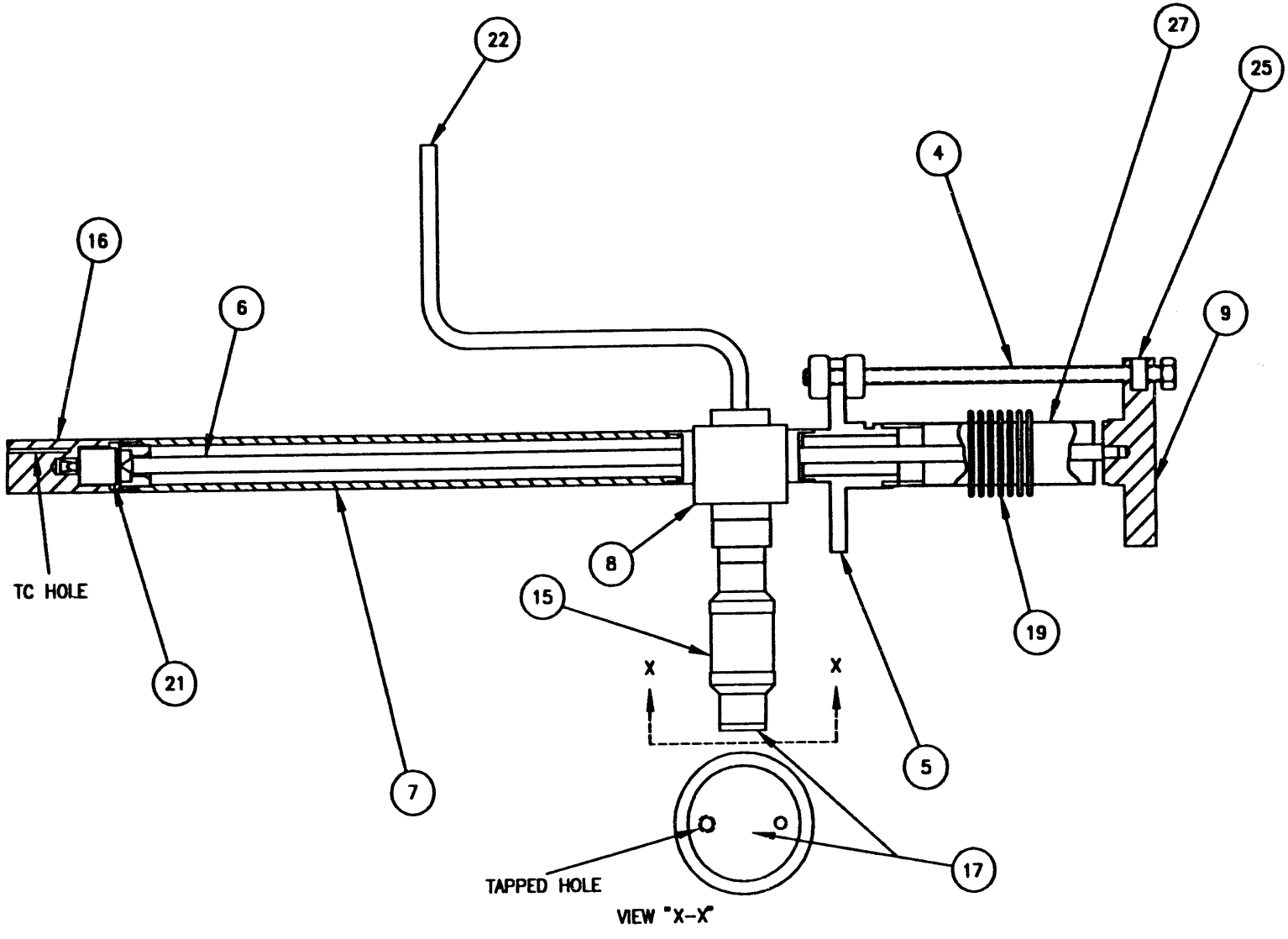

Figure B-1. Cesium Meter Schematic

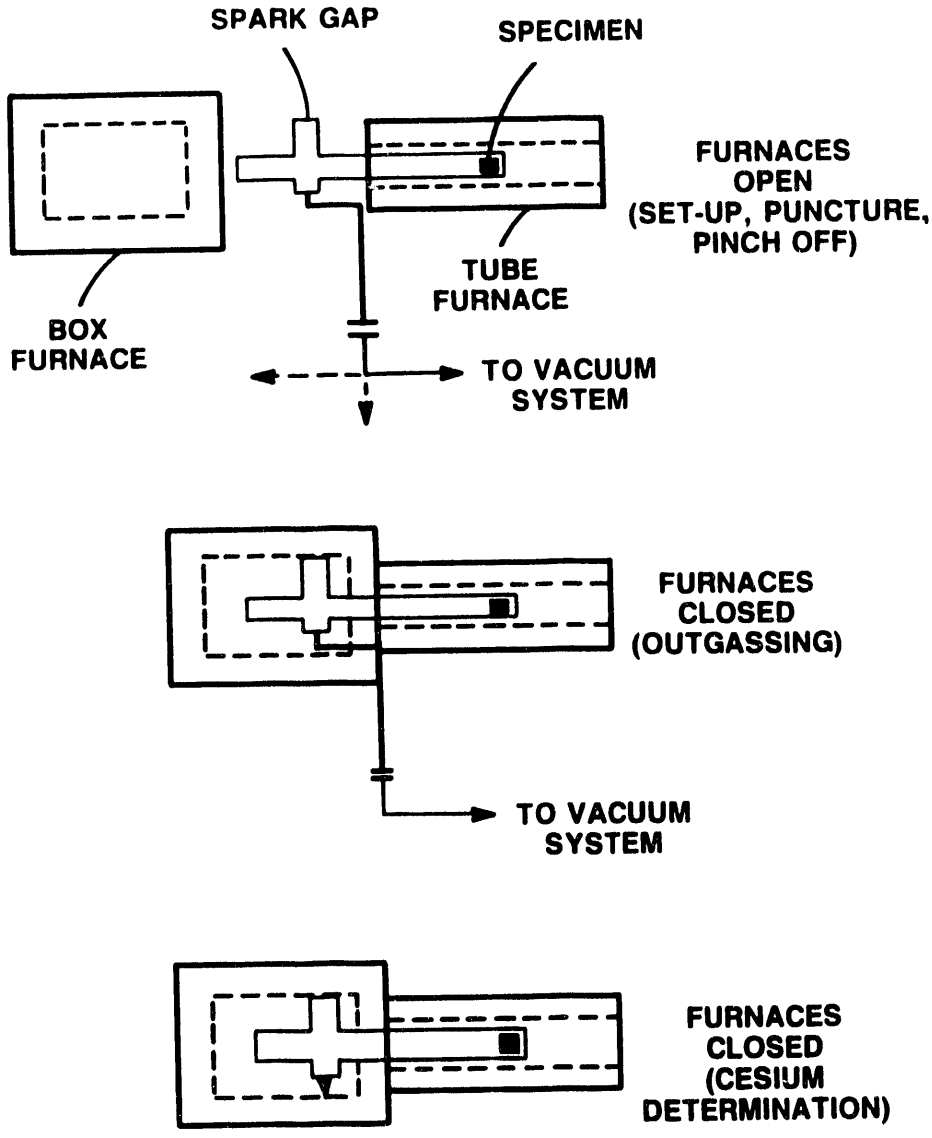

Figure B-2. Cesium Meter Furnace Arrangement

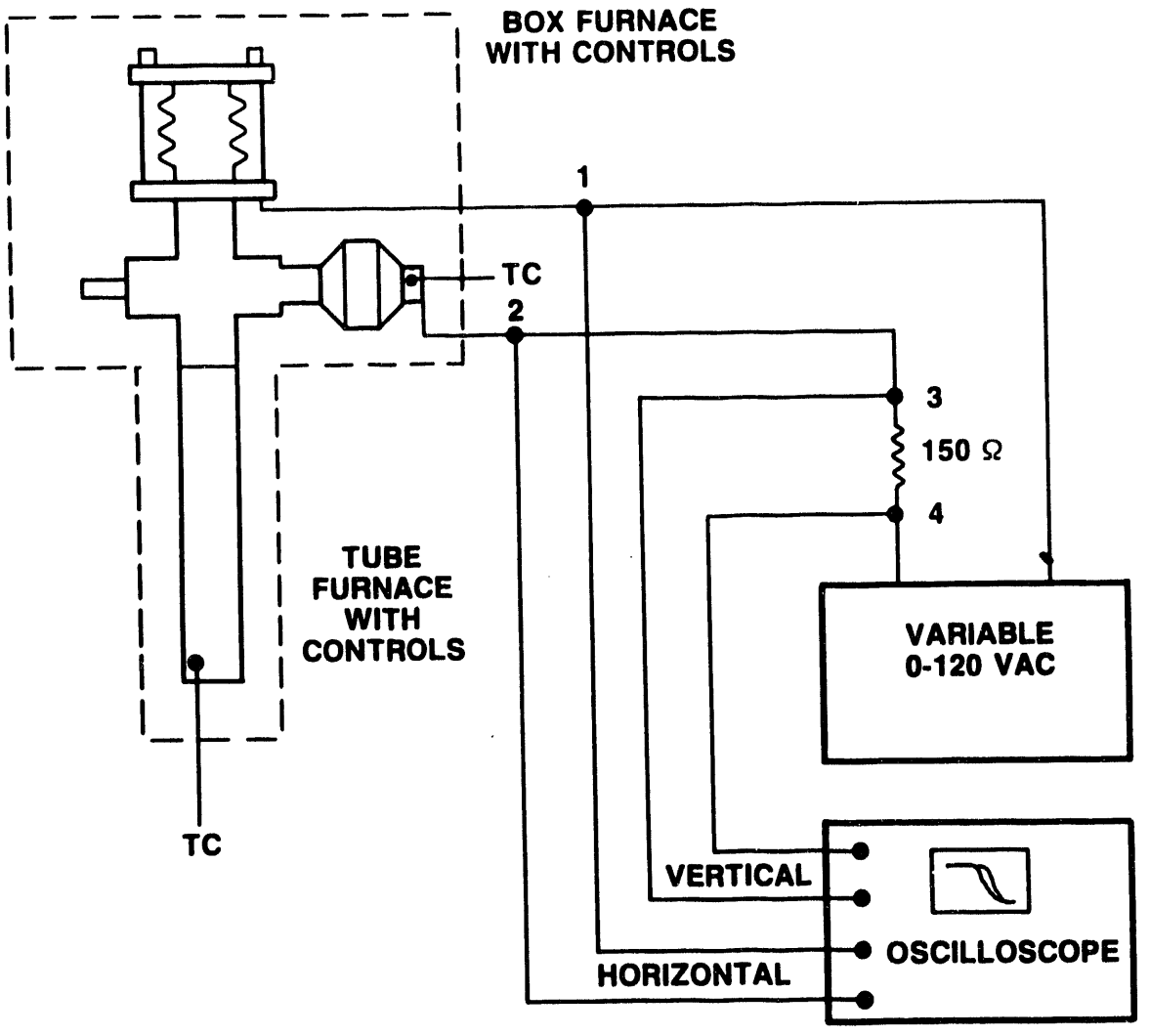

Figure B-3. Cesium Meter Instrument Schematic

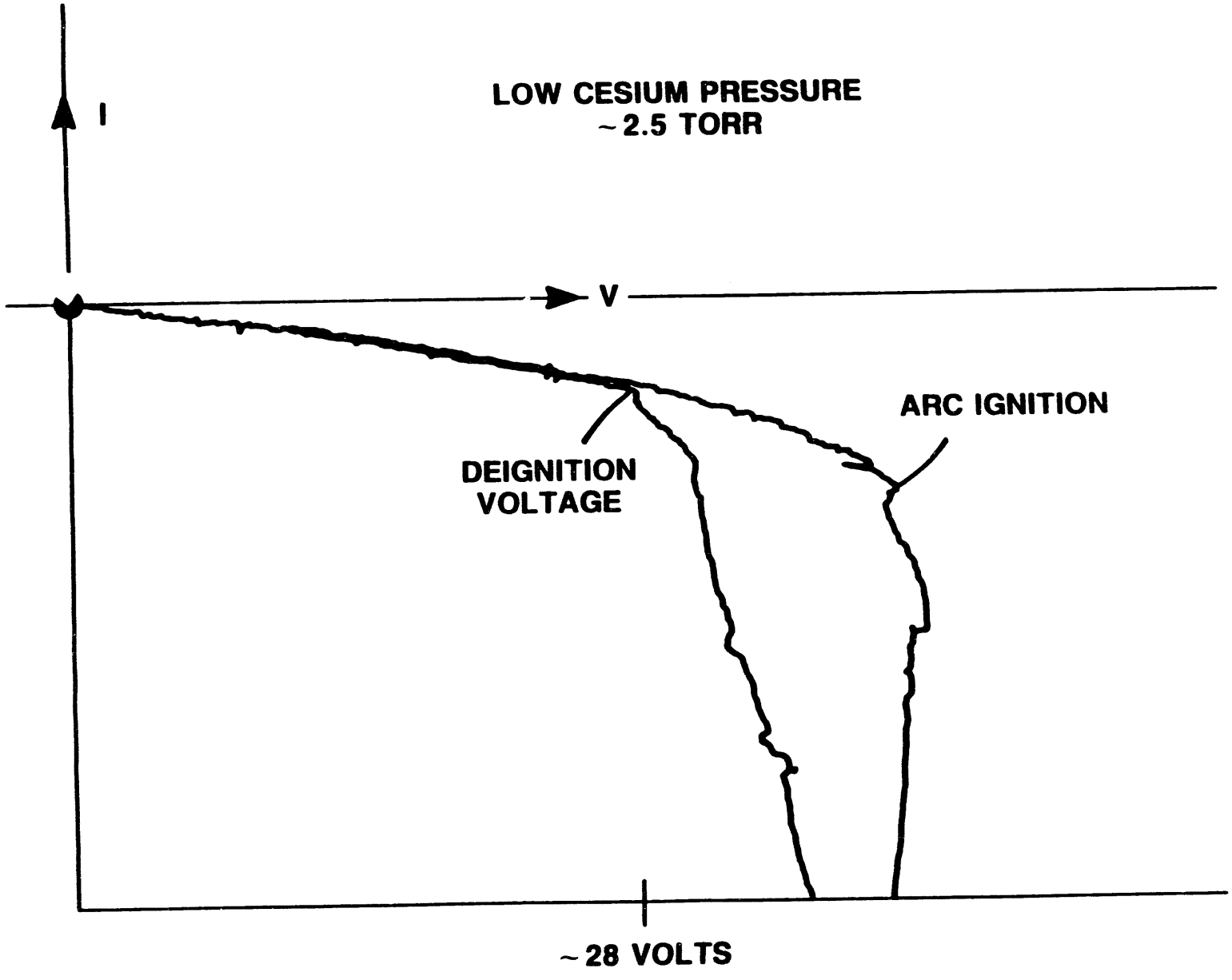

Figure B-4. Arc Voltage Current Curve

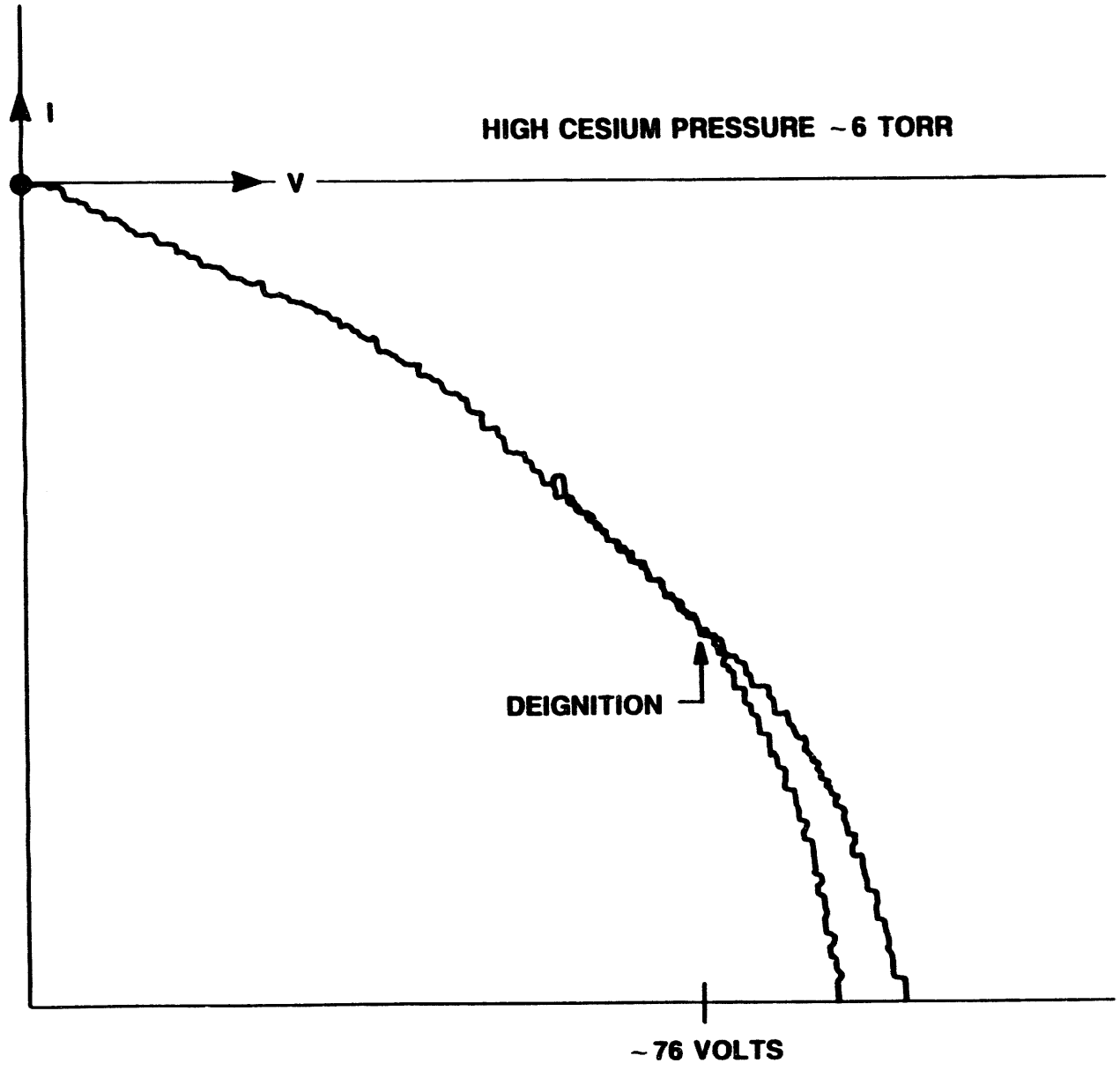

Figure B-5. Arc Voltage Current Curve

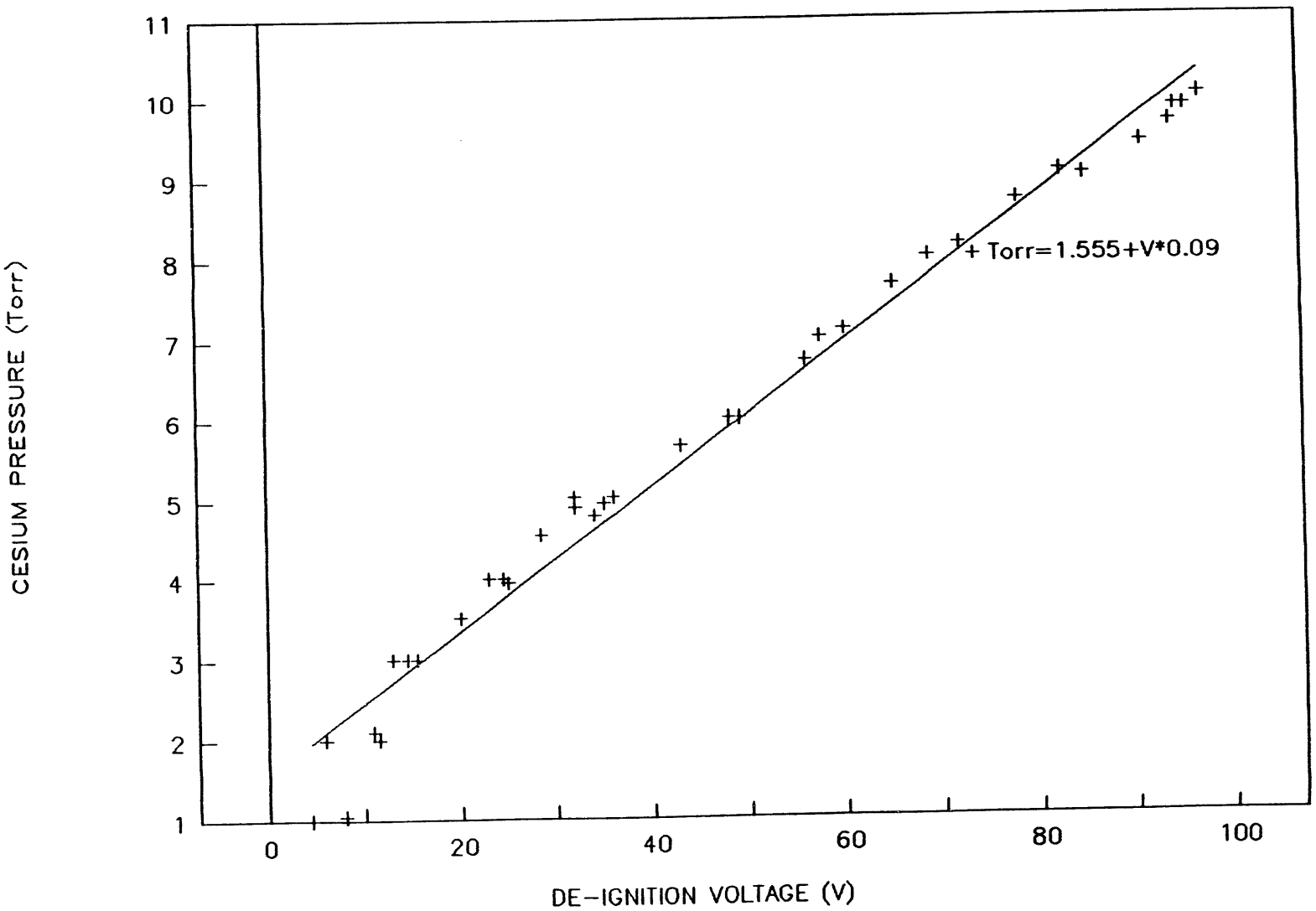

Figure B-6. Calibration Curve Cesium Pressure vs Deignition Voltage

APPENDIX C

PRESSURE-TEMPERATURE RELATIONSHIPS FOR IRRADIATED CESIUM-GRAPHITE RESERVOIRS

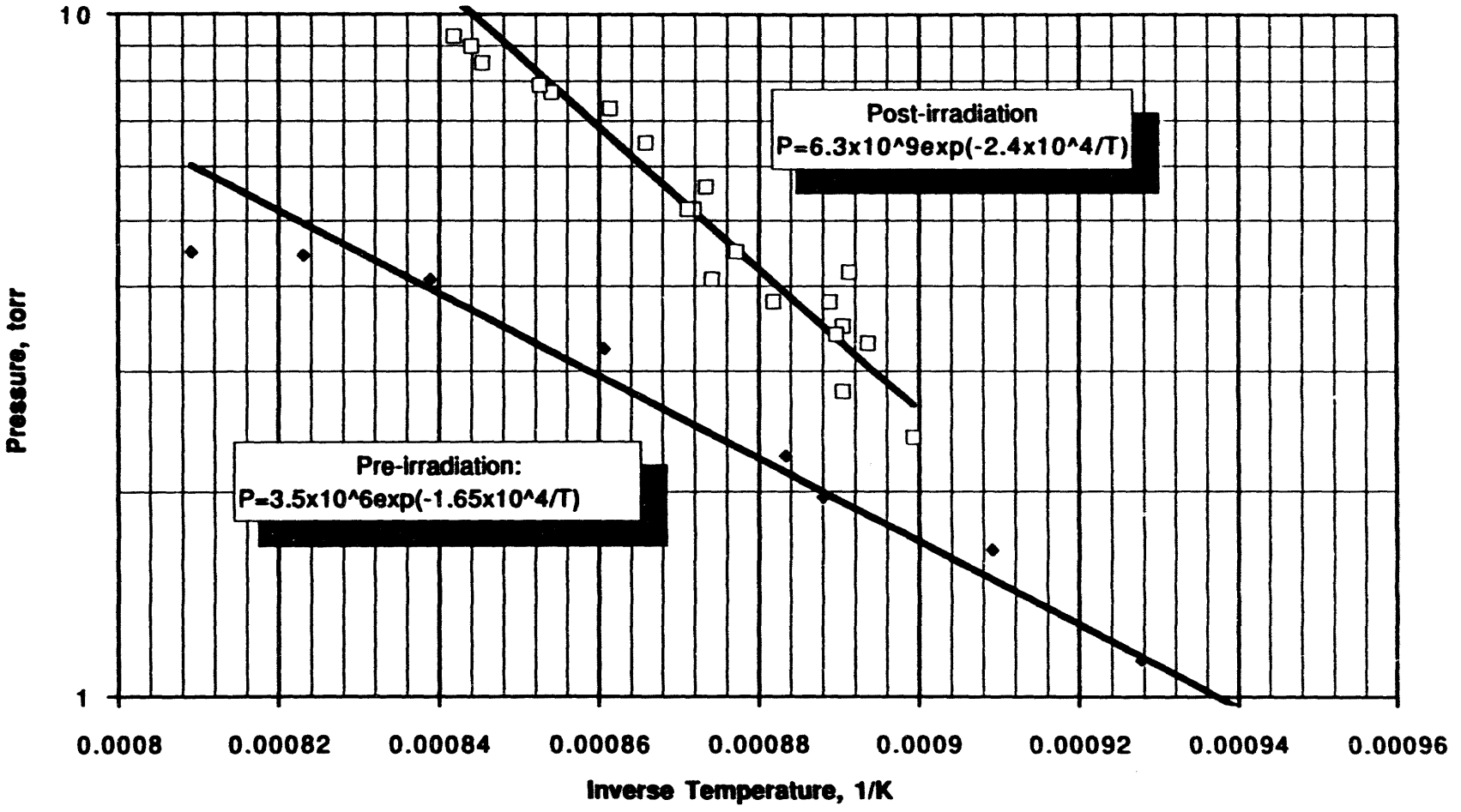

Figure C-1. UCA-2 Sample 199 D 222 mg Cs/gC

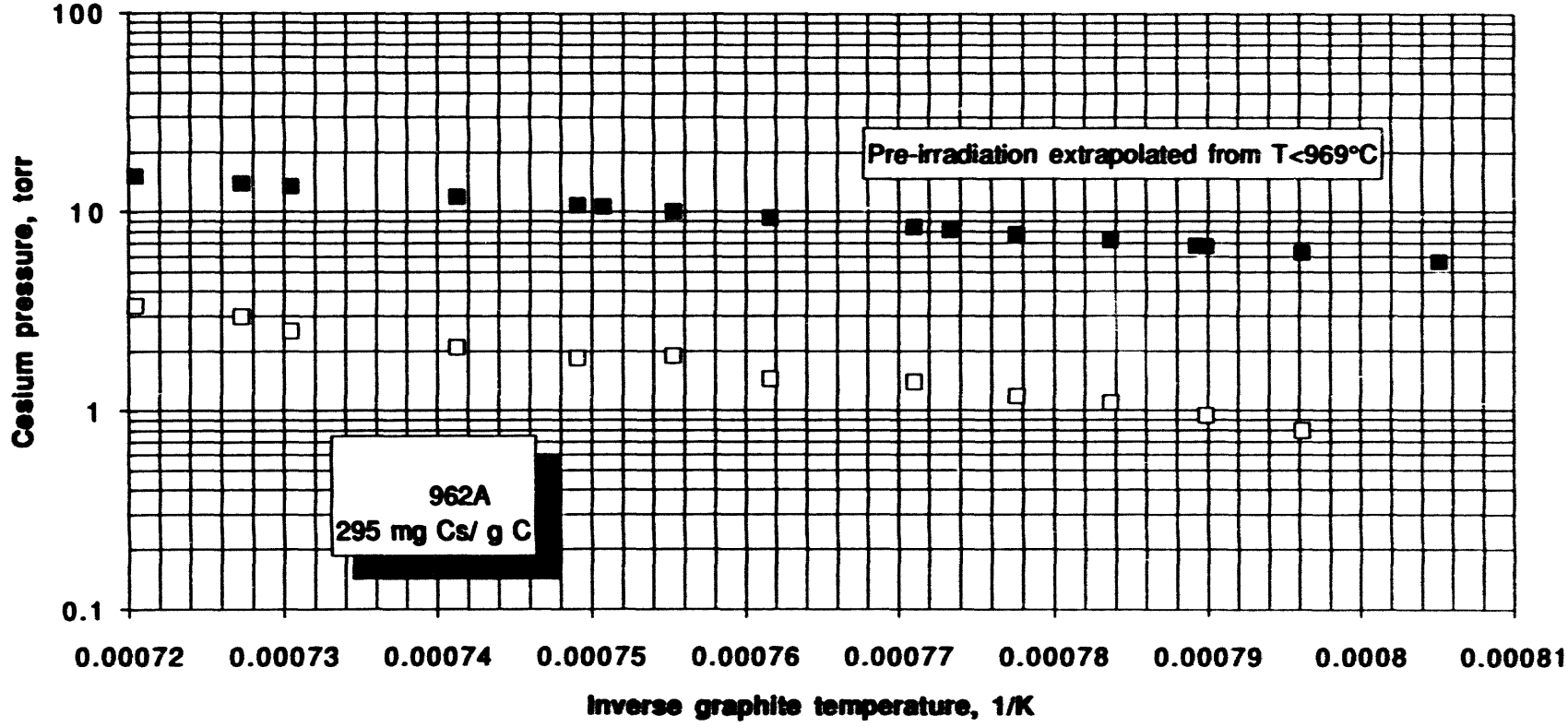

Figure C-2. UFAC-3 HOPG Reservoir, Closed Symbols, Pre-irradiation; Open Symbols, PIE

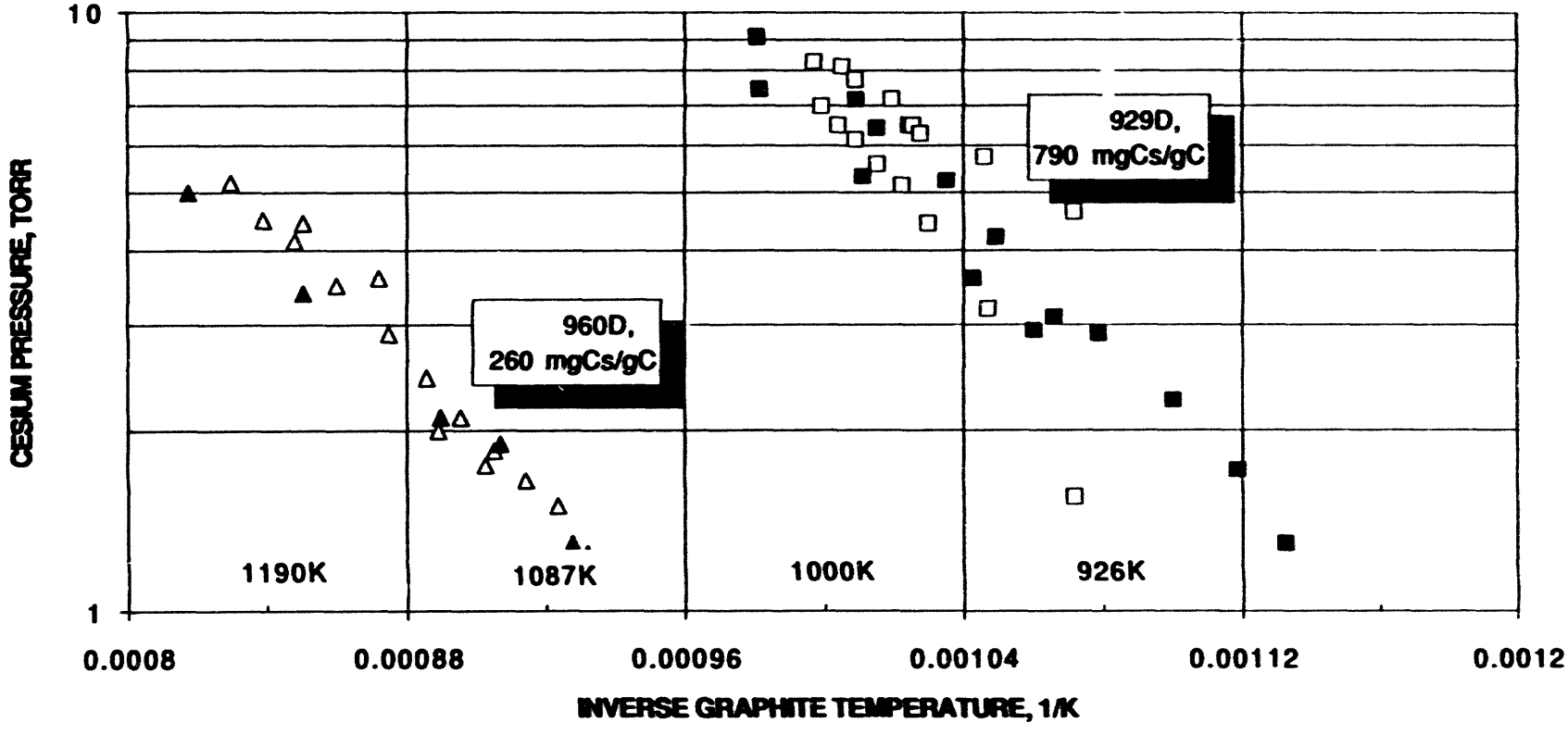

Figure C-3. UFAC-3 POCO Reservoirs, Closed Symbols, Pre-irradiation; Open Symbols, PIE

DATE

FILMED

6/29/94

END